DISSERTATIONES
PHYSICAE
UNIVERSITATIS
TARTUENSIS
133

KAJA PAE

Electron-phonon interactions in local degenerate electronic states in solids

DISSERTATIONES PHYSICAE UNIVERSITATIS TARTUENSIS
133

DISSERTATIONES PHYSICAE UNIVERSITATIS TARTUENSIS
133

KAJA PAE

Electron-phonon interactions in local degenerate electronic states in solids

UNIVERSITY OF TARTU
Press
1632

This study was carried out at the University of Tartu

The dissertation was admitted on 8.05.2024 in partial fulfilment of the requirements for the degree of Doctor of Philosophy in Physics, and was allowed for defense by the Council of the Institute of Physics, University of Tartu.

Supervisor: Prof. Vladimir Hizhnyakov, University of Tartu, Estonia

Opponent: Prof. Boris Tsukerblat, Ben-Gurion University of the Negev, Beer-Sheva, Israel

Defense: 20.06.2024 at the University of Tartu

The research presented in this thesis is supported by the Estonian Science Foundation projects no. TK114, IUT2-27, ETF7741 and SF0180013s07.

ISSN 1406-0647 (print)
ISBN 978-9916-27-547-4 (print)
ISSN 2806-2523 (pdf)
ISBN 978-9916-27-544-3 (pdf)

University of Tartu Press
www.tyk.ee

CONTENTS

LIST OF PUBLICATIONS

The thesis is based on the following seven publications, which are referred to in the text by Roman numerals.

I Hizhnyakov, Vladimir; Pae, Kaja; Vaikjärv, Taavi (2012). Vibronic Transitions to a State with Jahn-Teller Effect: Contribution of Phonons. M. Atanasov et al., Vibronic Interactions and the Jahn-Teller Effect: Theory and Applications (179–191). Springer.

II Hizhnyakov, Vladimir; Pae, Kaja; Vaikjärv, Taavi (2012). Optical Jahn-Teller effect in the case of local modes and phonons. Chemical Physics Letters, 525–526, 64–68, 10.1016/j.cplett.2011.12.066.

III Pae, Kaja; Hizhnyakov, Vladimir (2013). Optical Jahn-Teller effect: contribution of phonons. Journal of Physics: Conference Series, 428, 012011.10.1088/1742-6596/428/1/012011.

IV Pae, Kaja; Hizhnyakov, Vladimir (2013). Nonadiabaticity in a Jahn-Teller system probed by absorption and resonance Raman scattering. Journal of Chemical Physics, 138 (10), 104103, 10.1063/1.4792835.

V Pae, Kaja; Hizhnyakov, Vladimir (2014). Time-dependent Jahn-Teller problem: Phonon-induced relaxation through conical intersection. Journal of Chemical Physics, 141 (23), 234113, 10.1063/1.4903814.

VI Pae, Kaja; Hizhnyakov, Vladimir (2016). Quantum friction of pseudorotation in Jahn-Teller system: Passage through conical intersection. Journal of Chemical Physics, 145, 064108-1–064108-14, 10.1063/1.4959601.

VII Pae, Kaja; Hizhnyakov, Vladimir (2017). Ground state in $E \otimes e$ Jahn-Teller and Renner-Teller systems: Account of nonadiabaticity. Journal of Chemical Physics, 147 (8), ARTN 084107.10.1063/1.4986883.

Author's contribution

All the publications were developed in close collaboration with the listed researchers. All the calculations for $E \otimes e$ Jahn-Teller problem were performed by author of the thesis also the visualization and interpretation of the results of calculations (in addition to $E \otimes e$-problem, Publications I and II regarded also pseudo Jahn-Teller effect, which was studied by Taavi Vaikjärv). The author of the thesis contributed significantly to writing the manuscript of Publications III–VII.

PUBLICATIONS NOT INCLUDED IN THE THESIS

VIII Hizhnyakov, V.; Boltrushko, V.; Pae, K.; Vaikjarv, T. (2011). Zero-phonon lines: Novel manifestations of vibronic interactions in impurity centres of solids. Optika i Spektroskopiya, 111 (3), 398–406.

IX Hizhnyakov, V.; Pae, K.; Boltrushko, V.; Köppel, H. (2018). Vibronic states in conical intersections: manifestations of centrifugal energy and non-adiabaticity in optical spectra of Jahn-Teller systems. Journal of Physics: Conference Series, 1148, 012002.10.1088/1742-6596/1148/1/012002.

ABBREVIATIONS

APES	adiabatic energy surfaces
JTE	Jahn-Teller effect
PJTE	pseudo Jahn-Teller effect
RRS	resonance Raman scattering
RTE	Renner-Teller effect
RWA	rotating wave approximation
$J_1 = J$	rotational pseudomomentum (angular momentum of pseudorotation) for linear vibronic interaction
J_2	rotational pseudomomentum (angular momentum of pseudorotation) for quadratic vibronic interaction
$D = k_1^2/2$	Jahn-Teller stasbilization energy (for graphs and calculations it is represented in $\hbar\omega_0$ units)
k_1 and k_2	parameters of the linear and quadratic coupling
λ^2	phonon interaction strength
ω_0	frequency of the main (local) mode
ω_M	maximum value of the phonon frequency

1 INTRODUCTION

1.1 Coupling of electrons and vibrations

The mass of atomic nuclei or ions in molecules and solids exceeds the mass of electrons several thousands times. Born-Oppenheimer approximation utilizes this significant mass difference to effectively separate the motion of electrons and nuclei. In this approximation, it is assumed that the rapid motion of electrons instantaneously responds to the much slower motion of nuclei. This separation of time scales greatly simplifies the process of solving the Schrödinger equation and determining the wave function and energies of quantum states.

The Born-Oppenheimer approximation is sufficiently valid in conventional dielectric systems where the energy of the electronic state significantly differs from other electronic states, particularly in comparison to vibrational quanta. However, in many systems, electronic levels may have equal or close energy values. In such cases, the adiabatic approximation may fail due to electronic transition between these levels induced by electron-vibrational (vibronic) non-adiabatic interaction. The interplay between electronic and ionic motion gives rise to several important and intriguing physical phenomena, including phase transitions resulting from changes in external conditions, relaxation of electronic excitations and spins in a lattice, the electrical resistance of metals, superconductivity, ultrasonic attenuation, and others in extended systems and some less prominent phenomena in localized systems.[1]

Vibronic interaction, which refers to the coupling of electrons and vibrations, can be observed in spectra of optical absorption, Raman scattering, and relaxation of excited states of impurity centres, among others. When degenerate electronic and vibrational states are present in a molecular system or crystal, vibronic interaction leads to the Jahn-Teller effect (JTE). In such cases, electronically degenerate electronic states in molecular systems or crystals undergo spontaneous symmetry breaking, resulting in the splitting of energy levels and a lowering of the system's potential energy. If we neglect accidental degeneracy (i.e. degeneracy not caused by symmetry) then a degenerate electronic state is always consistent with some kind of symmetry in nuclear configuration.[2] In 1937 Hermann Arthur Jahn and Edward Teller formulated a theorem stating that all nonlinear nuclear configurations are unstable for an orbitally degenerate electronic state.[2] Jahn and Teller used group theory to prove the theorem, showing that there are nontotally symmetric normal displacements of nuclear configuration for all the symmetry groups corresponding to any degenerate electronic configuration.[2] As a result, the mechanism responsible for symmetry breaking in nonlinear molecular systems is known as the Jahn-Teller effect.

The instability induced by the Jahn-Teller effect is generally considered negligible if the degenerate electronic states are fully occupied and do not participate in the molecule's or ion's binding, such as degenerate electrons in inner atomic

shells and if perturbation caused by the displacements of nuclei is small. This effect is also absent when the highest occupied state (HOMO) is fully occupied. The extent to which the system's energy is lowered due to vibronic coupling is referred to as the Jahn-Teller stabilization energy E_{JT}, which serves as a signature characteristic of JTE. If $\frac{E_{JT}}{\hbar\omega} \approx 1$ (where $\hbar\omega$ is an energy quantum of a vibration involved in the coupling), then the presence of JTE is noticeable. If $\frac{E_{JT}}{\hbar\omega} \gg 1$, then a strong JTE is present in the system.

To explain JTE qualitatively one might say that it is an effect of the interplay between electronic states and vibrations: it involves mixing of electronic states by vibrations, and mixed electronic states in turn influence the nuclear motion, resulting in special coupled electron-nuclear dynamics. It appears, that such coupled dynamics influences all the properties of the polyatomic system.[3]

The distortion of the system may also occur in case of pseudo-degeneracy – that is the circumstance if energy gap between mixing electronic states is relatively small compared to the energy of the vibrational interaction.[3] This scenario is referred to as the pseudo Jahn-Teller effect (PJTE). Mixing of electronic and vibrational states and lowering of symmetry takes also place in linear molecules, but as a higher-order effect of quadratic vibronic interaction. Special feature of vibronic coupling in linear molecules is the lack of first order coupling. This symmetry-breaking effect is known as Renner-Teller effect (RTE). Typical examples of early study of RTE included compounds like CO_2, NH_2[4,5] etc.

It has been proved that any instability in high-symmetry configurations of any system originates from the Jahn-Teller effect (in the case of degenerate states), the pseudo Jahn-Teller effect (in the case of pseudo degenerate states), or Renner-Teller (in the case of degenerate states in linear systems).[3] The JTE theory is applicable not only to chemically bonded systems: mixing of electronic and vibrational states and corresponding instabilities may also appear in case of molecule formation from atoms, intermolecular interaction, and chemical reactions.[6,7] Structural transformations, even in these cases, are often considered as pseudo-Jahn-Teller effects, where electronic states of rather different energies become mixed due to strong vibronic interaction, leading to structural changes in molecules.

There exists a longstanding tradition of studying vibronic effects at the Institute of Physics of Tartu University. The investigation of impurity centres with vibronic coupling began in the 1960s and has continued to the present day. Key contributors to Jahn-Teller theory include Nikolai Kristofel, Vladimir Hižnjakov, Peet Konsin, Vello Loorits, Imbi Tehver, Teet Örd, Aleksei Sherman and Olev Sild. Much of this research builds upon the earlier work of these scientists. The 12th and 23rd Jahn-Teller Symposia were held in Tartu in 1994 and 2016, respectively.

1.2 The role of the Jahn-Teller effect in modern physics and current state of the art

Jahn-Teller effect plays a crucial role in explaining several topics in modern physics. According to the standard model, the symmetry breaking of the Higgs boson field is responsible for the appearance of non-zero masses of elementary particles.[8] This spontaneous symmetry breaking, associated with degeneracy or pseudodegeneracy, is something inherent to the physical universe.[7] The evolution of the universe after the Big Bang is governed by different types of spontaneous symmetry breaking.[3] In condensed matter, spontaneous symmetry breaking is typically realized through Jahn-Teller coupling[7], making it an origin of several specific properties of matter.

The Bardeen-Cooper-Schrieffer theory of superconductivity considers electron-phonon coupling of electron and phonon plane waves, but not local excitations, leading to the JTE. The rearrangement of the system induced by electron-phonon interaction does not occur in real space, but in the momentum (quasimomentum) space: Cooper pairs of charge carriers are formed in momentum space and in energy spectrum appears a gap (the order parameter). In case of broad-band metal with widely delocalized electrons the JT coupling is weak and may be neglected due to the fact that mean difference of energies of electrons is large compared to energy of phonon quanta.[3] In systems with narrow bands, such as high-temperature superconductivity, the JTE becomes significant,[3] resulting in many interesting phenomena like ferroelectric, ferromagnetic and combined phase transitions with complex temperature dependence.[9,10]

The important argument by Nobel Prize winner A. Müller in favour of the existence of high-temperature superconductivity (discovered by Müller) in cuprate superconductors was the Jahn-Teller effect, which is observed in cuprates and caused by the electron interaction with nontotally symmetric vibrations. This effect leads to a significant narrowing of the conducting bands, facilitating the phase separation at the nanoscale and markedly reducing the screening of the electric field associated with optical phonons. This decrease in shielding results in an enhanced electron-phonon interaction with these phonons and, in turn, to an increase in the critical temperature of superconductivity. Refs. 84–86 have demonstrated that unscreened long-range pairing may originate from both totally symmetric A_{1g} and nontotally symmetric B_{1g} phonons, with the A_{1g} phonons making the dominant contribution. Both interactions attract charge carriers, forming Cooper pairs. However, the contribution of short-range totally symmetric phonons is only partially attractive – charge carriers with similar energies are attracted to one another, while they repel each other in the opposite scenario. In contrast, the contribution of nontotally symmetric phonons is essentially different, primarily being attractive.[84–86] Hence, they may play a more significant role in pairing than short-range totally symmetric phonons. Therefore, considering the phonon-mediated pairing in superconductors it is essential to take into account

the symmetry of contributing phonons. This may be crucial for superconductors with open Fermi surfaces. In such crystals, several order parameters may coexist, even in single-band cases, potentially leading to the emergence of Leggett modes. Consequently, the Jahn-Teller effect can lower the symmetry of the order parameter.

In 2015 was reported a discovery of new type of state in matter, which was called Jahn-Teller metal, where a doped superconductor lattice showed conducting behaviour alongside Jahn-Teller distortion.[11] A superconductor Cs_3C_{60} lattice was doped with rubidium. The change of distance between the carbon-60 anions, caused by doping, changes the electronic properties of the system making the conducting band narrower. It was reported that as a result of the doping the insulator phase develops into a new state, where it is conducting and has Jahn-Teller distortion at the same time (localized electrons coexist with conducting ones (metallicity), and the on-molecule (local) distortion persists).[11]

Conical intersections of potential surfaces of vibronic systems with the Jahn-Teller or pseudo-Jahn-Teller effect are crucial for physical and chemical processes in solids. The main importance of conical intersection lies in the fact that the nonadiabatic interactions of valence electrons with phonons are strongly enhanced near the conical intersection. Understanding these nonadiabatic processes requires a nonperturbative account of nonadiabaticity and, therefore, belongs to the most fundamental problems of physical chemistry and chemical physics.

Vibronic coupling also plays a vital role in photophysics and photochemistry. For instance, the photostability of DNA and other biomolecules relies on ultrafast radiationless decay enabled by mixing excited electronic states. Initial ground state is reached by relaxation trough conical intersection(s), as a result UV photons are absorbed and conveyed into vibrations (heat).[12, 13] Organic matter is generally poorly resistant to UV radiation, and vibronic coupling near the conical intersections of these materials is the key mechanism for the loss of photostability.[14] Conical intersections direct relaxation to certain coordinates. Currently it is believed that vibronic coupling is also responsible for the effective energy transporting mechanism in photosynthesis.[15]

However, ultraviolet radiation can lead to illnesses like skin cancer due to the photochemical formation of thymine dimers in DNA chains.[16, 17] Note that the nuclear acids that make up DNA – adenine, guanine and cytosine – are the most resistant among nuclear acids to damage by ultraviolet radiation. Thymine, which also is present in DNA is less resistant – thymine dimers, which can be formed under the influence of ultraviolet radiation, can cause skin cancer. The formation of the thymine dimer in DNA is the result of the vibronic conversion of the photoexcited thymine molecule and the neighbouring thymine molecule into a chemically bound thymine pair. This transformation is accompanied by the emission of phonons into DNA and the environment; that is it is a result of electron-phonon coupling in vibronic system with degeneracy. A dimer presents a defect in DNA that disrupt DNA functioning and can cause diseases.

These examples highlight the diverse impact of the Jahn-Teller effect across various fields of physics and chemistry, and here are mentioned only a few. However, it can be argued[3] that this effect influences most areas of physics and chemistry in some manner.

2 AIM OF THE THESIS

2.1 Jahn-Teller effect in solids and phonon continuum of the bulk

Interactions between optical electrons and surrounding atoms, stemming from the cooperative motion of vibrational normal modes, give rise to electron-phonon interaction, commonly known as vibronic interaction. This is one of the most important interactions of molecular systems and impurity centres in crystals, fundamentally shaping their properties. In the case of degenerate or quasi-degenerate electronic states, this interaction leads to a crucial phenomenon – the Jahn-Teller effect.[1–11]

One of the most notable distinctions between the Jahn-Teller effect in crystals compared to molecules lies in the existence of a phonon quasi-continuum, including approximately Avogadro's number of modes. These modes contribute significantly to the electron-phonon interaction responsible for this effect.[3,18–23] The presence of this continuum renders existing methods tailored for molecular systems inadequate. However, the presence of this continuum also gives rise to a novel phenomenon in crystals compared to individual molecules – the irreversible nature of vibronic dynamics, leading to the relaxation of vibronic excitations. The aim of the thesis is to develop a method, which enables to calculate JTE effect in excited state of impurity centre of a crystal taking into account phonon continuum and, thereby, energy relaxation, and to use this method to study (optical) properties of the impurity centre.

Previous methods, including the multi-configurational time-dependent Hartree approximation[24–30] – an algorithm to solve time-dependent Schrödinger equation – have limitations in handling only a small number of vibrational coordinates. The primary constraint of this approximation lies in the exponential growth of calculations and inaccuracies as the number of vibrational coordinates increases. This turns impossible to use the method for describing the irreversible time evolution of the vibronic systems with a continuous energy spectrum and to take into account the long-range interactions, which essentially determine the vibrations in 3D systems.[Pub. II]

O'Brien proposed in Ref. 31 to replace the consideration of the multimode effects by the consideration of one efficient single JT active mode with an addition quadratic interaction of the mode. To exclude other modes, O'Brien proposed a set of $\sim N_{\mathrm{Avogadro}}$ equations to determine the parameters of the effective quadratic interaction. Unfortunately, it is not known how to solve this set of equations. O'Brien's approach is, in fact, the opposite of our approach, which aims to account for N_{Avogadro} modes, and thus account for energy relaxation. O'Brien's approach is to replace all N_{Avogadro} modes with one mode, which essentially means ignoring relaxation. Analogous to O'Brien idea, but with illuminating all except $N \sim 10$ modes was used in Ref. 32. However, this procedure is

completely inapplicable for describing all other, weakly and strongly excited states and does not provide anything for understanding phenomena such as the temporal evolution of the Jahn-Teller system, including vibrational relaxation.

Publications I–VI propose replacing linear vibronic interaction with quadratic vibrational interaction. Unlike O'Brien in these works $\sim N_{\text{Avogadro}}$ phonon coordinates are not illuminated, but they are explicitly taken into account. Specifically, it is demonstrated in **Publication II** that the Jahn-Teller linear vibronic interaction with non-totally symmetric modes of phonon continuum can be effectively replaced by the interaction of Jahn-Teller active vibrational modes with phonons. Taking into account the effects caused by the latter interaction is much simpler and can be done by standard methods of quantum field theory used to describe interactions in phonon continuum in crystals. As a result, the proposed transformation of the Jahn-Teller Hamiltonian of multimode systems enables the development of a completely quantum mechanical method (in **Publications I–III**). This method enables, for the first time, strict quantum mechanical calculations of relaxation of vibronic systems and the optical spectra of impurity centres in crystals and large molecules with the JTE in the excited state, while considering the non-totally symmetric phonon continuum. The method enabled for the first time the rigorous consideration of processes involving the phonon continuum, which is inevitably necessary for describing irreversible relaxation processes.

The method functions effectively when the contribution of phonons is weaker than the contribution of the main (local and pseudo-local) JT mode. It enables the consideration of an arbitrary vibronic interaction with a few (pseudo)local modes and weak interaction with an arbitrary number of other modes, including the $\sim N_{\text{Avogadro}}$ modes of the phonon continuum.[Pub. II] The method allows to consider the time evolution of vibronic system using stationary (localized) vibronic basis. Additionally, the method allows for the calculation of the time evolution of vibronic systems and their vibronic (optical) spectra by calculating the time evolution due to the Jahn-Teller effect in the excited electronic state. Replacing in this method the linear vibronic interaction with the phonon continuum by the quadratic interaction of the main Jahn-Teller active local (pseudo-local) modes with phonons allows for the division of the solution of the complex problem of simultaneously considering vibronic interactions with fundamental modes and phonons into two simpler problems of taking into account these mutual interactions in turn. At first, only the strong vibronic interaction with the main local modes is considered, which can be done numerically with high precision. Then, as a second step the interaction of these modes with phonons is considered, using numerically determined vibronic states as the basis. The proposed method is general. However, in the thesis calculations are carried out only for impurity centers with $E \otimes e$-problem – that is doubly degenerate vibrational mode is interacting with doubly degenerate electronic state.

The developed method is first applied to calculate absorption (in **Publication II**) and 1st and 2nd order Raman scattering spectra (in **Publication IV**) for

impurity centres of crystals with $E \otimes e$ JTE in excited state (in case of electronic transition from nondegenerate to twofold-degenerate state) taking phonon continuum into account.

It should be particularly noted that using this method, it became possible for the first time to consider the relaxation of vibronic systems through a conical intersection within a strictly quantum theory framework (in **Publication V**). In particular, the method can be used to study phonon-induced relaxation through conical intersection accompanied by the energy loss of the excited vibronic system to the bulk by emission of phonons. This process determines the chemical and photochemical transformations of molecules and impurity centres. Therefore it presents one of the most important phenomena caused by the vibronic interactions with phonon continuum (with $\sim N_{\text{Avogadro}}$ bath modes (phonons)) – the energy loss of the excited vibronic system. Note, that in majority of molecular systems the relaxation takes place, at least partly, by passing through the conical intersections of potential energy surfaces, which cannot be considered using the adiabatic approximation. Moreover, the passing through the conical intersection is accompanied by the enhancement of the effects of nonadiabaticity. The developed method takes this enhancement fully into account, allowing for the first time to give a rigorous fully quantum-mechanical solution of this problem (in **Publications V–VI**). Applying the method allows also to calculate time-dependence of the distribution function of the basic configurational coordinate and to visualize long-time range energy relaxation through the conical intersection. This enables to understand qualitatively the temporal dynamics of the system near conical intersection.

In **Publication V** relaxation from excited vibronic state with minimal rotational pseudomomentum (angular momentum of pseudorotation) $J = \left|\frac{1}{2}\right|$ was investigated taking into account only vibronic levels with $J = \left|\frac{1}{2}\right|$ as a possible relaxation path. In **Publication VI** relaxation from vibronic state with non-minimal value of the rotational pseudomomentum was considered, taking into account all vibronic levels with $J \geq \left|\frac{1}{2}\right|$ as a possible path for the radiationless energy relaxation.

2.2 Ground state of $E \otimes e$ vibronic systems and Renner-Teller systems

The symmetry of the ground state in $E \otimes e$ vibronic systems and Renner-Teller systems has been a longstanding subject of debate. **Publication VII** investigates, whether the ground state of JT $E \otimes e$-system is nondegenarete A_1-state or doubly degenerate E-state. The thesis aims to investigate the ground state and lowest excited state for various combinations of linear and quadratic coupling strengths.

According to the calculations, depending on the combination of the 1st and 2nd order vibronic interaction parameters, the ground state can be either nondegenerate A_1-state or doubly degenerate E-state. Additionally, the thesis calculates the parameter values necessary for the transition from a degenerate ground state to a nondegenerate one.

In his early works[33, 34] Bersuker proposed that for strong vibronic coupling, the ground state is nondegenerate A_1-state, while the first excited state is doubly degenerate E-state. O'Brien[35] studied tunnelling motion in an $E \otimes e$-system as the hindered rotation, finding that the ground state belongs to E-representation and the first excited state belongs to A_1-representation.[Pub VII] Similarly, Ham argued that ground state is E-state,[36] as the vibrational wave function changes the sign under 2π rotation in vibrational coordinates, indicating two states with opposite sign in the ground state. Berry's work[37] suggests that this sign change arises from a geometrical phase – electronic part of the wave function changes sign due to the vibronic coupling if transported around a circuit. That is, with such a turn of the deformation, the system goes into another state. This is possible if this other state exists.

It is important to note that the geometrical phase described by Berry has clear meaning in adiabatic approximation: i.e. if electronic wavefunction parametrically depends on the coordinates of nuclei.[37] This requirement is well met if the system is far from degenerate configuration. However, in cases of significant nonadiabaticity, such as near the conical intersection, the concept of the Berry phase may become less effective.[Pub VII] Therefore, Ham's explanation holds in the adiabatic approximation.

As a result of studies by O'Brien and Ham it was believed that the symmetry of the ground state of the vibronic system is the same as the symmetry of the initial electronic state. But in 1996 it was shown by Moate et al.[38] and Manini et al.[39] that in JT $H \otimes h$-problem in case of some vibronic interaction strength the ground state is nondegenerate. Koizumi and Bersuker[40] later showed that the same holds for $E \otimes e$-systems if dynamical instability is removed by positive quartic anharmonicity. They considered the cases with the first, the second and, the fourth order terms. Koizumi and Bersuker found that in case of strong quadratic coupling, the system exhibits four conical intersections. As the wavefunction of the ground state moves far from the conical intersections and coupling is strong, then the adiabatic approximation is fulfilled and the electronic wave function does not change the sign after the circular transportation, which means that ground state is nondegenate.[41]

Bersuker's and Koizumi's work, along with subsequent studies by several authors,[3, 42–46] has led to the conclusion that in the adiabatic approximation, the ground state is degenerate if the dominant motion occurs around an odd number of APES (adiabatic potential energy surface) conical intersections and nondegenerate if the number is even. However, the boundary values of the linear and quadratic vibronic coupling parameters corresponding to the transition from a

doubly degenerate ground state to a nondegenerate one remained unresolved. To solve this problem, it is necessary to perform calculations of the ground and first excited vibronic states with full consideration of non-adiabaticity. This problem is addressed as one of the aims of the thesis.

3 $E \otimes e$-PROBLEM

3.1 Linear and quadratic vibronic interaction

In case of $E \otimes e$-problem, a doubly degenerate electronic state E becomes coupled by a doubly degenerate vibrational mode e. There are several other types of Jahn-Teller systems, such as: $T \otimes e$, $T \otimes t_2$, $T \otimes (e + t_2)$, $T \otimes h$, $G \otimes (g + h)$, just to name some more common. Here T or t denote triple degeneracy (electronic and vibrational respectively), G or g for fourfold degeneracy, and h for fivefold degeneracy. As mentioned in the introductory part of the thesis, the symmetry of the system's configuration is the reason for degenerate states (there might also be accidental degeneracies, but those are not the focus of interest in the current thesis). The symmetries of configurations that produce degenerate terms are known from group theory.[3] Interaction of electrons of nondegenerate electronic states and nucleus can only cause totally symmetric displacements of nuclear configuration, thus not affecting the symmetry of the system.[3] However, electrons of degenerate electronic states distort the nuclear configuration, producing non-totally symmetric distortions, which are predicted by the Jahn-Teller theorem.[3]

Molecules and impurity centres with C_3-symmetry axis and doubly degenerate electronic state possess the $E \otimes e$-problem. This includes triangular, triangular-pyramidal, tetrahedral, octahedral, cubic, icosahedral, pentagonal, and hexagonal molecular systems. The thesis studies three types of vibronic interaction, which may occur in these systems: 1) linear vibronic coupling, 2) purely quadratic vibronic coupling, 3) linear and quadratic vibronic coupling. In most cases, to describe the special effects in molecular system caused by vibronic interaction, it is enough to take into account linear and quadratic terms of coupling.

If there is no vibronic coupling, the electronic wave function is independent of the nuclear coordinates, which means that Born-Oppenheimer approximation can be applied. In case of linear vibronic coupling, there is a correlation between electronic and vibrational motions. In this case, potential energy has axial symmetry in the space of coordinates of the Jahn-Teller active two-fold degenerate e-modes. The vibronic states here are characterized by half-integer quantum number of pseudorotations. If the linear vibronic coupling is very weak, then, qualitatively speaking, the system still vibrates in essentially the same manner as in case of lack of vibronic coupling , but the vibratory motion causes small mixture of partner degenerated electronic states.[1] In the case of significant linear vibronic coupling, the distorted configuration of the system rotates, entraining electronic states with the rotation of the distortions.

In Fig.1, a triatomic molecule and its configuration changes in physical space are depicted. Circles denote the trajectory of rotating nuclei for first order vibronic coupling. In case of quadratic vibronic coupling, the nuclear motions take place in the neighbourhoods of three potential minima, which are denoted as bold points.[1] The system moves from one potential minima neighbourhood to another via a tunnelling process.[1]

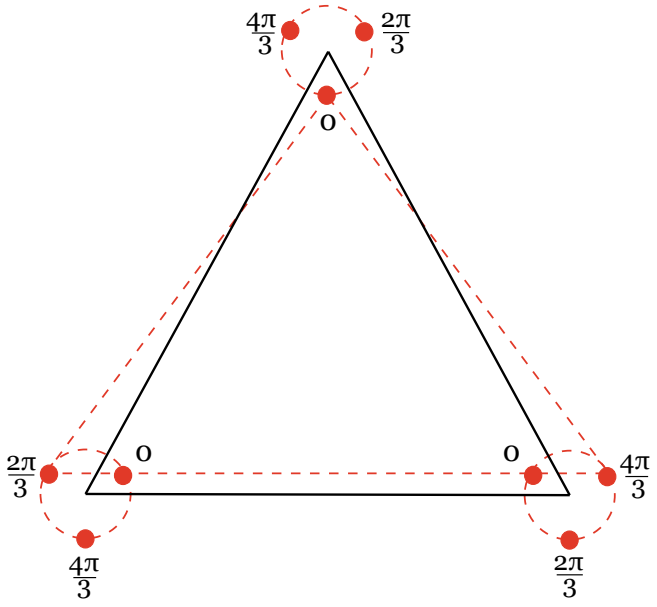

Fig. 1. Distortions of triatomic molecule X_3. First order vibronic coupling causes atoms to move along the circles. In APES of the linear $E \otimes e$-problem it means moving along the bottom of the trough of the lowest sheet – see Fig. 2. Taking second order coupling into account can be found minima denoted with bold points. The dashed triangle corresponds to the point $Q_\varepsilon = 0$, $Q_\theta = \rho$ in Fig. 3.[3]

When only linear coupling occurs, all vibronic states are doubly degenerate (analogue of Kramers degeneracy). If linear and quadratic vibronic coupling is present, there also exist nondegenerate states whose behaviour is similar to electronic (orbital) singlets.[1]

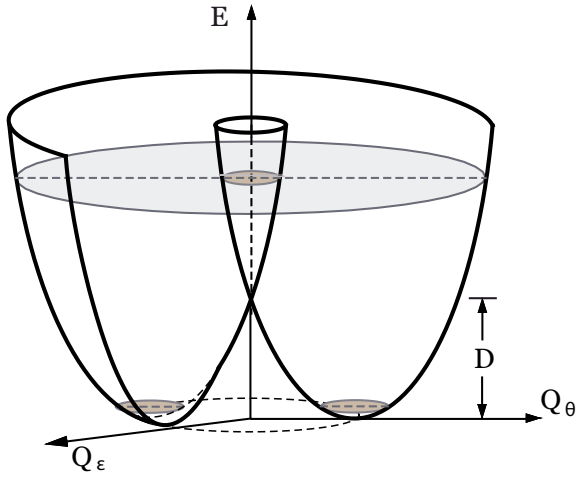

Fig. 2. Potential energy surface of linear $E \otimes e$-problem: doubly degenerate electronic state E interacting linearly with a doubly degenerate vibrational mode e.

A common example of Jahn-Teller $E \otimes e$-problem are octahedral complexes. Vibronic interaction causes for octahedral complex a tetragonal distortion – compressing (or extending) the complex along one of the three fourfold axes and at the same time extending (or compressing) along the other two axes.[3] The tetragonally extended configuration coincides with the minima in the bottom of the warped "Mexican hat" APES and compressed configurations corresponds to the maxima (saddle points).[47] The states associated with the upper potential have been interpreted as representing a motion in which the electronic part is out of phase with the nuclear coordinates,[48] as the nuclear angle changes twice as quickly as electronic angle, while in lower potential, the electronic and nuclear part move in phase.[1]

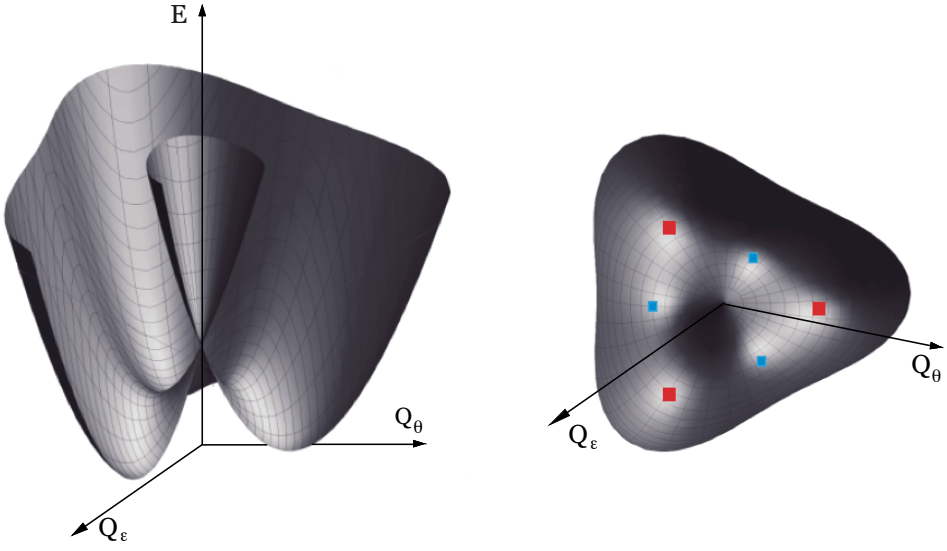

Fig. 3. Potential energy surface of $E \otimes e$ Jahn-Teller system with quadratic vibronic interaction. Right: bottom view of the potential, three minima are denoted with red squares in which the low energy motion is concentrated, and three saddle points are denoted with blue squares.

The eigenstates of the vibronic $E \otimes e$-system are used as a basis to solve several problems in the thesis. Eigenvectors and eigenvalues for $E \otimes e$-problem were found by Longuet-Higgins et al.[49] The following is an overview of the principles how the eigenvalue problem was solved in Refs. 3 and 49.

The vibronic Hamiltonian[3] of Jahn-Teller $E \otimes e$-problem is

$$H = H_0 \cdot I + \hat{V}_1 + \hat{V}_2 . \tag{1}$$

Here H_0 is the Hamiltonian of the two-fold degenerate *e*-vibrations, which is Hamiltonian of two-dimensional harmonic oscillator

$$H_0 = -\frac{1}{2}\left(\frac{\partial^2}{\partial Q^2} + \frac{\partial}{Q\partial Q} + \frac{\partial^2}{Q^2\partial\varphi^2}\right) + \frac{Q^2}{2}, \tag{2}$$

where Q and φ are the polar coordinates of the oscillator. I is 2 × 2 unit matrix, $\hat{V}_1$ and $\hat{V}_2$ are the operators of the linear and quadratic vibronic coupling. In the basis of electronic states $|\pm 1/2\rangle_e$ of *E*-representation with pseudomomentum half these operators can be presented as follows:

$$\hat{V}_1 = k_1 Q\left(\sigma_1 \cos\varphi + \sigma_2 \sin\varphi\right), \qquad \hat{V}_2 = \left(k_2/2\right)Q^2\left(\sigma_1 \cos 2\varphi - \sigma_2 \sin 2\varphi\right), \tag{3}$$

where σ_i are Pauli matrices, k_1 and k_2 are the parameters of the linear and quadratic coupling.[Pub VII] k_1 and k_2 are signature parameters of JTE – they characterize the measure of coupling between the electronic structure and nuclear displacements, i.e, the measure of influence of the nuclear displacements on the electron distribution and, conversely, the effect of the changes in the electron structure upon nuclear dynamics.[3] k_1 and k_2 can be taken to be positive. For the sake of simplicity for the calculations is taken $\hbar = \omega_0 = 1$, where ω_0 is the frequency of the main oscillating mode.

In case of linear $E \otimes e$-problem, the unperturbed system is a dimeric oscillator with energies $E_n = \hbar\omega_0(n + \frac{1}{2}), n = 0,1,2,...$. The angular momentum of the nuclei is defined by the quantum number $m = n, n-2, ..., -n+2, -n$. Eigenstates of unperturbed Hamiltonian H_0 are described with two quantum numbers $|n, m\rangle$. Eigenstates of linear vibronic Hamiltonian $H = H_0 \cdot I + \hat{V}_1$ are described also with two quantum numbers $|v, J_1\rangle$.[49] The vibronic energy level quantum number $v = 0, 1, 2,...$ is an analogue to the quantum number n. The total angular momentum of the electrons and nuclei is defined by quantum number of pseudo-rotation $J_1 = m \pm \frac{1}{2}, m = 0, \pm 1, \pm 2, ...$ (the effective angular momentum of the electrons in the doubly degenerate state is defined by quantum numbers $\pm\frac{1}{2}$).[3] J is preserved in case of linear vibronic intearaction. The operator $\hat{V}_1$ commutes with the momentum operator $\hat{J}_1 = -i\partial/\partial\varphi + \sigma_3/2$ and has half-integer eigenvalues $J_1 = \pm\frac{1}{2}, \pm\frac{3}{2}, \pm\frac{5}{2}, ...$[49] Operator $\hat{V}_1$ couples the vibrational states of harmonic oscillator in the way indicated by broken lines in Fig. 4.

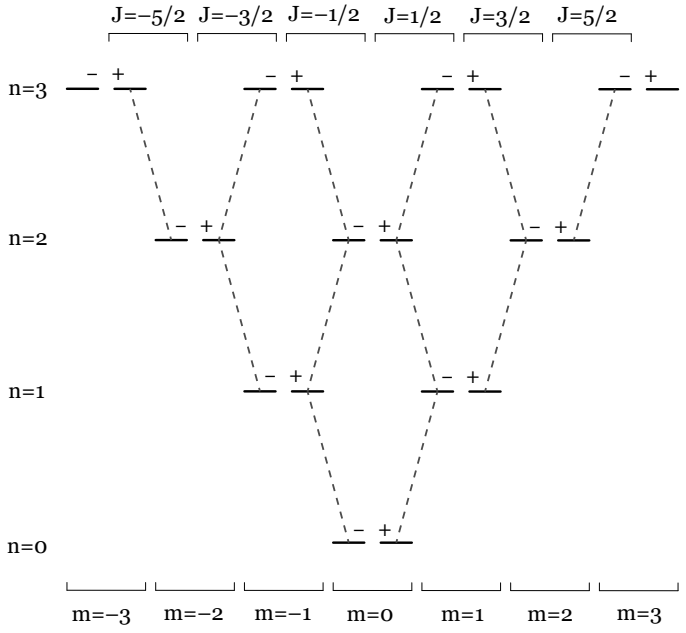

Fig. 4. Coupling diagram of vibrational levels of harmonic oscillator in case of linear vibronic interaction. Horizontal lines are energy levels of harmonic oscillator. Broken lines connect the states coupled by operator $\hat{V}_1$ in Eq. (1). "+" and "–" denote electronangular momentum $\pm\frac{1}{2}$.[49]

H and $\hat{J}_1$ commute, therefore they have common eigenvectors $|v\rangle$
H $|v\rangle = E|v\rangle$, $\hat{J}_1|v\rangle$, and eigenvectors $|v\rangle$ can be presented in the form

$$|v\rangle = \begin{pmatrix} |v+\rangle e^{i(J_1-1/2)\varphi} \\ |v-\rangle e^{i(J_1+1/2)\varphi} \end{pmatrix}. \tag{4}$$

To find the eigenstates of vibronic system, we need to find solutions for the following vibrational equation:

$$\left(H_0 \cdot I + \hat{V}_1\right)\begin{pmatrix} |v+\rangle \\ |v-\rangle \end{pmatrix} = E_v \begin{pmatrix} |v+\rangle \\ |v-\rangle \end{pmatrix}. \tag{5}$$

We use eigenfunctions of harmonic oscillator as a bases and get for $J_1 > 0$ the eigenstates of $H_0 \cdot I + \hat{V}_1$:

$$|v_J\rangle = \sum_n C_{2n;v,J}\,|2n+J-1/2, J-1/2\rangle|+\rangle_e + C_{2n+1;v,J}\,|2n+J+1/2, J+1/2\rangle|-\rangle_e. \tag{6}$$

The amplitudes $C_{l,v}$ and the energies E_v are the solutions for the following matrix equation,[49] it can be solved numerically, using several hundres[32, 50, 51] or thousands[52, 53] basic vibrational states:

$$\begin{pmatrix} J+1/2 & \sqrt{(2J+1)D} & 0 & 0 & 0 \ldots \\ \sqrt{(2J+1)D} & J+3/2 & \sqrt{2D} & 0 & 0 \ldots \\ 0 & \sqrt{2D} & J+5/2 & \sqrt{(2J+3)D} & 0 \ldots \\ \ldots & \ldots & \ldots & \ldots & \end{pmatrix} \begin{pmatrix} C_0 \\ C_1 \\ C_2 \\ \ldots \end{pmatrix} = E \begin{pmatrix} C_0 \\ C_1 \\ C_2 \\ \ldots \end{pmatrix}. \quad (7)$$

Here $D = k_1^2 / 2\omega_0$ is known as the Jahn-Teller stabilization energy, which corresponds to the depth of the JT potential in the representation of normal coordinates (see Fig. 2). In my bachelor's thesis,[53] several vibronic energy spectra were calculated in case of $J_1 = \frac{1}{2}, \frac{3}{2}, \frac{5}{2}, \frac{7}{2}, \frac{9}{2}$ and $D = 0.1, 0.6, 1, 2, 3, 10, 100, 400, 1000, 10000$. The energy of a vibrational quantum is typically ~0,01 *eV*–0,05 *eV*. For a vibronic interaction strength of $D = 100$, the vibronic interaction energy is ~1 *eV* – 5 *eV*. In this order is the vibronic interaction energy in case of electronic transition from *p*-orbital to *d*-orbital. If the transition occurs from an *s*-orbital to a *p*-orbital, the vibronic coupling energy can be up to 5 *eV*.

Linear and quadratic coupling parameters of the vibronic interaction are independent; the quadratic coupling is not necessarily insignificant compared to the linear coupling. If the quadratic coupling is sufficiently large, the form of the APES changes essentially – besides the central conical intersection, three lateral conical intersections also occur.[3] Such quadratic coupling affects the spectral properties and the tunnelling splitting of the system.[3] The ground state of the $E \otimes e$-system depends on the strength of linear and quadratic coupling. It can be either doubly degenerate *E*-state or nondegenerate state of A_1-representation. This issue and the calculation of eigenstates of quadratic vibronic coupling are discussed in Section 3.4 and **Publication VII**.

3.2 $E \otimes e$-problem and conical intersections in experiment

There are various methods to detect vibronic interaction. If a molecule undergoes Jahn-Teller distortion, the symmetry of the molecule is reduced, and this is manifested in UV-VIS absorption spectra as the splitting of bands. It can also be observed with IR and Raman vibrational spectroscopy.[54] Today, the most common methods to detect vibronic coupling are the laser-induced florescence (LIF) spectroscopy (enabling the study of JTE in the excited electronic state) and laser-excited dispersed fluorescence (LEDF) spectroscopy (for studying the ground electronic state).[55, 56]

As was mentioned above, molecules and impurity centres with a C_3-symmetry axis and a doubly degenerate electronic state exhibit the $E \otimes e$ JT effect. A wide range of such systems has been studied experimentally, as the Jahn-Teller effect is an important feature for determining the properties of these systems. Probably the most extensively studied are molecules of the $E \otimes e$ JT problem in trimers X_3 with general form: like H_3, O_3, Ag_3, Cu_3, Au_3, and many others. A detailed review of investigations of Jahn-Teller effect in such molecules is given in Ref 6. Sufficiently complete data also exist for CX_3Y molecules. There are also numerous experimental studies of MX_3-type molecules, C_3H_3, XCH_3, XCD_3, XCF_3-type molecules, and molecules with benzene cationе.[6]

There are also experimental studies of impurity centres in crystals with $E \otimes e$-problem, especially for *Cu(II)* octahedral complexes in various crystals. Ultrasonic experiments, applicable to any JTE problem, have been used to determine vibronic parameters of JTE, such as the linear vibronic constant k_1, and as a result, APES for the impurity centre with JTE were reconstructed.[57, 58] Temperature-dependent ultrasound attenuation and phase velocity measurements were applied.[57, 58] For example, in Ref 57, $ZnSe{:}Fe_2+$ with $E \otimes e$-problem was studied.

As mentioned in the introduction, conical intersections are crucial to explain photophysical and photochemical properties, which has made them a focus of experiments in recent decades. Ultrafast femtosecond spectroscopy techniques like time-resolved pump-probe photoelectron spectroscopy make it possible to study dynamics around conical intersections.[59] In Ref. 60, the relaxation of XUV-excited benzene cation with a VIS/NIR pulse was studied. Two fast relaxation timescales (11 ± 3 fs and 110 ± 20 fs) were measured, which were interpreted as passing two sequential conical intersections.

A good review of recent (experimental) works on the JTE can be obtained in the proceedings of the latest Jahn-Teller symposia.[61, 62]

3.3 Slonczewski resonances

Slonczewski has shown in his paper[63] that quasi-stationary states exist above the conical intersection inside the conical area of the potential. These states involve collective motion of electrons and nuclei in which the instantaneous distortion of nuclear configuration is opposite in sense to the static distortion appropriate to the instantaneous electronic state[63], i.e., the electronic part is out of phase with the nuclear coordinates. If the system moves on the upper branch of the APES, then the Jahn-Teller distortional forces are balanced by pseudocentrifugal forces[63] (here vibrational motion becomes pseudorotational motion), while motion on the lower part of APES is elastically stabilized. Quasi-stationary states of the upper potential, termed Slonczewski resonances, owe their stability to the steep walls of the inner conical part of the potential, resulting in a higher movement frequency compared to the main vibrational frequency. Hence, the impact of non-adiabaticity on corresponding motion remains relatively minor.

The thesis explores the relaxation from Slonczewski resonances to closely located levels of the external potential, rather than through Slonczewski resonances located relatively far away. This is due to the fact that in cases of strong vibronic interaction, the steepness of the potential energy within the upper inner part, or conical section, is significant (see Fig. 2 and Fig. 17 left). Consequently, quantum motion within this conical region results in the emergence of high-energy quantum levels. Slonczewski resonances play a dominant role in governing the quantum dynamics of the excited Jahn-Teller state. The current thesis demonstrates that they give rise to several intriguing purely quantum mechanical effects.

The quantum states corresponding to Slonczewski resonances can be approximated by considering only the central conical part of the potential energy. The energies and wave functions of these resonances can be derived by quantizing states within such a truncated potential, using the boundary condition of reversing the wave function to zero for a zero value of the radial coordinate. Although motion within the upper inner part of the potential interacts with the motion outside it, this interaction is weak in the case of strong vibronic coupling and can be neglected. As the vibronic interaction strength increases, the truncated part of the potential moves further away from the central conical part, resulting in reduced interaction between the inner and outer parts of the adiabatic potential energy surface (APES) and minimizing the truncation effect on the states within the conical intersection.

Fig. 5 illustrates the absorption spectrum[53] of the $E \otimes e$ Jahn-Teller problem, calculated using the eigenvalue problem defined by Eq. (7). The lines within the spectrum for $E > 0$ (inside the cone of the potential) belong to the upper branch of the potential, while line groups in the region $20 < E < 50$ denote Slonczewski resonances.

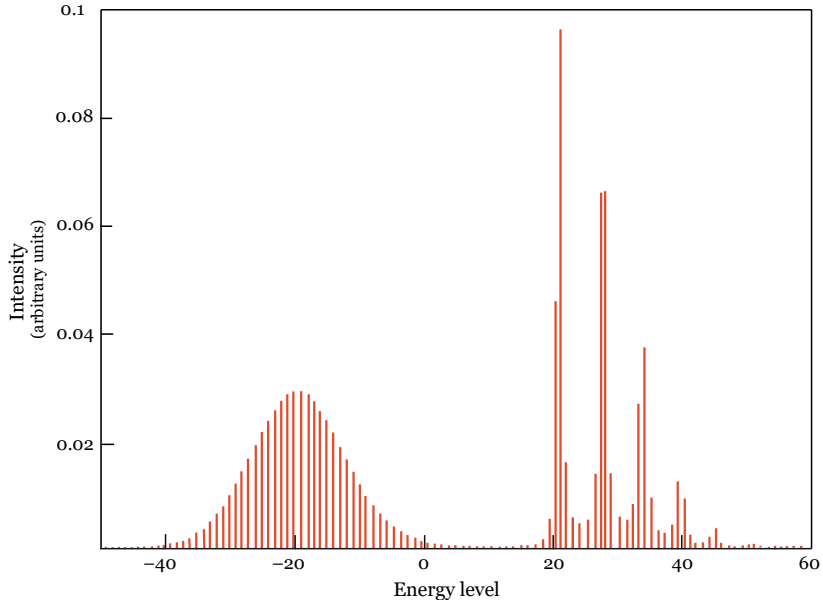

Fig. 5. Absorption spectrum for $D = 100$, $J = 5/2$, $n = 2000$. Stronger vibronic interaction increases the number of the resonances. Increasing pseudomomentum J means that resonances are more distinctively grouped, shifted upwards in the potential and the number of resonances is also bigger. Zero level of potential energy is taken to intersect the conical intersection.

To describe Slonczewski resonances, the wave function of the vibronic state corresponding to Slonczewski resonances with the given J is presented in the form

$$\psi = \xi^{-1/2} \begin{pmatrix} F(\xi) e^{i(J-1/2)\varphi} \\ G(\xi) e^{i(J+1/2)\varphi} \end{pmatrix},$$

where ξ is the radius and $\phi = -(1/2)\arctan(2k\xi^2/J)$ is the angle of the polar coordinates of the wave function.[Pub VI] We get the following equation for the wave functions[49]

$$\left(H_{0J} + K - E \cdot I\right)\Psi = 0,$$

where

$$H_{0J} = \frac{1}{2}\left(-\frac{d^2}{d\xi^2} + \xi^2 + \frac{J^2}{\xi^2} + \left(\frac{d\phi}{d\xi}\right)^2 + U_0\Theta(-\xi)\right)\cdot I + \sqrt{\left(\frac{J^2}{2\xi^2}\right)^2 + k^2\xi^2}\begin{pmatrix} 1 & 0 \\ 0 & -1 \end{pmatrix}. \quad (8)$$

Here and below $\begin{pmatrix} 0 & 1 \\ 1 & 0 \end{pmatrix} = \sigma_x$, $i\begin{pmatrix} 0 & 1 \\ -1 & 0 \end{pmatrix} = \sigma_y$, $\begin{pmatrix} 1 & 0 \\ 0 & -1 \end{pmatrix} = \sigma_z$ are Pauli Matrices.

The diagonal part of the Hamiltonian of the radial motion $(H_{0J})_{11}$ describes the vibronic states of the system above the conical intersection in the adiabatic approximation.[Pub VI] Off-diagonal operator K describes non-adiabatic effects:

$$K = \frac{3J\kappa}{2}\left[\frac{\xi^2}{J^2 + 4k^2\xi^6}, \frac{d}{d\xi}\right]_+ \begin{pmatrix} 0 & 1 \\ -1 & 0 \end{pmatrix},$$

here $[...]_+$ is anticommutator.[Pub VI]

3.3.1 Results

In the thesis are found:

1) the energies of the Slonczewski resonaces (**Publication VI**, Section 3.3.1),
2) their contribution to the relaxation process (**Publication V**, Chapter 6),
3) speeding up of pseudorotation due to Slonczewski resonaces (**Publication VI**, Chapter 7).

1) Energies of the Slonczewski resonaces.

By using the diagonal term $(H_{0J})_{11}$ of Hamiltonian in Eq. (8). the stationary Schrödinger equation for the excitations inside the conical intersection can be obtained:

$$\left(-d^2/dr^2 + r - \varepsilon + u_0\Theta(r)\right)F = 0, \quad u_0 \to \infty. \tag{9}$$

For $r > 0$, this is equation of quantum motion in the presence of constant force. Therefore for $r > 0$ the solution of this equation is the Airy function.[64]

$$F(\omega) = \frac{1}{\sqrt{\pi}}\int_0^\infty \cos\left(\frac{u^3}{3} + \omega u\right)du, \quad \omega = r - \varepsilon. \tag{10}$$

The border condition $F = 0$ for $r \le 0$ defines the allowed values of ω. The first 10 values of ω_n are: –2.34, –4.09, –5.52, –6.79, –7.95, –9.02, –10.04, –11.01, –11.94, –12.83.[Pub VI]

The presented values of ω_n determine the energies of the Slonczewski resonances $E_{D,J}^{(0,n)} = -\omega_n D^{1/3}$ in the zeroth approximation, which does not take into account the pseudorotation term $J^2/2\xi^2$ and the potential energy term $\xi^2/2$. Taking these terms into account in the first order of the perturbation theory, we get the following energy corrections:

$$\delta E_{D,J}^{(n)} = \int_{\omega_n}^{\infty} F^2(\omega)\left(\frac{J^2 D^{1/3}}{(\omega_n-\omega)^2} + \frac{(\omega_n-\omega)^2}{4D^{1/3}}\right)d\omega \Bigg/ \int_{\omega_n}^{\infty} F^2(\omega)d\omega. \qquad (11)$$

As a result, the energies of the resonances are:

$$E_{D,J}^{(n)} = \left(-\omega_n + \eta_n J^2\right) D^{1/3} + C_n D^{-1/3}, \qquad (12)$$

where $D = k^2/2$ is the Jahn-Teller stabilization energy, n is order number of the Slonczewski resonance, ω_n (n = 1,2,3,...) are energies of the Airy function with zero values at the origin, η_n are the dimensionless parameters of the order of unity. In Eq. (12) the term ηJ^2 describes the dependence of the resonance energy on the pseudorotation momentum, while the $\propto C_n$ term takes into account the potential energy $\xi^2/2$. The first 3 values of ω_n are: $\omega_1 = -2.34$, $\omega_2 = -4.09$, $\omega_3 = -5.52$. The corresponding values of the parameters η_n and C_n are equal to: $\eta_1 = 1.12$, $\eta_2 = 0.82$, $\eta_3 = 0.70$, $C_1 = 0.13$, $C_2 = 1.4$, $C_3 = 3.0$.[Pub VI] Additional values of ω_n, η_n and C_n are given in Appendix B of Pub VI. The values of the resonance energies corresponding to above ω_n, η_n and C_n are presented in Table 1. Numerical calculations given in the thesis show that these states play an essential role in relaxation through the conical intersection.

Table 1. Energies of the Slonczewski resonances.[Pub VI]

	Theory (Eq. (12))				Calculations[53]			
	$E_{D,J}^{(1,T)}$				$E_{D,J}^{(1,C)}$			
D\J	1⁄2	3⁄2	5⁄2	9⁄2	1⁄2	3⁄2	5⁄2	9⁄2
10	5.3 (5.0)	8.5 (7.7)	11.0 (9.5)	15.7 (13.0)	6	8	10	13
100	13.4 (12.8)	18.5 (16.4)	23.6 (20.3)	33.9 (28.0)	13		20	
400	21.3 (20.3)	29.4 (26.3)	37.5 (32.3)	53.7 (44.5)	20	26	32	44
1000	28.9 (27.5)	39.9 (35.7)	50.9 (43.9)	72.9 (60.3)	27	35		60
	$E_{D,J}^{(2,T)}$				$E_{D,J}^{(2,C)}$			
D\J	1⁄2	3⁄2	5⁄2	9⁄2	1⁄2	3⁄2	5⁄2	9⁄2
10	10.3	12.7	15.0	17.4	10	12	14	17
100	21.2	26.4	31.2	36.6	21	27		
400	33.2	41.7	49.3	57.9	32	39	45	55
1000	45.1	56.4	61.7	78.3	44	54		71
	$E_{D,J}^{(3,T)}$				$E_{D,J}^{(3,C)}$			
D\J	1⁄2	3⁄2	5⁄2	9⁄2	1⁄2	3⁄2	5⁄2	9⁄2
10	14.1	15.6	17.17	20.1	11			19
100	27.9	31.1	34.3	40.8	27		33	
400	43.6	48.8	54.0	64.3	43	49	52	63
1000	59.0	66.0	723.0	86.9	59	65		86

2) Contribution of Slonczewski resonaces to relaxation process.

The thesis investigates the influence of Slonchewski resonances on the relaxation of the distribution function in the case of quasi-monochromatic excitation of an impurity center with $E \otimes e$ JTE in an excited state. The parameters of the study are outlined in Capter 6 and in **Publication V**. Here are summarized some results from this study concerning the properties of the Slonczewski resonances. Relaxation occurs through the emission of phonons into the bulk. Initially, relaxation from vibronic levels $|v > 0, J = 1/2\rangle$ was examined, with the condition that relaxation path passes through the vibronic levels $|v > 0, J = |1/2|\rangle$ (in **Publication V**). The time evolution of the distribution function was calculated for various strengths of vibronic interaction. Detailed discussion on the calculation method and results for this type of relaxtion can be found in Chapter 6.

According to calculations, the evolution of distribution function in the region of small configurational coordinate Q exhibits a non-monotonous dependence on time due to the Slonczewski resonance (Fig. 18). When the most intense line in a Slonczewski resonance (in a line group) or the next line to the right (within the same group) is excited, the distribution function spreads wider initially, and the maximum of distribution function is reached later (e. g Fig. 18 c, d, e, and h, i, j).[Pub V] Conversely, if the level to the left of the most intense vibronic line in the Slonczewski group is excited, the maximum of the distribution function is attained at zero time and zero configurational coordinate value (e. g Fig. 18 a, b, and f, g).[Pub V]

3) Speeding up of pseudorotation due to the resonaces.

As a next step, the relaxation processes of various cases were calculated: relaxation of purely rotating states $|v = 0, J > 1/2\rangle$, combined vibrational-rotational states $|v > 0, J = 1/2\rangle$, and relaxation of vibronic levels $|v > 0, J > 1/2\rangle$ (in **Publication VI**). The details of relaxation and the calculation method are discussed in more detail in Chapter 7.

Two purely quantum mechanical effects were discovered, which lack analogues in classical physics. Firstly, in the vicinity of the resonances, there is an increased probability that in the course of relaxation the vibronic levels with bigger rotational pseudomomentum compared to the initial level's pseudomomentum become populated. This means that the pseudorotation speeds up in the course of relaxation (Fig. 29). Secondly, calculations indicate a higher probability near the Slonczewski line group for the change in the direction of pseudorotation – the rotational pseudomomentum of the final state has opposite sign compared to the initial state. [Pub VI]

3.4 Ground state in Jahn-Teller and Renner-Teller systems

In **Publication VII**, an algorithm was developed to address the longstanding question regarding the symmetry of the ground state in $E \otimes e$ Jahn-Teller problem: whether it is degenerate E-state or nondegenerate A_1-state. The symmetry of the ground state is a crucial property for understanding the measured results of the system. The thesis investigates the ground and lower excited states of the $E \otimes e$ Jahn-Teller system with linear and quadratic vibronic coupling, considering nonadiabaticity.

To calculate vibronic states, second quantization is applied:

$$H_0 = (\hat{a}_+^+\hat{a}_+ + \hat{a}_-^+\hat{a}_- + 1)\cdot I,$$
$$\hat{V}^{(1)} = k_1\begin{pmatrix} 0 & \hat{a}_+ + \hat{a}_-^+ \\ \hat{a}_- + \hat{a}_+^+ & 0 \end{pmatrix},\ \hat{V}^{(2)} = \frac{k_2}{2}\begin{pmatrix} 0 & (\hat{a}_+^+ + \hat{a}_-)^2 \\ (\hat{a}_-^+ + \hat{a}_+)^2 & 0 \end{pmatrix}, \tag{13}$$

here $\hat{a}_\pm$ and $\hat{a}_\pm^+$ are the destruction and creation operators of phonons with momentum ±1. In the second quantization basis, the linear vibronic interaction of the $E \otimes e$-problem has a simple structure: represented by purely non-diagonal 2×2 matrixes with non-diagonal elements given by operator $\hat{a}_+ + \hat{a}_-^+$ and its conjugated operator $\hat{a}_+^+ + \hat{a}_-$. From the structure of quadratic vibronic interaction $V^{(2)}$ it follows that consideration of this interaction can be essentially simplified if we extract consisting $\hat{a}_-^+\hat{a}_+$ and $\hat{a}_+^+\hat{a}_-$ terms conserving the number of phonon excitation. Due to this conservation law these interaction terms can be taken into account analytically using proper vibrational basis. This essentially simplifies the calculations of effects caused by the quadratic vibronic interaction $V^{(2)}$. Considering only operators $\hat{a}_-^+\hat{a}_+$ and $\hat{a}_+^+\hat{a}_-$ corresponds to rotating wave approximation (RWA). The calculations are made by using the wave functions in the rotating wave approximation (RWA) as the basis states.

As was mentioned above, the operator $\hat{V}_1$ commutes with the momentum operator $\hat{J}_1 = -i\partial/\partial\varphi + \sigma_3/2$ and has half-integer eigenvalues $J_1 = \pm\frac{1}{2}, \pm\frac{3}{2}, \pm\frac{5}{2}, \ldots$.[49] The operator $\hat{V}_2$ commutes with the momentum operator $\hat{J}_2 = -i\partial/\partial\varphi + \sigma_z$ and has integer eigenvalues $J_2 = 0, \pm1, \pm2, \ldots$.[41] In the basis of the eigenstates of $\hat{J}_1$ operator $\hat{V}_1$ conserves momentum J_1 and operator $\hat{V}_2$ describes the processes with the change in the momentum J_1 by ±3. As in this basis operator $\hat{V}_1$ describes the creation/destruction of electronic excitation with the unit momentum simultaneously with the creation/destruction of a phonon with the unit momentum of the opposite sign and operator $\hat{V}_2$ describes the creation/destruction of electronic excitation with the unit momentum simultaneously with the creation/destruction of two vibrational quanta with two units of the momentum of the same sign.[Pub VII]

Therefore, in the basis of the eigenstates of $\hat{J}_1$, operator $\hat{V}_1$ conserves momentum, and operator $\hat{V}_2$ mixes vibronic levels with J_1 and $J_1 \pm 3$. Similarly, in the bases of the eigenstates of $\hat{J}_2$ operator $\hat{V}_2$ conserves momentum J_2 and operator $\hat{V}_1$ describes the processes with the change in the momentum J_2 by ± 3.[Pub VII] It is interesting to note, that linear vibronic interaction causes vibronic states to behave as fermions due to half-integer angular momentum values, while quadratic vibronic interaction leads to bosonic behaviour due to integer angular momentum values. It would be interesting to examine the interaction of two vibronic systems and study their bosonic or fermionic properties.

For systems with both linear and quadratic vibronic coupling, calculations are performed in two steps. First, the eigenvalue problem (7) for linear vibronic coupling (of Hamiltonian $H_0 \cdot I + \hat{V}_1$) is solved to obtain the eigenstates (6), which are then used as a basis for calculating eigenstates of quadratic vibronic coupling. In this basis they are given by the eigenvalues and the eigenfunctions of the energy matrix $W_{v,,J;v',,J'} = E_{v,,J}\delta_{v,,v'}\delta_{J,,J'} + V^{v,,J}_{v',,J'}$, where $V^{v,,J}_{v',,J'} = \langle \psi_{v,,J} | \hat{V}_2 | \psi_{v',,J'} \rangle$ represents the quadratic vibronic coupling in the (v, J) basis.[Pub VII] As was mentioned above, only the processes with changes in pseudomomentum J_1 by ± 3 are allowed. Therefore, only $V^{v,,J}_{v',,J'}$ terms with $J' = J \pm 3$ differ from zero,[65] resulting in three-diagonal block-form for $W_{v,,J;\, v',,J'}$.

$$\hat{W} = \begin{pmatrix} \hat{E}_{J_1} & \hat{V}^{(2)}_{J_1} & (0) & (0) \\ \hat{V}^{(2)}_{J_1} & \hat{E}_{J_1+3} & \hat{V}^{(2)}_{J_1+3} & (0) \\ (0) & \hat{V}^{(2)}_{J_1+3} & \hat{E}_{J_1+6} & \dots \\ (0) & (0) & \dots & \dots \end{pmatrix},$$

$$\hat{E}_{J_1} = \begin{pmatrix} \hat{E}_{0,J_1} & 0 & 0 & (0) \\ 0 & \hat{E}_{1,J_1} & 0 & (0) \\ 0 & 0 & \hat{E}_{2,J_1} & (0) \\ (0) & (0) & (0) & \dots \end{pmatrix}, \hat{V}^{(2)}_{J_1} = \begin{pmatrix} V^{0,J_1}_{0,J_1} & V^{0,J_1}_{1,J_1} & V^{0,J_1}_{2,J_1} & \dots \\ V^{1,J_1}_{0,J_1} & V^{1,J_1}_{1,J_1} & V^{1,J_1}_{2,J_1} & \dots \\ V^{2,J_1}_{0,J_1} & V^{2,J_1}_{1,J_1} & V^{2,J_1}_{2,J_1} & \dots \\ \dots & \dots & \dots & \dots \end{pmatrix}. \tag{14}$$

The matrix elements are following:

$$\begin{aligned} V^{v,,J_1>0}_{v',,J_1+3} = \frac{k_2}{4} \sum_{n\geq 0} a^{(v',,J_1+3)}_{2n} \Big[& a^{v,,J_1}_{2n+1} \sqrt{(n + J_1 + 5/2)(n + J_1 + 3/2)} \\ & + 2a^{(v,,J_1)}_{2n+3} \sqrt{(n + J_1 + 5/2)(n+1)} + a^{(v,,J_1)}_{2n+5} \sqrt{(n+2)(n+1)} \Big], \end{aligned} \tag{15}$$

$$V^{v,,-\frac{1}{2}}_{v',\frac{5}{2}} = \frac{k_2}{4} \sum_{n\geq 0} a^{\left(v',\frac{5}{2}\right)}_{2n} \sqrt{(n+1)(n+2)} \left(a^{\left(v,\frac{1}{2}\right)}_{2n} + 2a^{\left(v,\frac{1}{2}\right)}_{2n+2} + a^{\left(v,\frac{1}{2}\right)}_{2n+4} \right), \tag{16}$$

$$V^{\nu,-\frac{3}{2}}_{\nu',\frac{3}{2}} = \frac{k_2}{4}\sum_{n\geq 0}(n+1)\left[\sqrt{\frac{n+2}{n+1}}\left(a_{2n}^{\left(\nu,\frac{3}{2}\right)}a_{2n+2}^{\left(\nu',\frac{3}{2}\right)} + a_{2n+2}^{\left(\nu,\frac{3}{2}\right)}a_{2n}^{\left(\nu',\frac{3}{2}\right)}\right) + 2a_{2n}^{\left(\nu,\frac{3}{2}\right)}a_{2n}^{\left(\nu',\frac{3}{2}\right)}\right]. \quad (17)$$

If only quadratic vibronic interaction is present ($k_1 = 0$, $k_2 \neq 0$), the JTE manifests as the Renner-Teller effect (there is no first order vibronic coupling in linear molecules). To investigate the second order coupling, it is helpful to split the $\hat{V}^{(2)}$ term in the Hamiltonian $\hat{H}_2 = H_0 \cdot I + \hat{V}^{(2)}$ into two: $\hat{V}^{(2)} = \hat{V}_2^{(0)} + \hat{V}_2^{(1)}$, where

$$\hat{V}_2^{(0)} = k_2\begin{pmatrix} 0 & \hat{a}_+^+\hat{a}_- \\ \hat{a}_-^+\hat{a}_+ & 0 \end{pmatrix}, \quad \hat{V}_2^{(1)} = \frac{k_2}{2}\begin{pmatrix} 0 & \hat{a}_+^{+2} + \hat{a}_-^2 \\ \hat{a}_-^{+2} + \hat{a}_+^2 & 0 \end{pmatrix}. \quad (18)$$

The operator $\hat{V}_2^{(0)}$ conserves the number of phonons, while $\hat{V}_2^{(1)}$ changes phonon number by two. Using the RWA, only contribution of operator $\hat{V}_2^{(0)}$ is considered. As a result, the energy matrix takes on a block-three-diagonal matrix with 2 × 2 blocks:

$$\hat{H}_2^{(0,J_2)} = \begin{pmatrix} \hat{E}_{0,J_2} & \hat{V}^{(2)}_{0,J_2} & (0) & (0) & \ldots \\ \hat{\tilde{V}}^{(2)}_{0,J_2} & \hat{E}_{1,J_2} & \hat{V}^{(2)}_{1,J_2} & (0) & \ldots \\ (0) & \hat{\tilde{V}}^{(2)}_{1,J_2} & \hat{E}_{2,J_2} & \hat{V}^{(2)}_{2,J_2} & \ldots \\ \ldots & \ldots & \ldots & \ldots & \ldots \end{pmatrix}. \quad (19)$$

Here

$$\hat{E}_{0,J_2} = E_{0,J_2} = J_2,\ \hat{V}^{(2)}_{0,J_2} = \frac{k_2}{2\sqrt{2}}\sqrt{J_2\left(J_2+1\right)}\,(1,1), \quad (20)$$

$$\hat{E}_{n\geq 1,J_2} = \begin{pmatrix} E^-_{J_2,n} & 0 \\ 0 & E^+_{J_2,n} \end{pmatrix},\ \hat{V}^{(2)}_{n\geq 1,J_2} = \begin{pmatrix} -V^{(2,+)}_{n,J_2} & V^{(2,-)}_{n,J_2} \\ -V^{(2,-)}_{n,J_2} & V^{(2,+)}_{n,J_2} \end{pmatrix}, \quad (21)$$

$$V^{(2,\pm)}_{n,J_2} = \left(k_2/4\right)\left(\sqrt{(n+J_2)(n+J_2+1)} \pm \sqrt{n(n+1)}\right)\left(1+\delta_{n,0}\left(\sqrt{2}-1\right)\right). \quad (22)$$

$\hat{\tilde{V}} \equiv \hat{V}^+$ is the transposed matrix, (0) denotes a square matrix with zero elements, and (1,1) is the single-row matrix with two unit elements.[Pub VII] Hamiltonian (19) can be easily diagonalized. Then the obtained new basis can be used to take into account the (rest) term $\hat{V}_2^{(1)}$ in the Hamiltonian $\hat{H}_2$.

3.4.1 Results

Calculations were performed for two scenarios: 1) considering purely quadratic vibronic interaction, and 2) including linear coupling using the eigenfunctions of Hamiltonian with purely quadratic vibronic coupling as the basis for quadratic interaction. The obtained results align with previous research indicating that when weak (or absent) second order coupling combines with any first order coupling, the ground state is degenerate E-state while the first excited state is nondegenerate A_1-state. However, with strong second order interaction and weak (or absent) first order interaction, the nondegenerate state becomes the ground state. Corresponding vibronic coupling parameters k_1 and k_2 were calculated.

1) Purely quadratic interaction.

Used algorithm facilitated calculations for quadratic vibronic interaction strength $k_2 \leq 1 - 10^{-7}$. It was found that the ground state becomes a singlet in the region $0.929 < k_2 < 1$, while in the region $k_2 < 0.929$, the ground state is a doublet. Matrix sizes of 784 × 784 were employed for calculations in Eq. (19). The results are concluded in Fig. 6.

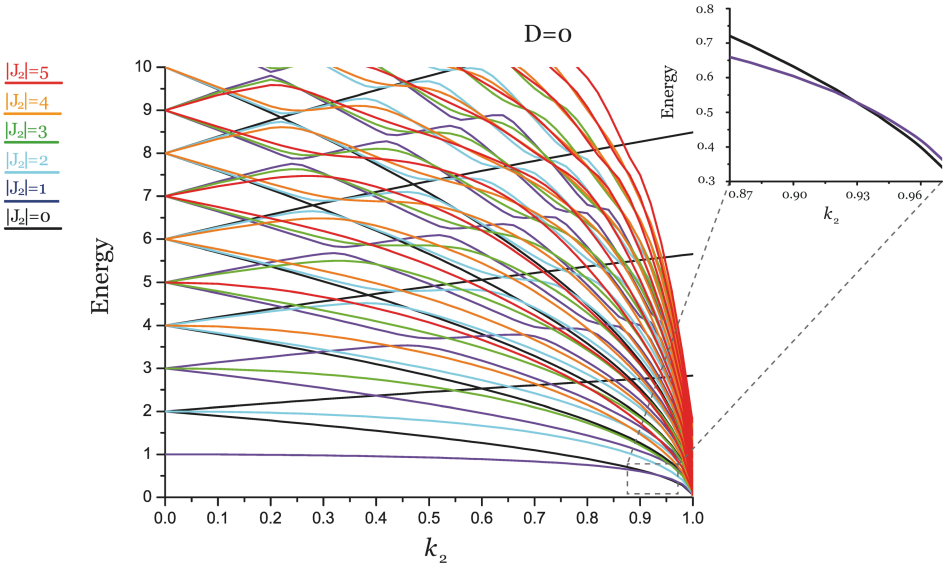

Fig. 6. Energy levels of the $E \otimes e$-system's vibronic states (in $\hbar\omega_0$ unit values) under purely quadratic vibronic coupling for various rotational momentum J_2, varying with the quadratic vibronic coupling parameter k_2. In case of $k_2 < 0.9$ results similar to those in Ref. 66 were observed. Coloured lines with $J_2 \neq 0$ represent E-states, while black lines with $J_2 = 0$ denote A_1-states. Ground state degeneracy differs: it is doubly degenerate for $k_2 < 0.929$ region and nondegenerate $0.929 < k_2 < 1$. Note the level crossing with different J_2 and avoided crossing with similar J_2.[Pub VII]

2) Linear and quadratic coupling.

Qualitative considerations based on Berry phase from works of Berry[37] and Zwanzinger et al.[17] suggest that if k_2 is significant and k_1 is small, the ground state coordinates encircle four conical intersections, leading to a singlet ground state.[Pub VII] Our calculations corroborate this, indicating that the nondegenerate state becomes ground state if $1 - k_2 < 0.07$ and $k_1 < 0.8$ The results are summarized in Fig. 7.

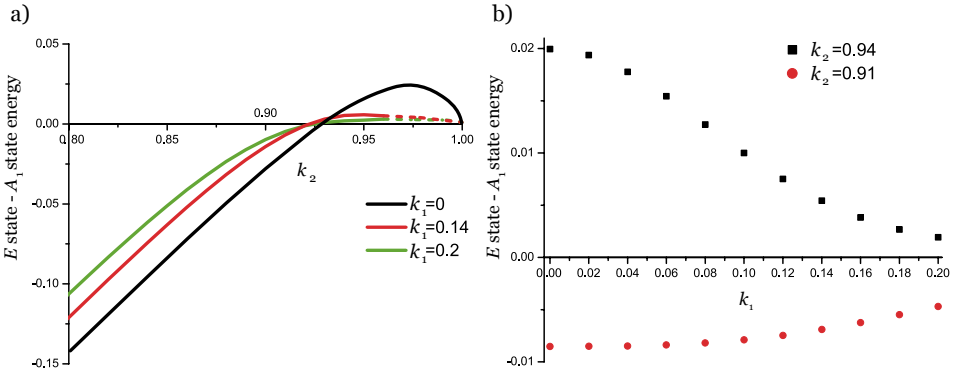

Fig. 7. A) Energy level differences between the lowest E and A_1-state, in case of weak linear vibronic coupling (k_1) and strong quadratic coupling (k_2). B) Differences in the same levels for $k_2 = 0.94$ and $k_2 = 0.91$ across various k_1.[Pub VII]

In summary, detailed calculations involving a large number of vibronic states of the Jahn-Teller $E \otimes e$-system with linear and quadratic vibronic interactions were conducted in the thesis. In the case of strong quadratic interaction, the analytical basis of RWA was introduced, which allowed significant simplification of the calculations. The parameter relations between linear and quadratic vibronic interactions were established, delineating the transition from a twice degenerate to a non-degenerate ground state.

4 INTERACTION WITH PHONON BATH

4.1 Transformation of vibronic Hamiltonian

This chapter provides an overview of the method that enables to calculate JT $E \otimes e$-problem taking phonon continuum into account. Section 2.1 highlighted the primary limitations of previous multimode approaches, such as the restricted number (typically around 10) of contributing vibration coordinates, inability to describe irreversible time behaviour characteristic of systems with a continuous spectrum, and impossibility of incorporating long-range interactions essentially determining the vibrations of 3D systems.

In Section 3.1 was given the Hamiltonian of the two-fold degenerate e-vibrations (Eq. (2)) and the amplitudes and energies of the system, where is interaction between two-fold degenerate e-vibrations and two-fold degenerate electronic state E (Eq. (7)). To describe vibrational systems with j number of normal modes, normal coordinates are commonly employed. In this representation, the Hamiltonian of vibrations in harmonic approximation assumes a general diagonal form

$$H_v = \frac{1}{2}\sum_{\alpha}\sum_{j\geq 0}\left(-\frac{\partial^2}{\partial x_{j\alpha}^2} + \omega_{j\alpha}^2 x_{j\alpha}^2\right), \tag{23}$$

where α counts the representations and the rows of representations of the symmetry group of the system, j are the number of normal modes of a given representation, x_j represent normal coordinates, and $\omega_{j\alpha}$ are their frequencies. This diagonal basis of vibrational Hamiltonian is also commonly used for describing vibronic interactions in degenerate or quasi-degenerate electronic states. For instance, using this basis, the vibronic interaction Hamiltonian with e-vibrations in the E-state of a trigonal centre can be expressed analogously to Eq. (1)

$$H = H_v \cdot I + \hat{V}, \tag{24}$$

$$\hat{V}_1 = \kappa\left(\sigma_x Q_x + \sigma_y Q_y\right), \tag{25}$$

where I is 2×2 unit matrix, $\alpha = x, y$ denotes two rows of e-representation, x_j are normal coordinates of vibrations, $\hat{V}$ is the vibronic interaction term that incorporates linear and quadratic terms with respect to configurational coordinates Q_α belonging to e-representation, and σ_x and σ_y are Pauli matrices. In solids and typically in molecules, a large number $N \gg 1$ of normal coordinates contribute to these configurational coordinates resulting in

$$Q_\alpha = \sum_{j=0}^{N} \overline{e}_j x_{j\alpha}, \tag{26}$$

where $\overline{e}_j$ are normalized components polarization vectors.

However, in real systems, the primary contribution to vibronic interaction arises from only a few local or pseudolocal vibrations, while the contribution from all other modes (in solids of the order of Avogadro number) is significantly smaller. Nevertheless, this contribution plays a crucial role in the irreversible time evolution of vibronic systems with a continuous energy spectrum, leading to relaxation of excited states of the centre, including passing through conical intersections.

A potential solution to this problem involves a two-step resolution. Initially we numerically find eigenstates and eigenvalues of the vibronic Hamiltonian, accounting only for these few modes that contribute significantly to the vibronic interaction. Then, as a second step we consider the effect of all the other modes using the found basis. However, realizing this approach in the representation of normal coordinates is complicated by the difficulty of finding vibronic matrices (containing the Pauli matrices in the $E \otimes e$-problem) in the vast basis of the numerically found vibronic states.

Publication II (see also Publications III and IV) proposed a solution to this difficulty by employing a coordinate basis different from normal coordinates. The basis was selected so that the configurational coordinates involved in the vibronic interaction belong to the set of the used independent coordinates. Obviously, the vibrational Hamiltonian is not diagonal in this basis but it remains quadratic. Notably, in the case of weak interactions with the phonon continuum, the non-diagonal quadratic term takes on a simple factorized form, where the main coordinate is one of the factors and a linear combination of phonons is another factor. As a result, this quadratic interaction depends linearly on the coordinates of the main mode(s) and also linearly on the coordinates of phonons. This simple interaction replaces the vibronic interaction with the phonon continuum. It is essential that the found form of the quadratic interaction is convenient for the description of the effect of phonon continuum while the coordinate of the main mode has simple form in the numerically found vibronic basis. The linear phonon part can be effectively handled for an arbitrary number of modes by applying the cumulant expansion of the evolution operator concerning this interaction. Below is presented the derivation of the quadratic interaction term that replaces the vibronic interaction with phonons, while also considering small correction terms that were previously overlooked. The rows and columns of the matrices correspond to the two electronic states of E-representation of the center. However, they can also belong to electronic states of different centres.

4.2 Local mode of $E \otimes e$-problem

The vibronic interaction in case of $E \otimes e$-problem is described by the Eqs. (25) and (26). Let us consider the row α and omit subscript α. Here we investigate the case when the main contribution to this interaction is given by the local mode described by the normal coordinate x_0. In this case one can take $\overline{e}_j = e_j\left(\delta_{j0} + \lambda\right)\Big/\sqrt{1+\lambda^2}$, $\sum_{j\geq 1} e_{1j}^2 = 1$, giving

$$Q = \left(1+\lambda^2\right)^{-1/2}\left(x_0 + \lambda q_1\right), \tag{27}$$

where λ is small dimensionless parameter ($\lambda \ll 1$), $q_1 = \sum_{j\geq 1} e_{1j} x_j$. In this case the vibronic interaction can be presented in two terms: $\hat{V} = \hat{V}_0 + \hat{V}_1$, where

$$\hat{V}_0 = \kappa \sum_{\alpha=x,y} \sigma_x x_{0\alpha} \tag{28}$$

accounts for the vibronic interaction with local mode,

$$\hat{V}_1 = \kappa \sum_{\alpha=x,y} \sum_{j\geq 1} \sigma_\alpha e_j x_{j\alpha} \tag{29}$$

takes into account the vibronic interaction with phonons.

Let us introduce coordinate

$$Q_1 = \left(1+\lambda^2\right)^{-1/2}\left(q_1 - \lambda x_0\right) \tag{30}$$

which is orthogonal to Q. The back transformation reads

$$x_0 = \left(1+\lambda^2\right)^{-1/2}\left(Q - \lambda Q_1\right),$$

$$q_1 = \left(1+\lambda^2\right)^{-1/2}\left(Q_1 + \lambda Q\right).$$

We introduce coordinates q_l, $l \geq 2$ orthogonal to coordinates x_0 and q_1 (obviously they are also orthogonal to coordinates x_0 and Q_0). Using these coordinates the doubled potential energy of phonons gets the form

$$2U = \omega_0^2 x_0^2 + \sum_{l\geq 1}\sum_{l'\geq 1} D_{ll'} q_l q_{l'} = \omega_0^2 x_0^2 + D_{11} q_1^2 + 2\sum_{l\geq 2} D_{1l} q_1 q_l + \sum_{l\geq 2}\sum_{l'\geq 2} D_{ll'} q_l q_{l'}. \tag{31}$$

Note that $D_{ll'}$ $(l, l' \geq l)$ is the dynamical matrix of phonons with ω_j^2 being its eigenvalues. Expressing in Eq. (31) x_0 and q_1 via Q_0 and Q_1 we get

$$2U = \left(1+\lambda^2\right)^{-1}\left((\omega_0^2 + \lambda^2 D_{11})Q_0^2 + (D_{11}+\lambda^2)Q_1^2 - 2\lambda Q_0 Q_1(\omega_0^2 - D_{11})\right) + \\ + 2\left(1+\lambda^2\right)^{-1/2}\sum_{l\geq 2} D_{1l}(Q_1 + \lambda Q_0)q_l + \sum_{l\geq 2}\sum_{l'\geq 2} D_{ll'}q_l q_{l'}.$$

We keep now only terms up to λ^2 included. This gives

$$2U = \bar{\omega}_0^2 Q_0^2 + \bar{D}_{11}Q_1^2 - 2\lambda Q_0\left((\omega_0^2 - D_{11})Q_1 - \sum_{l\geq 2} D_{1l}q_l\right) \\ + 2(1-\lambda^2/2)\sum_{l\geq 2} D_{1l}Q_1 q_l + \sum_{l\geq 2}\sum_{l'\geq 2} D_{ll'}q_l q_{l'}, \tag{32}$$

where

$$\bar{\omega}_0^2 = \omega_0^2 + \lambda^2(D_{11} - \omega_0^2), \tag{33}$$

$\bar{D}_{11} = D_{11} - \lambda^2(D_{11} - \omega_0^2)$. Let us introduce new variables $Q_1' = Q_1$ and $Q_l' = q_l(1 + \lambda^2/2)$, $l \geq 2$. We get

$$2U_0 \cong \bar{\omega}_0^2 Q_0^2 + \sum_{l\geq 1}\sum_{l'\geq 1}\bar{D}_{ll'}Q_l' Q_{l'}' - 2\lambda Q_0\left((\omega_0^2 Q_1 - \sum_{l\geq 1} D_{1l}Q_l'\right),$$

where $D'_{ll'} = D_{ll'} + \lambda^2(\omega_0^2\delta_{1l}\delta_{1l'} - \mathrm{D}_{1l'}\delta_{il})$. The quadratic form given by the double sum can be diagonalized introducing new normal coordinates $x_j' = \sum_l e'_{lj}Q_l'$. New polarization vectors here e'_{lj} satisfy the standard equation $\sum_{l'} D'_{ll'}e'_{l'j} = \omega_j^2 e'_{lj}$. (Here we take into account that a single weak point defect does not change the frequencies of bulk phonons). This equation allows to find the changed polarization vectors e'_{lj}. Indeed, according to this equation

$$\sum_{l'} D_{ll'}e'_{l'j} + \lambda^2\delta_{l1}\left(\omega_0^2\delta_{l'1} - D_{1l'}\right)e'_{l'j} = \omega_j^2 e'_{lj}. \tag{34}$$

From this equation it follows that $e'_{lj} = e_{lj}$ if $l \neq 1$, while e'_{1j} slightly (up to $\propto \lambda^2$ term) differs from e_{1j}. Taking into account the basic ration for phonons $\sum_l D_{ll'}e_{lj} = \omega_j^2 e_{l'j}$ we get

$$e'_{1j} = e_{1j}\left(1 + \lambda^2\left(\omega_0^2 - \omega_j^2\right)\Big/\left(D_{11} - \omega_j^2\right)\right). \tag{35}$$

Now we can present U in the form

$$U \cong \frac{1}{2}\bar{\omega}_0^2 Q_0^2 + U'_{ph} - \lambda Q_0 \sum_{j\geq 1}\left(\omega_0^2 - \omega_j^2\right) e_{1j} x'_j, \tag{36}$$

where $U'_{ph} = \sum_j \omega_j^2 x'^2_j / 2$,

$$x'_j = x_j + \lambda^2 Q_1 e_{1j}\left(\omega_0^2 - \omega_j^2\right) / \left(D_{11} - \omega_j^2\right) \tag{37}$$

are new, slightly changed normal coordinates. Consequently account of small terms in the order of λ^2 leads to a small change of the polarization vector e_{1j} and the frequency of the main mode. If λ is small then $x'_j = x_j$.

Let us introduce the creation ($\hat{a}_j^+$) and destruction ($\hat{a}_j$) operators of the main mode and phonons. Then

$$\begin{aligned} Q_0 &= \sqrt{\hbar / 2\bar{\omega}_0}\,(\hat{a}_0 + \hat{a}_0^+), \\ x'_j &= \sqrt{\hbar / 2\bar{\omega}_0}\,(\hat{a}_j + \hat{a}_j^+). \end{aligned} \tag{38}$$

In this representation the transformed Hamiltonian of the E-state gets the form

$$H = \tilde{H}_v + H' + \hat{V}_0, \tag{39}$$

where

$$\tilde{H}_v = \hbar \sum_{\alpha=x,y}\left(\tilde{\omega}_0(\hat{a}_{\alpha 0}^+ \hat{a}_{\alpha 0} + 1/2) + \sum_{j\geq 1}\omega_j(\hat{a}_{\alpha j}^+ \hat{a}_{\alpha j} + 1/2)\right), \tag{40}$$

$$H' = \lambda \sum_{\alpha=x,y}\sum_j \vartheta_j(\hat{a}_{\alpha 0} + \hat{a}_{\alpha 0}^+)(\hat{a}_{\alpha j}^+ + \hat{a}_{\alpha j}), \tag{41}$$

$\vartheta_j = e_{1j}\hbar(\omega_0^2 - \omega_j^2)/2\sqrt{\omega_0\omega_j}$. Consequently, transformed Hamiltonian replaces the vibronic interaction with phonons $\hat{V}_1$ by the quadratic interaction of the main mode with phonons H'.

In certain scenarios, the primary source of vibronic interaction arises from the engagement with pseudo-local modes. Appendix A of **Publication VI** demonstrated that, even in such cases, the part of the Hamiltonian describing the vibronic interaction with phonons can be replaced by a factorized correction to the vibrational Hamiltonian. One factor involves the coordinate of the pseudo-local mode, while the other factor comprises a linear combination of phonon coordinates.

This transformation remains applicable even when the vibronic interaction includes higher order terms conserning configurational coordinates. For example, one can include the second order terms taking

$$\hat{V} = \sigma_x \left(k_1 Q_x + k_2 (Q_x^2 - Q_y^2) \right) + \sigma_y \left(k_1 Q_y - 2k_2 Q_x Q_y \right).$$

4.3 A few remarks on the vibronic interaction

In last section was considered the scenario if two electronic states belong to one centre. In this case the different rows and columns of the vibronic matrix correspond to two electronic states of the same centre. However, the presented Hamiltonian transformation is general and can describe different impurities. For instance, it remains valid even if the basic electronic states belong to two different centres. In this case, the configurational coordinate Q that mixes both states corresponds (up to a constant) to the distance between the canters. If this coordinate is the sole contributor to the interaction, then the problem simplifies to the well-known dimer problem. The presented transformed Hamiltonian can account for the contribution of phonons to the dimer.[67–69] This approach may prove useful for the consideration of closely spaced centres, where the overlapping integral of the wave functions of the centres (which determines the vibronic interaction of the dimer) has remarkable value.

There are numerous crystals with the Jahn-Teller effect, including some with $E \otimes e$ Jahn-Teller effect in the ground state. In some of these systems, pseudo-rotation or tunnelling excitation occurs in this state. These low energy excitations notably interact with bulk phonons. This interaction is responsible, for instance, for sound attenuation in these systems. Additionally, phonons may be responsible for cooperative effects leading to phase transitions. A successful theory of these phenomena requires an understanding of the interaction of phonons with low-energy vibronic states in these systems. The presented method of accounting for vibronic interaction with phonons via effective quadratic interaction of phonons with vibrations responsible for Jahn-Teller effect may offer a new approach to this problem. For example, it may allow for the deteremination of strength of vibronic interaction with phonons responsible for transitions between tunnelling and other low energy vibronic excitations.

4.4 Vibronic interaction of spaced-apart impurities

A centre (defect) in a crystal introduces a disturbance to the lattice vibrations. If the ground electronic state of the centre is non-degenerate, then the perturbation in harmonic approximation is expressed as $\hat{V} = (Q\kappa Q)/2$, where κ is the tensor describing the change of the dynamical matrix, and Q is the vector of configurational coordinates. This perturbation alters the zero-point energy of the lattice. When two centres perturb the same phonons, they differently renormalize the zero-point energy compared to two independent centres. As demonstrated by Maradudin et. al,[70] this leads to the interaction of impurities. It is interesting to note that this interaction (like gravity) is attractive and long-range.

If the ground electronic state is degenerate or quasi-degenerate, then the aforementioned theory does not apply. In such cases, we must additionally consider the vibronic interactions, which may be more significant. Here, two centres interact vibronically with the same phonon continuum, resulting in their coupling. This method enables the description of effects caused by cooperative vibronic coupling through phonons. Specifically, for two centres the vibronic interaction with phonons can be replaced by an interaction linear with respect to Jahn-Teller modes and phonons. As a result we get $\mathrm{H}' = H_1' + H_2'$, where $H_{1(2)}'$ describes interactions including the local modes of the centres number 1 and 2, along with corresponding packets of phonon coordinates. It is important that these Hamiltonians include the same phonon continuum. This common phonon continuum leads to an interaction that can be explicitly determined, for instance, by applying a unitary transformation that illuminates the linear couplings with phonons and then averaging the resulting Hamiltonian over vibronic states of impurities. This interaction obtained in this manner can be particularly significant for systems nearing structural phase transitions. We intend to revisit this question in the future using the method outlined here.

4.5 Debye-van Hove model for phonons

The Debye-van Hove model of phonons, which describes non-totally symmetric acoustic phonons, was employed for all calculations in this thesis. The density of states function $\rho(\omega) = (16/\pi\omega_M^4)\omega^2\sqrt{\omega_M^2 - \omega^2}$ behaves accurately near both ends of the spectrum, at $\omega \to 0$ and, at $\omega \to \omega_M$, where ω_M is the maximum value of the phonon frequency.

Fig. 8 represents function $v^2(\omega) = \rho(\omega)(\omega^2 - \omega_0^2)^2/2\hbar\omega\omega_0$, which illustrates the frequency dependence of the interaction with phonon continuum distribution. As we describe the interaction of main mode with phonon continuum, the main mode ω_0 is excluded from the distribution. Calculations are conducted under low-temperature conditions $T \ll \hbar\omega_0/k_B$, enabling only phonon-induced downward transitions between vibronic levels with the energy difference $\leq \hbar\omega_M$.

The frequency of the local mode was taken as unity (ω_0=1), and the maximum value of the phonon frequency was set to ω_M = 1,3. As the average energy difference of the vibronic levels equals ω_0, choosing ω_M = 1,3 allows transitions only between neighbouring levels. The approximate value of the local mode vibrational frequency in crystals is $\omega_0 = 10^{13}$ sec^{-1}, so for crystals, the time unit in the graphs of relaxation calculations is 0,1 ps.

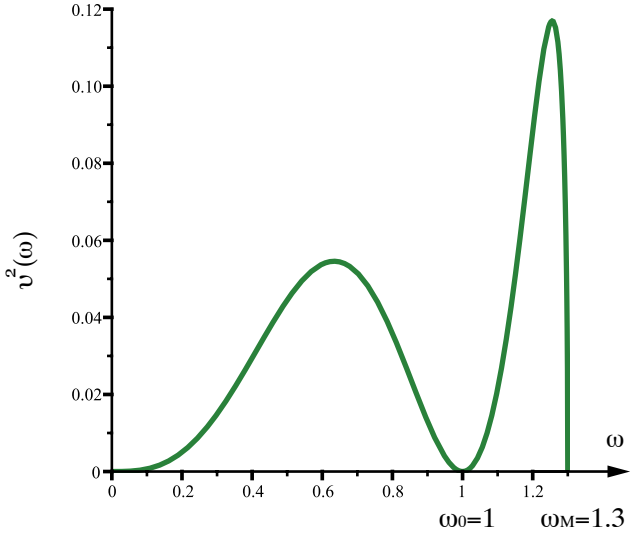

Fig. 8. Debye-van Hove model of phonons, which describes the non-totally symmetric acoustic phonons. Graph illustrates the frequency dependence of the interaction with phonon continuum distribution, the main mode ω_0 is excluded.[Pub VI]

5 RESONANT RAMAN SCATTERING COMPARED TO ABSORPTION

Experimental investigation of the Jahn–Teller effect often involves optical probing, specifically through measurements of absorption and resonance Raman scattering (RRS). RRS provides detailed information about vibronic excitations in the ground electronic state by measuring the excitation spectra known as Raman excitation profiles (REPs) of various vibrations.[71] The widespread use of tunable lasers in Raman spectroscopy has facilitated a thorough study of resonant Raman scattering. It has been recognized that the Raman excitation profile, which illustrates the dependence of the Raman effect on the excitation frequency, can offer more comprehensive insights into the vibronic system compared to conventional absorption techniques. Unlike the absorption spectrum, REP not only provides information about the entire vibronic interaction but also offers separate details about the Raman active modes. This makes the REP method of Raman spectroscopy especially important for systems governed by multiple modes, such as polyatomic molecules or solid-state defect systems.

The aim of the thesis and **Publication IV** is to investigate the absorption and RRS spectra of impurity centres with JT $E \otimes e$-effect and to explore the influence of nonadiabaticity on the dynamics of the JT system. Special attention was devoted to the impact of the vast number of Avogadro bath modes (phonons) of the crystal[3, 19–23] on the Jahn-Teller active configurational coordinates. To account for the bath modes, the method outlined in Chapter 4 and **Publication II** was employed. This fully quantum-mechanical approach allows for the description of spectral lines resulting from the excitation of active local and pseudo-local Jahn-Teller modes, as well as the phonon wings of these spectral lines. Previous calculations by other authors were performed using the quasi-classical approximation for absorption[72–74] and RRS,[75, 76] neglecting the phonon continuum.

As mentioned earlier, the currently available theories, including the multi-configurational time-dependent Hartree approximation,[24–30] only enable the study of the dynamical JT effect in systems with a small number of contributing vibrational coordinates (typically around 10 or fewer). This limitation highlights a fundamental drawback of the Hartree approximation – it is not suitable for describing the relaxation of the centre associated with the creation of phonon waves in the continuum that transmit energy from the centre to the crystal. Additionally, the method fails to account for Fano effects – asymmetric spectral line shapes resulting from the interference of the contributions of discrete and continuous states in absorption and RRS. The considerations presented in the **Publication IV** takes into account this process of phonon emission for the first time, including the manifestations of Fano effect for phonons interacting with local modes. This analysis has led to the identification of several Fano resonances resulting from the interference of channels with zero phonon and those with phonon support in the absorption and RRSs spectra.

5.1 Raman Fourier amplitudes and phonon contribution

The method of resonant Raman Fourier amplitudes (developed in Ref. 77) was used to calculate the Raman excitation profiles in **Publication IV**. This approach enabled the first fully quantum mechanical calculations of the profiles of Jahn-Teller systems, considering the contribution of the phonon continuum to the active Jahn-Teller coordinates. Additionally, fully quantum-mechanical calculations of the absorption spectra of Jahn-Teller systems were performed for the first time, also considering the phonon continuum. To this end the cumulant expansion of the Raman Fourier amplitudes was applied with respect to the interaction of the main Jahn-Teller active mode with phonons H':

$$A_f(t) = \Theta(t)\left\langle f \left| \mu_\beta^+ e^{it(H+V_0+H')} \mu_\alpha \right| 0,0 \right\rangle . \tag{42}$$

Here $|0,0\rangle$ and $|f\rangle$ represent the initial (zero-point) and final states of the main (Jahn-Teller active) local (pseudolocal) mode of the optical centre and phonons, μ_α and μ_β are 2-row single column matrices of the electronic matrix elements, $|f\rangle = |0,0\rangle$ corresponds to Fourier transform of absorption for $t \geq 0$ (the case of zero temperature was considered).[Pub IV] Considering the first two cumulants, the following equation for the Raman Fourier amplitudes was found:

$$A_f(t) \cong \Theta(t) \sum_\nu C_{f\nu} C_{0\nu} e^{iE_\nu t + g_\nu(t)} . \tag{43}$$

Here, $C_{f\nu}$ are numerically found amplitudes of the expansion of the vibronic state ν with energy E_ν of the Jahn-Teller effect with respect to state number f of the Jahn-Teller active mode, and $g_\nu(t)$ is the Fourier transform of the one-phonon excitations, given by Eq. (33) in Publication IV. The absorption and REPs calculations were performed for different JT interaction strengths in the ground mode and different phonon interaction strengths. The Debye-van Hove model introduced in Section 4.5 was utilized to model phonons and calculate the absorption spectra and REPs.

5.2 Results

In calculations, the transformation relations between the Fourier amplitudes of the resonant Raman scattering and the Fourier transform of the absorption spectrum were used for the basic model of linear vibronic coupling and for more complex models, including linear noncondonal interaction, frequency shifts and mixing of modes with electronic excitation, the Jahn-Teller effect and inhomogeneous broadening.

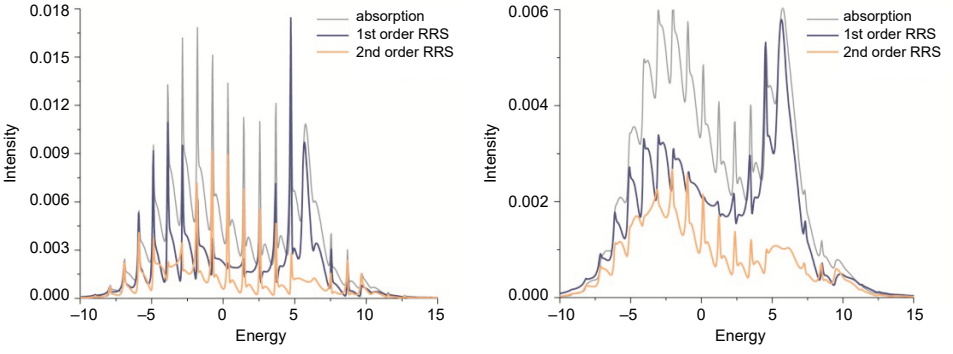

Fig. 9. Absorption spectrum and Raman excitation profiles (REPs) of first and second order trigonal center with $E \otimes e$ Jahn-Teller effect in the excited state for $\omega_M = 1{,}3\omega_0$ and Jahn-Teller stabilization energy $D = 10\hbar\omega_0$. Left: Phonon interaction strength $\lambda^2 = 0{,}1$, right: $\lambda^2 = 0{,}15$. Pub. III

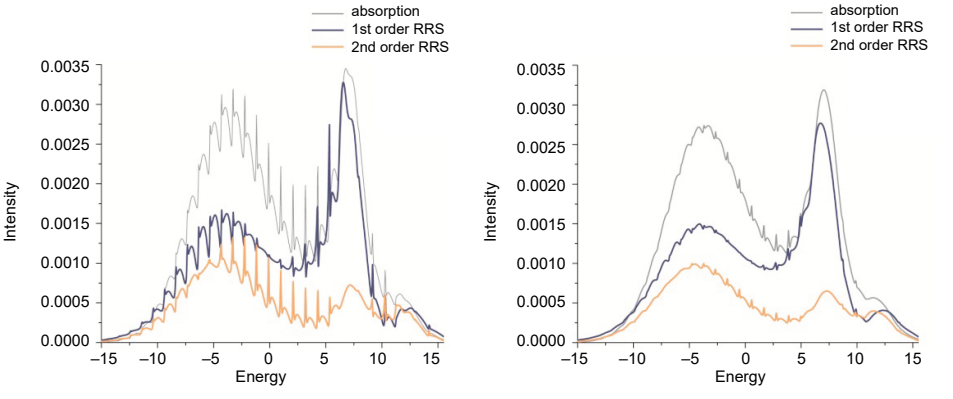

Fig. 10. Similar to Fig. 9, but for $D = 20\hbar\omega_0$. Pub. III

Fig. 9 and Fig. 10 show an increase in the effects of non-adiabaticity in RRS. Indeed, in Fig. 9 and Fig. 10 the first-order REP gain compared to the absorption for the medium frequencies corresponding to the spectral position of the conical intersection. This central region of the REP is attributed to the generation of a quantum of the Jahn-Teller vibration with a momentum $|m| = 1$ near the conical intersection caused by non-adiabaticity. Additionally, sharp minima are observed at the boundary between the lines and wings of the phonon continuum, indicating the presence of Fano effects. It is noteworthy that these Fano minima are more pronounced in the first-order REPs than in absorption spectra, attributed to the increased generation of low-frequency phonons due to non-adiabaticity.

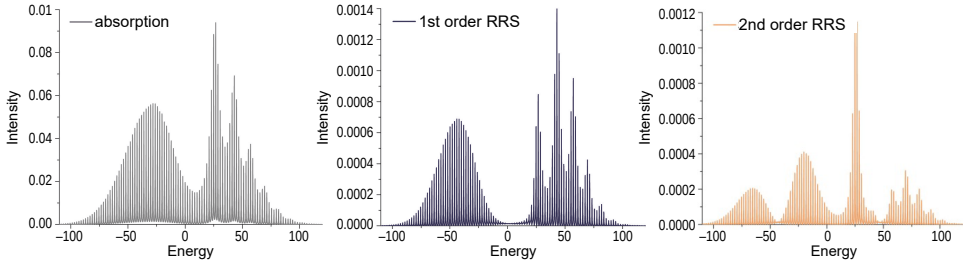

Fig. 11. Similar to Fig. 9, but for $D = 1000\hbar\omega_0$, $\lambda^2 < 0{,}01$. [Pub. III]

Fig. 11 clearly illustrates the enhancement of high-energy Slonczewski resonances in REPs compared to absorption spectra (which is also evident in Fig. 9 and Fig. 10, albeit to a lesser extent). This phenomenon signifies the stimulated quantum process of generating vibrational quanta: the higher the vibrational excitation at the conical intersection, the higher the probability of creating a vibrational quantum in the RRS process. In cases of a very large D corresponding to a very strong Jahn-Teller interaction, this amplification effect surpasses the increase in non-adiabaticity observed under moderate D. Furthermore, additional minima are observed in the second-order REPs in Fig. 11, indicating the interference of different RRS channels processes in the creation of two vibrational quanta with varying total rotational momentum $m = 0$ and $|m| = 2$.

6 PHONON-INDUCED RELAXATION THROUGH CONICAL INTERSECTION

In **Publication V** is studied the energy dissipation process of an impurity centre with an excited Jahn-Teller $E \otimes e$, particularly exploring scenarios where energy is dissipated without radiation through the influence of $\sim N_{\text{Avogadro}}$ bath modes (phonons). The time dependence of the distribution function of the configurational coordinate and relaxation through conical intersection was visualised. The calculations are conducted in case of optical excitation of the impurity centre by a spectrally selective and nonselective light pulses.

As mentioned earlier, near the conical intersection of APES, the electronic states and vibrational states are strongly mixed. This mixing is believed to speed up chemical and photochemical reactions and non-radiative electronic transitions.[59, 78] However, despite being a widely acknowledged qualitative statement, rigorous theoretical support has been lacking due to the absence of nonperturbative methods for addressing the non-adiabaticity arising from the interaction of Jahn-Teller-type systems with the phonon continuum.

To calculate the interaction of Jahn-Teller centre with phonon bath and describe the relaxation through conical intersection was employed the method described in Chapter 4 and **Publication II**. This method reveals that the linear vibronic interaction can be replaced by a purely vibrational quadratic interaction, which is the product of the coordinate of the main active Jahn-Teller mode and the configuration coordinate, which is a linear combination of phonon coordinates. As was described above, by calculating vibronic states considering local modes of the impurity centre (that is solving $E \otimes e$-problem by solving Eq. (7)) and subsequently utilizing them as a basis for computing the quadratic vibrational interaction of the Jahn-Teller mode with phonons, we streamline the process.

An important aspect in the case of a conical intersection in the $E \otimes e$-problem is the presence of the Berry phase, which leads to a half-integer quantum number of angular momentum in vibronic levels.[79] During the energy relaxation process considered here, phonons are emitted, which also have angular momentum (the latter belongs to the doubly degenerate e-representation). Therefore, due to the conservation of the total angular momentum, the angular momentum of the main vibronic system (which includes only few local modes) is altered during relaxation. To account for this effect, the master equation for the population factors of vibronic levels was derived and numerically solved. Knowing the population density of vibronic levels allowed to calculate the time-dependence of the distribution function of the basic configurational coordinate and to visualise long-time range energy relaxation through the conical intersection.[Pub V] It is also shown, that Slonczewski resonances affect the relaxation through conical intersection. In current chapter and **Publication V** is studied the relaxation process taking into account only vibronic levels with pseudomomentum (total angular momentum) $J = |1/2|$ (for simplicity, the subscript 1 for linear vibronic interaction is omitted in current and next chapter, so J denotes first order vibronic coupling).

6.1 Master equation and phonon contribution

Density operator formalism was employed to calculate the relaxation of excited Jahn-Teller state interacting with the phonon continuum. Utilizing the transformed Hamiltonian Eq. (41) obtained earlier, Hamiltonian of the interaction causing relaxation was derived. The matrix elements of density operator are:

$$\hat{\rho}_{\nu\nu'} = \left\langle 0_{ph} \left| e^{-it(H+H')} \right| \nu \right\rangle \left\langle \nu' \left| e^{it(H+H')} \right| 0_{ph} \right\rangle, \tag{44}$$

where $|0_{ph}\rangle$ denotes the zero-point state of phonons. Applying interaction representation $\hat{\rho}(t) = e^{itH}\,\hat{\rho}e^{-itH}$, the time derivative of the density operator is $\dot{\hat{\rho}} = -i\langle 0_{ph}|[\tilde{H}', \hat{\rho}]|0_{ph}$.[Pub V] By using Eq. (41), the time derivative of the density operator up to second order can be presented in the following form:

$$\dot{\hat{\rho}}(t) = \lambda^2 \int_0^t d\tau G(\tau) \sum_\alpha a_{0\alpha}(t) \left[a_{0\alpha}^+(t-\tau)\hat{\rho}(t) - \hat{\rho}(t-\tau)a_{0\alpha}^+(t-\tau \right] + Hc\,. \tag{45}$$

Here the correlation function $G(\tau) = \sum_j e_j^2 \left\langle 0_{ph} \left| a_{\alpha j}(\tau) a_{\alpha j}^+ \right| 0_{ph} \right\rangle = \sum_j \upsilon_j^2 e^{-i\omega_j \tau}$ describes phonon excitations.

In cases of strong Jahn-Teller coupling in the impurity centre and weak coupling with phonons, the diagonal elements of the density matrix can be used to calculate the relaxation time, as the non-diagonal elements change much faster compared to diagonal elements. The characteristic reciprocal time of non-diagonal elements are $\sim\sqrt{D}\,\omega_0$, where $D \gg 1$, while for the diagonal elements, which depend only on weak interaction with phonons the characteristic reciprocal time is at least λ^2 times smaller than $\sqrt{D}\,\omega_0$.[Pub V]

For large time limit in Eq. (45) the $\hat{\rho}\,(t-\tau)$ may be replaced by $\hat{\rho}\,(t)$. In this case the Eq. (45) reduces to the master equation in the Lindblad form.[80] Considering that operator H' conserves the rotation momentum J and by using Eq. (6) for Lindblad form the time derivative of diagonal elements of density matrix gets the standard form of the master equation:

$$\dot{\rho}_{\nu\nu} \approx -\gamma_\nu \rho_{\nu\nu} + \sum_{\nu' \neq \nu} \gamma_{\nu\nu'}\, \rho_{\nu'\nu'}\,. \tag{46}$$

The first term on the right side of master equation describes the rate of decay of the state $|\nu\rangle$ due to transitions from this level to other levels with creation of phonons, the second term describes the transitions from all other levels. $\rho_{\nu'\nu'}$ describes other diagonal elements of the density matrix with the same J as $\rho_{\nu\nu}$.

The decay rate of the state $|v\rangle$ is $\gamma_v = \sum_{v'} \gamma_{vv'}$:

$$\gamma_{vv'} = \lambda^2 \left| A_{vv'} \right|^2 \int_{-t}^{t} d\tau G(\tau) e^{i(E_v - E_{v'})\tau}, \tag{47}$$

where interaction between the states $|v\rangle$ and $|v'\rangle$ is described with matrix elements $A_{vv'}$ of the interaction Hamiltonian H':

$$A_{vv'} = \left\langle v'_- \left| \left(a_{0+} + a_{0-}^+ \right) \right| v_+ \right\rangle + \left\langle v'_+ \left| \left(a_{0-} + a_{0+}^+ \right) \right| v_- \right\rangle, \tag{48}$$

where

$$\begin{aligned} \left| v_- \right\rangle &= \left\langle + \left| v \right\rangle = \sum_n C_{2n,v} \left| 2n, J - 1/2 \right\rangle, \right. \\ \left| v_+ \right\rangle &= \left\langle - \left| v \right\rangle = \sum_n C_{2n+1,v} \left| 2n+1, J + 1/2 \right\rangle \cdot \right. \end{aligned} \tag{49}$$

Using the above-given equations, the equation for interaction matrix elements becomes:

$$A_{vv',J} = \sum_n \left[C_{2n+1,v,J} \left(\sqrt{n + J + 1/2}\, C_{2n,v',J} + \sqrt{n+1} C^{(J)}_{2n+2,v'} \right) + C_{2n,v',J} \left(\sqrt{n + J + 1/2}\, C_{2n,v',J} + \sqrt{n+1} C_{2n+2,v,J} \right) \right], \tag{50}$$

where $C_{n,v,J}$ are the solutions of the Eq. (7) for $J = 1/2, 3/2, 5/2, \ldots$ and for the eigenvalue E_v. As was mentioned above, this chapter studies the relaxation process taking into account only vibronic levels with pseudomomentum (total angular momentum) $J = |1/2|$. In this case

$$A_{vv'} = \sum_n \sqrt{n+1} \left[C_{2n+1,v} \left(C_{2n,v'} + C_{2n+2,v'} \right) + C_{2n+1,v'} \left(C_{2n,v} + C_{2n+2,v} \right) \right]. \tag{51}$$

Calculations of $\gamma_{vv'}$ can be simplified by taking into account that with a large time limit t

$$\gamma_{vv'} = 2\pi\lambda^2 \left| A_{vv'} \right|^2 \upsilon^2 \left(E_v - E_{v'} \right), \tag{52}$$

where $\upsilon^2(\omega)$ is the Fourier transform of $G(t)$.

Phonon function $\upsilon^2(E_v - E_{v'})$ has finite width, determined by the width of the phonon spectrum (see Fig. 8), the exception are the lowest levels corresponding to the lowest pseudo-rotation states. Therefore, for every v the function $\upsilon^2(\omega)$

essentially differs from zero only for the nearest v'. The one-phonon transition from the level v is possible to the next lower level v' and the possible transitions to the level v come only from the one higher level v'. The fact that transitions are possible only between nearest levels simplifies the solution of the master equation (46).

6.2 Time-dependence of the distribution function

Two types of optical excitations were examined: firstly, where all vibronic levels with $J = \pm 1/2$ are excited, resulting in an initial population density of vibronic levels given by equation[32, 49–51]

$$\rho_{vv}(t=0) = C_{0,v}^2 . \tag{53}$$

Secondly, quasi-monochromatic excitation where a specific vibronic level $|v_0\rangle$ is populated, leading to an initial population density of the vibronic levels as following:

$$\rho_{vv}(t=0) = \delta_{vv_0} . \tag{54}$$

If phonon interaction strength λ is small, relaxation rates γ_v are smaller than the energy differences between adjacent vibronic levels and the excitation with duration $\sim \omega_0^{-1}$ excites one or a few vibronic levels.

By employing the master equation (46), the evolution of population density for all vibronic levels can be calculated. It enables to calculate the time-dependence of the distribution function of the configurational coordinate $Q = \sqrt{x_{01}^2 + x_{02}^2}$ by means of equation

$$\begin{aligned} P(Q,t) &= \sum_v \rho_{vv}(t)\left(\langle + | v_Q\rangle\langle v_Q | +\rangle + \langle - | v_Q\rangle\langle v_Q | -\rangle\right) \\ &= \sum_v \rho_{vv}(t)\left(|\Psi_{v+}(Q)|^2 + |\Psi_{v-}(Q)|^2\right). \end{aligned} \tag{55}$$

Here $|v_Q\rangle$ represents the wave function of the vibronic state v,

$$\begin{aligned} \Psi_{v+}(Q) &= \sum_n C_{2n,v}\psi_{2n,0}(Q), \\ \Psi_{v-}(Q) &= \sum_n C_{2n+1,v}\psi_{2n+1,1}(Q). \end{aligned} \tag{56}$$

$\psi_{2n,0}(Q)$ is the wave function of the two-dimensional harmonic oscillator for the level with energy $2n\omega_0$ and momentum $m = 0$, $\psi_{2n+1,1}(Q)$ is the radial (i.e. $\varphi = 0$) part of the wave function of this oscillator for the level with energy $(2n + 1)\omega_0$

and the momentum $m = 1$ (the energy of the zero-point state is considered equal to zero).[Pub V] These functions satisfy the following recurrent relations (see Appendix of Publication V):

$$\psi_{2n,0}(Q) = \frac{1}{2^n\sqrt{\pi}n!}e^{Q^2/2}\left(\frac{d^2}{dQ^2}+\frac{1}{Q}\frac{d}{dQ}\right)^n e^{-Q^2}$$
$$\left|\psi_{2n+1,1}(Q)\right| = \frac{e^{i\varphi}}{2\sqrt{n+1}}\left(Q-\frac{d}{dQ}\right)\psi_{2n,0}(Q), \tag{57}$$

facilitating the calculation of the coordinate dependencies of several hundred wave functions, as illustrated in Fig. 12.

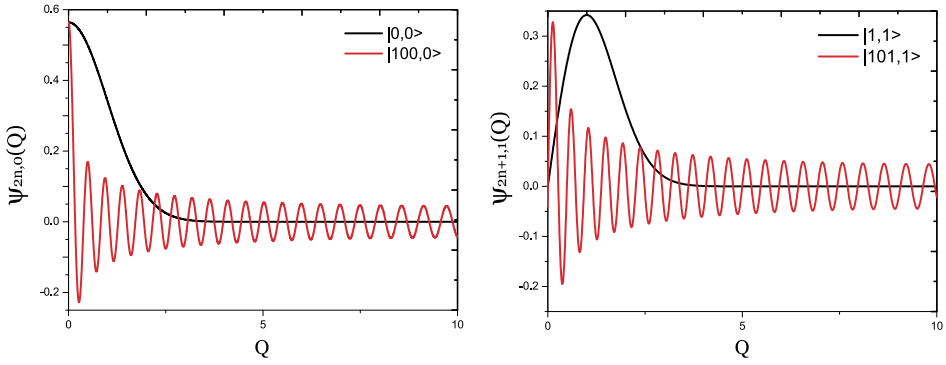

Fig. 12. Examples of the radial parts of wave functions $|0,0\rangle$, $|100,0\rangle$, $|1,1\rangle$ and $|101,1\rangle$ of 2-dimensional isotropic harmonic oscillator. Configurational coordinate Q is dimensionless.[Pub. V]

6.3 Results

The relaxation of the excited Jahn-Teller system from vibronic levels $|v > 0, J = 1/2\rangle$, restricted to paths through levels $|v > 0, J = |1/2|\rangle$, was explored under spectrally non-selective and spectrally selective excitations of electronic transitions $|A_1\rangle \rightarrow |E\rangle$. Fig. 13 depicts the APES of spectrally selective excitation and relaxation of the distribution function of configurational coordinate. The Debye-van Hove model was applied to describe the phonon density of states (see Section 4.5).

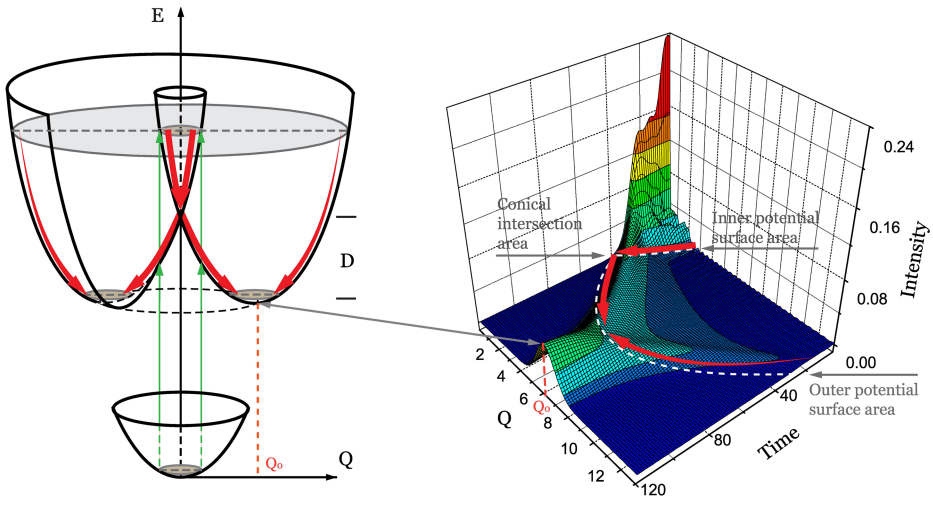

Fig. 13. Left: Scheme of APES depicting the Jahn-Teller $E \otimes e$-problem and electronic transitions in the configurational coordinate space. Right: Energy relaxation graph with quasi-monochromatic excitation; intensity axis corresponds to the value of the distribution function $P(Q,t)$. Note that graph depicts the "right half" of the potential. Relaxation process halts in the potential well around Q_0.[Pub. V]

6.3.1 Spectrally non-selective excitation

Under spectrally non-selective excitation (for example, excitation by a short light pulse), the initial distribution function comprises the sum of the distribution functions of all excited levels $|v\rangle$.[Pub V] The evolution of the distribution function was calculated for various parameters of linear vibronic coupling (from $D = 5$ to $D = 20$) and for various strengths of vibronic interaction with non-totally symmetric phonons (from $\lambda^2 = 0.05$ to $\lambda^2 = 0.2$).

As shown in Fig. 14, at small times, the distribution function primarily resides within the conical part of the potential (compare to Fig. 13, where on the distribution graph are marked half of the contours of the potential with dashed line). In the region of small coordinates, it can be detected that the peak of the distribution function first increases as the relaxation of the system moves towards the point of intersection of the surfaces. Additionally, there exists a discernible yet low distribution intensity near the outer surface of the potential. This underscores the significance of the effect of the turning points: the vibrating system tends to linger longer near these turning points compared to the intervals between them. Eventually, the relaxation process halts in the potential well at Q_0.

Given the typical vibrational frequency in crystals, on the order of $\omega_0 = 10^{13}\,Hz$, the time unit in the relaxation graphs approximates 0,1 ps. The characteristic time of total relaxation spans approximately 100–200 ω_0^{-1} (10–20 ps), while the characteristic time taken to traverse the conical intersection for the initial states considered in this chapter is around ~2–4 ps.

Fig. 15 illustrates similar parameters as in Fig. 14, with an increased interaction strength with phonons λ^2, resulting in a faster relaxation (the distribution function reaches quicker potential well, the region around Q_0).

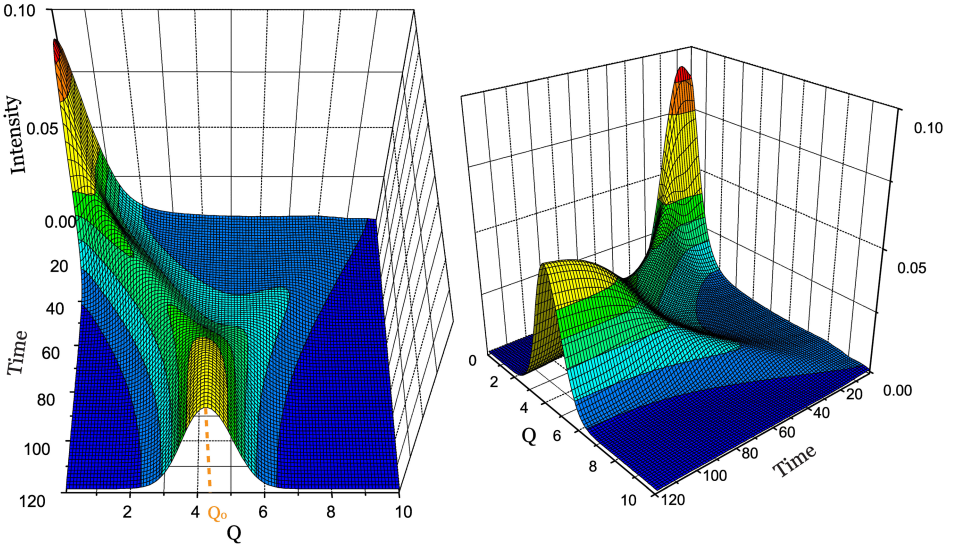

Fig. 14. Distribution function dependence of the configurational coordinate Q on time for spectrally nonselective excitation. $D=10$, $\omega_M=1.3$, $\lambda^2=0{,}1$. The typical time unit in case of crystals corresponds to 0,1 ps.[Pub. V]

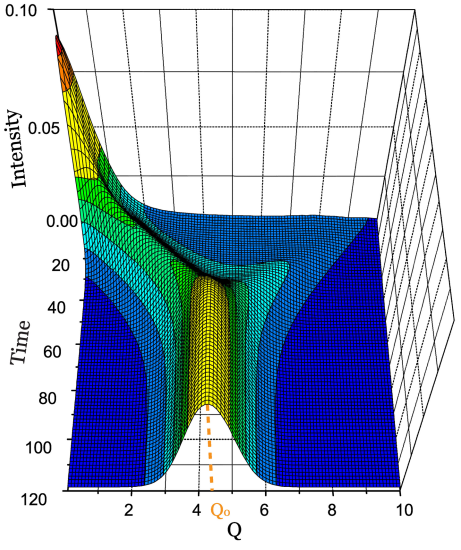

Fig. 15. Distribution function dependence of the configurational coordinate Q on time for spectrally nonselective excitation. $D=10$, $\omega_M=1{,}3$, $\lambda^2=0{,}15$.[Pub. V]

6.3.2 Spectrally selective excitation

Spectrally selective excitation was also studied. Here, the initial state $|A_1\rangle$ undergoes excitation with quasi-monochromatic light, leading to excitation of a specific vibronic level. Relaxation calculations were conducted across varying linear interaction strengths D, different strengths of vibronic interaction with nontotally symmetric phonons λ^2, and various excited levels.

Visualizing the population density of the vibronic levels (Fig. 16 b)), shows that each vibronic level above the conical intersection couples differently with phonons.[Pub V] Notably, the speed of relaxation near (above) the conical intersection is higher, indicative of the strongest nonadiabatic mixing of vibronic states in this region.[Pub V]

Fig. 16 c) illustrates the relaxation of the distribution function from the vibronic level $v = 7$, positioned below the conical intersection and Fig. 16 d) shows relaxation from level $v = 23$, situated above the conical intersection. If there is no relaxation through the conical intersection (as depicted in Fig. 16 c)), the two outermost higher peaks of the distribution function correspond to the inner and outer turning "points" of the potential.[Pub V] Corresponding distribution functions for $v = 7$ are depicted in Fig. 16 e), with their structures clearly discernible in the relaxation graph. If relaxation starts from the vibronic level above the conical intersection, the complex shape of distribution function inside the conical part of APES is evident, as shown in Fig. 16 d). Moreover, there is a noticeable intensity of the distribution function for large coordinate values, corresponding to the turning point of the vibrating system near the outer potential surface for relaxation below the conical intersection. However, the external turning point is scarcely visible in this figure when relaxation occurs above the conical intersection. This clearly demonstrates the importance of the conical intersection in relaxation, as the vibronic system really occurs inside the conic intersection; in a way, the system is dragged into a conical intersection. Indeed, the results presented here serve as compelling evidence, within the framework of strict quantum mechanical theory, of the profound significance of the conical intersection for the temporal evolution and relaxation of vibronic systems.

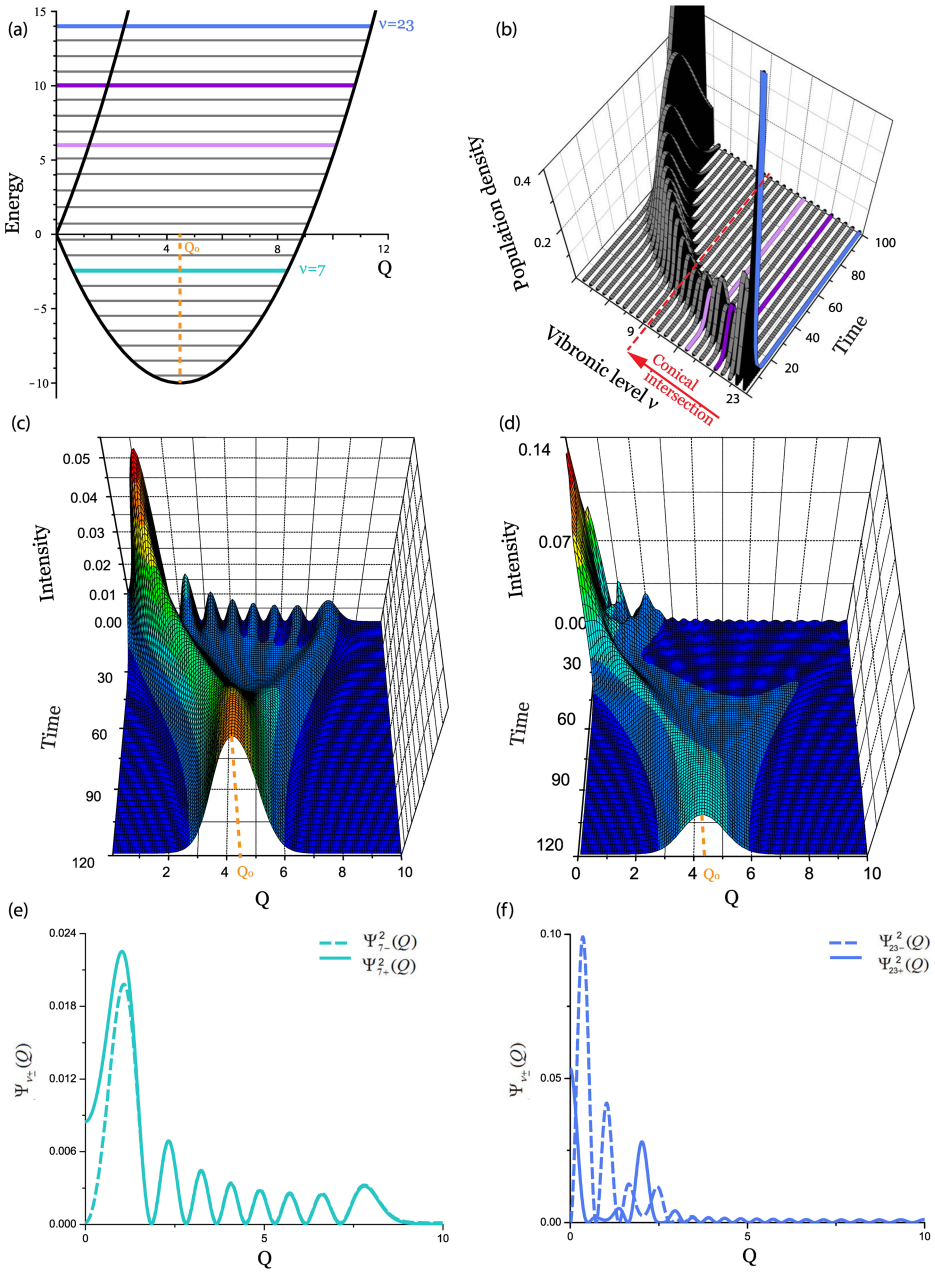

Fig. 16. Relaxation in the case of quasi-monochromatic excitation $D = 10$, $\omega_M = 1{,}3$, $\lambda^2 = 0{,}1$. A) APES and vibronic levels. Zero level of potential energy coincides with the conical intersection. B) Time dependence of vibronic level population (diagonal elements of density matrix). C) Time dependence of the distribution function of configurational coordinate Q in relaxation from $v = 7$, and D) in case of relaxation from $v = 23$. E) and F) Functions $\Psi^2_{v-}(Q)$ and $\Psi^2_{v+}(Q)$. Lower vibronic levels exhibit greater overlap of functions $\Psi^2_{v-}(Q)$ and $\Psi^2_{v+}(Q)$.[Pub. V]

6.4 Effect of Slonczewski resonances on relaxation through conical intersection

The evolution of the distribution function of the configurational coordinate within the conical part of the potential is rather nontrivial. This complexity arises from the presence of high-energy quantum levels known as Slonczewski resonances, which were introduced in Section 3.3.

In Fig. 17, the vibronic spectrum of the optical transition $|A_1\rangle \rightarrow |E\rangle$ is calculated for the case D=20. The line groups around the vibronic levels $v = 26$ and $v = 31$ represent the zero-point Slonczewski resonance and the first excited Slonczewski resonance, respectively.

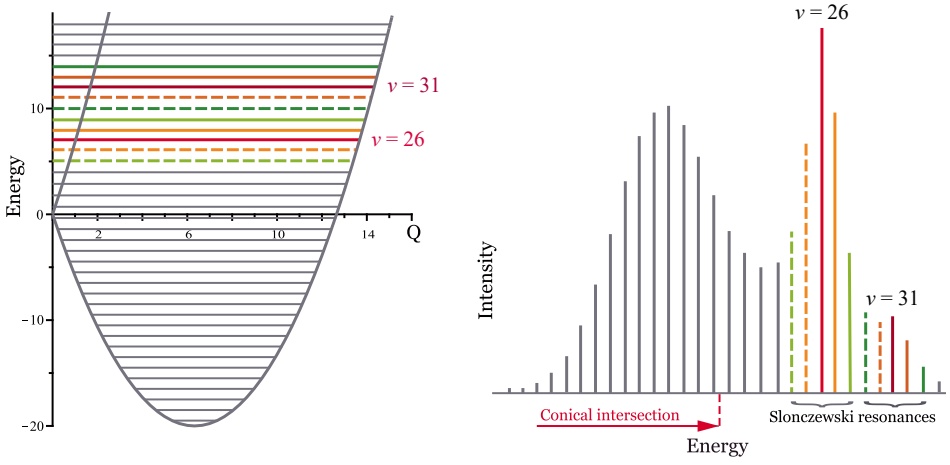

Fig. 17. Left: Vibronic potential for $D=20$. Right: Vibronic spectra for $D=20$. The spectral line groups around $v=26$ and $v=31$ vibronic levels are Slonczewski resonances. [Pub. V]

In Fig. 18, several cases of the relaxation process are depicted when a particular vibronic level is excited. As mentioned briefly in Section 3.3.1, it can be noted, that the non-monotonic behaviour of distribution functions depends on the position of the excited vibronic level within the Slonczewski line group of the absorption spectrum. If the most intense line within the Slonczewski resonance (or from the right within the same group) is excited, then the distribution function at small times is spread wider, and the maximum of distribution function is achieved later (for example, see Fig. 18, d, e, and h, i, j.[Pub V] Conversely, if the level to the left of the most intense vibronic line in the Slonczewski group is excited, then the maximum of the distribution function is situated at zero time at configurational coordinate zero (for example, see Fig. 18 a, b, and f, g).[Pub V]

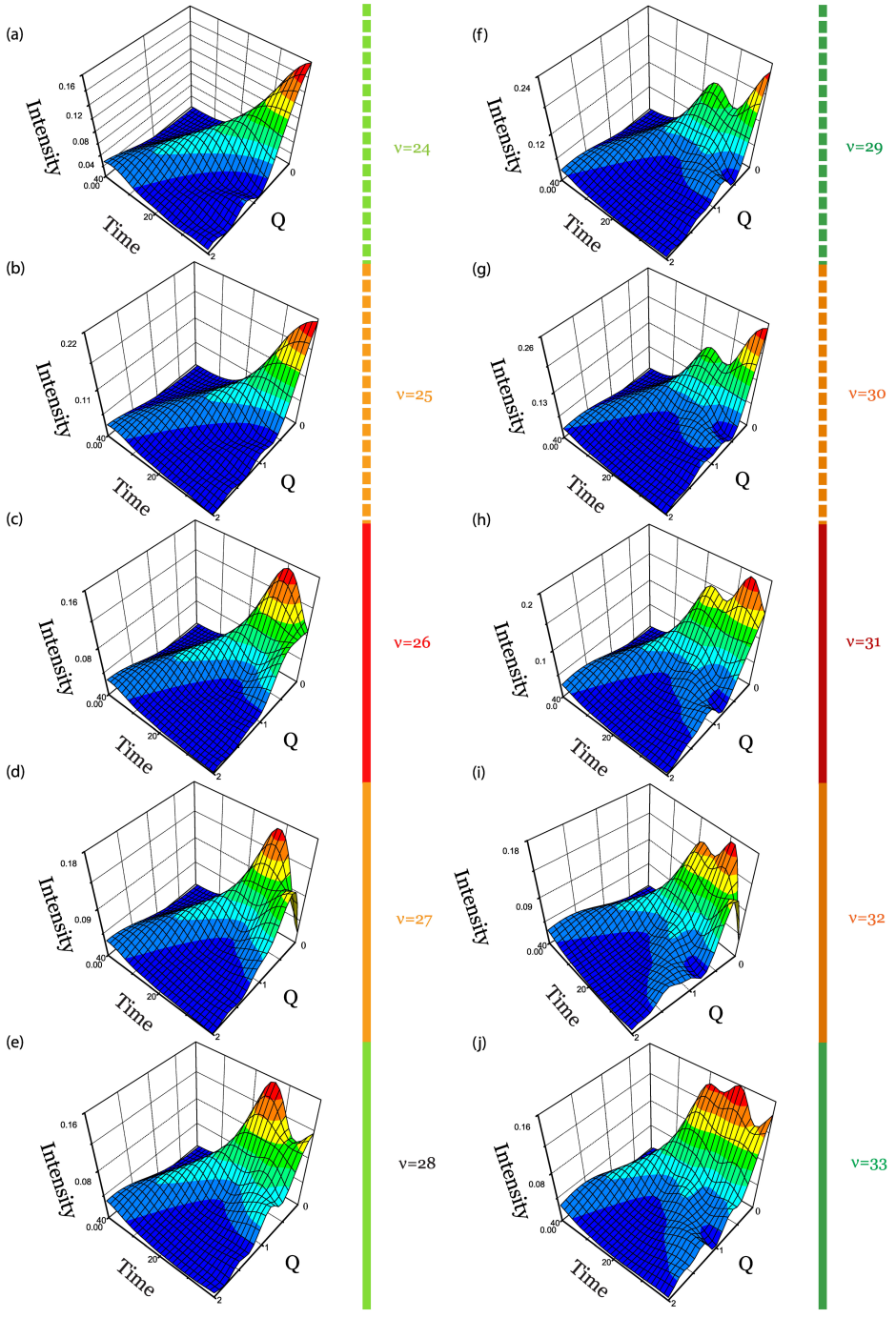

Fig. 18. Dependence of the distribution function of the configurational coordinate Q on time for quasi-monochromatic excitation $D=20$, $\omega_M=1{,}3$, $\lambda^2=0{,}1$, focusing on the area close to the conical intersection (origin of coordinates). Left column: Relaxation from levels belonging to the zeroth Slonczewski level. Right column: Relaxation from levels belonging to the first Slonczewski level. Note similarities in graphs row-wise, dependent on level position in Slonczewski resonance group.[Pub. V]

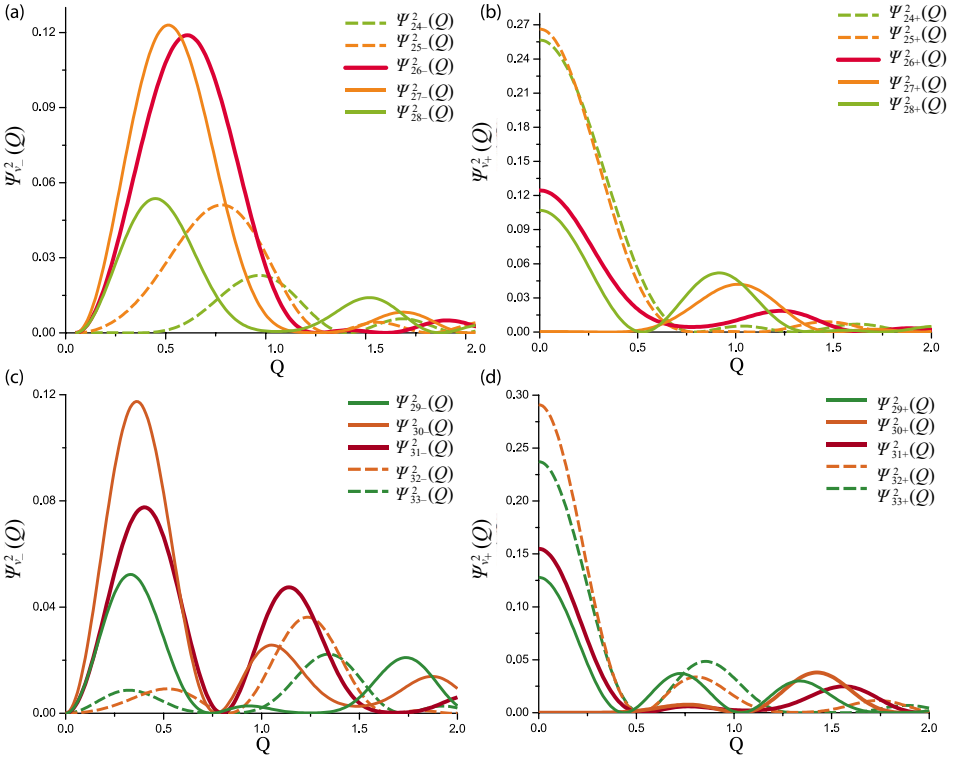

Fig. 19. Distribution functions of levels near Slonczewski resonances. Left column: Vibronic states with pseudorotation momentum quantum number –1/2. Right column: Vibronic states with the pseudorotation momentum quantum number +1/2. The maxima at small Q are due to Slonczewski resonances in conical intersections.[Pub. V]

To comprehend this behaviour, Fig. 19 presents the distribution functions of vibronic levels in Slonczewski resonances. The distribution functions of plus-states correspond to states with +1/2 electronic momentum quantum number and with the 0 vibrational momentum, while minus-states correspond to states with –1/2 electronic momentum quantum number and +1 vibrational momentum quantum number. [Pub V] Fig. 19 shows that below the levels $v = 26$ and $v = 31$, the plus-states have high peaks at the beginning of the coordinate, which explains the shape for relaxation graphs for levels $v = 24$, $v = 25$, $v = 29$ and $v = 30$. Above the levels $v = 26$ and $v = 31$ the plus-states have low or no peaks at the beginning of coordinate Q, but corresponding minus-states have high peaks. This explains the shape for relaxation graphs for levels $v = 27$, $v = 28$, $v = 32$, $v = 33$ and why the maximum intensity for the distribution function is achieved later. The non-monotonic shape of the relaxation graphs in Fig. 18 also arises from the fact that plus-states relax to the nearest minus-states with lower energy and vice versa.[Pub V]

7 QUANTUM FRICTION OF PSEUDOROTATION IN JAHN-TELLER SYSTEM

In the preceding chapter, the relaxation dynamics of the excited impurity centre with Jahn-Teller $E \otimes e$-problem was described, focusing solely on vibronic levels characterized by pseudomomentum (total angular momentum) $J = |1/2|$. This chapter and in **Publication VI** explores the relaxation process with an expanded scope, taking into account also the states with $J > |1/2|$. These excited vibronic states with $J > |1/2|$ can be attained through the excitation of the vibronic system with strong second order vibronic coupling. Random strains in the crystal can localize the tunnelling state of second order coupling to a specific minimum. Following the Franck-Condon principle, states with high pseudomomentum can be achieved through this excitation process. Since J is not a quantum number in the presence of both linear and quadratic vibronic coupling, using light of different frequencies, allows for the population of states with varying J. The excitation and relaxation processes are elucidated in Fig. 20.

Relaxation occurs through the emission of phonons with momentum ±1. Consequently, the pseudomomentum J predominantly decreases. This process can be called a quantum friction of pseudorotation. However, there exists a statistical probability that the momentum of the emitted phonon differs in sign from the pseudomomentum of the vibronic state, leading to instances where the pseudomomentum J of the excited Jahn-Teller centre may momentarily increase during relaxation. Such a process is absent in the classical limit, where the angular momentum of a rotating body can only decrease over time due to friction with the environment. Quantum effects are especially noticeable near the conical intersection, where the anomalous effects of friction during rotation are amplified due to the paramount importance of nonadiabaticity (the system's high rotational frequency), which has a purely quantum origin.

Utilizing the method outlined in Chapter 4, calculations of the relaxation of the $E \otimes e$-system were performed for various vibronic interaction strengths D and initial vibronic levels v with differing initial momentum of the pseudorotation J. Given the pivotal role of Slonczewski resonances in determining the special effects of relaxation kinetics, particular attention was devoted to studying them. Similar to the calculations of resonant Raman scattering spectra and relaxation in Chapter 5 and 6, the Debye-van Hove model was applied to simulate the phonon continuum.

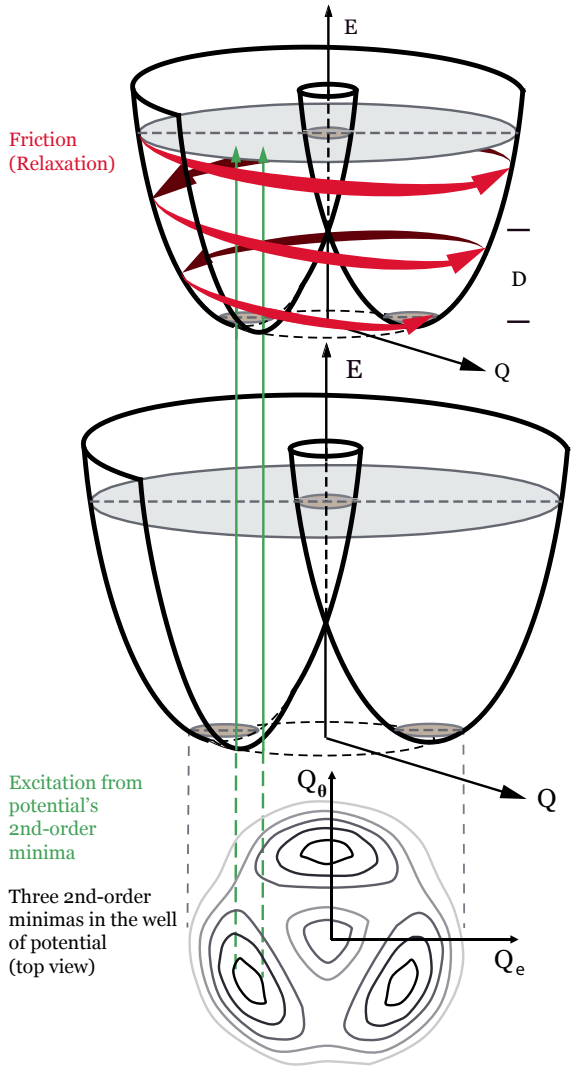

Fig. 20. Scheme of electronic transitions in configurational coordinate space. The lowermost part of scheme depicts a bottom view of APES with three minima of second order vibronic interaction. The second-order minima are in potential bottom as also depicted in Fig 3.[Pub. VI]

7.1 Vibronic states below conical intersection and Berry phase

A general description of high energy states above the conical intersection describing the Sloncezewski resonances, was given in Section 3.3. In this section, the distinctive characteristics of the energy spectrum below the conical intersection are described, focusing on vibronic states near the potential energy

minimum. For these states, the geometric phase or Berry phase plays a crucial role in determining the energy spectrum.

Berry demonstrated in 1984 that the adiabatic transportation of a wave function around a closed loop results in a geometrical phase factor[37] (in addition to dynamical phase factor predicted by the adiabatic theorem). In systems with a conical intersection, the adiabatically changing parameters encompass molecular coordinates, indicating singular relations between two parameters – mixed electronic and atomic motions in the case of a conical intersection. Longuet-Higgins highlighted in his seminal work on $E \otimes e$-problem[49] that half-integer rotational quantum number J is manifestation of the geometrical phase.

To present the results obtained regarding pseudo-rotation friction in the $E \otimes e$-system, it is beneficial to briefly reference the findings of Longuet-Higgins[49] et al. concerning pseudo-rotation in this system. The energy spectrum for pseudo-rotation can be derived from diagonal part of the Hamiltonian of the radial motion (Eq. (8)):

$$H_{0J} = \frac{1}{2}\left(-\frac{d^2}{d\xi^2} + \xi^2 + \frac{J^2}{\xi^2} + \left(\frac{d\phi}{d\xi}\right)^2 + U_0\Theta(-\xi) \right) \cdot I + \sqrt{\left(\frac{J^2}{2\xi^2}\right)^2 + k^2\xi^2} \begin{pmatrix} 1 & 0 \\ 0 & -1 \end{pmatrix}.$$

By using the diagonal term $(H_{0J})_{11}$ (in Section 3.3), the Hamiltonian of the adiabatic motion above the conical intersection of APES was found in **Publication VI**. The diagonal term $(H_{0J})_{22}$ of Eq. (8) gives the Hamiltonian of the adiabatic motion below the conical intersection of APES. To simplify the calculation of the energy of the lowest vibronic levels, certain approximations can be applied. Specifically, if the vibronic interaction is strong ($D \gg 1$) and considering that the potential minimum is located at $\xi = k = \sqrt{2D}$, ξ may be replaced by k in the J-dependent terms.[49] Consequently, the equation for the energy of (lowest) vibronic levels becomes:

$$E_{nJ} \approx \hbar\omega_0 (n + \frac{1}{2} - D) + \hbar\omega_0 \frac{J^2}{4D}\left(1 + \frac{J^2}{16D^2}\right), n = 0,1,2,\ldots . \tag{58}$$

Here, $\hbar\omega_0$ (n + 1/2) represents the energy of the radial vibrations, $-\hbar\omega_0 D$ is the Jahn-Teller stabilization energy, and $\hbar\omega_0 \frac{J^2}{4D}\left(1 + \frac{J^2}{16D^2}\right)$ denotes the energy of the pseudorotation.[Pub VI] Eq. (58) implies that the zero-point energy of the pseudo-rotation is nonzero. The energy spectrum of conventional rotation around a single axis is represented by $E_m = (\hbar^2 / 2I_C)m^2$, where $m = 0,1,2,\ldots$ is integer, I_C is the moment of inertia, hence the zero-point energy equals zero. However, considering circular transportation of the wave function around a closed loop, the electronic factor multiplies by –1 in the case of adiabatic process. In the $E \otimes e$-

problem, the phase of nuclear motion also changes, leading to a distinction between two components of the ground state of atomic motion, both of which are nontotally symmetric. This, in turn, is the reason, why the zero-point energy $E_{0,PR}$ holds a nonzero value.

7.2 Rates of vibronic transitions with emission of phonons

In Chapter 6, the rates of vibronic transitions were found, exclusively considering the states with $J = |1/2|$. The general matrix elements of the transition can be derived from the Hamiltonian describing the interaction with phonons in Eq. (41). The matrix elements of transitions $|v, J\rangle \rightarrow |v', J \pm 1\rangle$ are given by

$$\left\langle 1_{j,\mp} \middle| \left\langle v', J \pm 1 \middle| H' \middle| v, J \right\rangle \middle| 0 \right\rangle = \lambda \vartheta_j S^{(v,v')}_{J,J\pm1} \,, \tag{59}$$

where $|1_{j,\pm}\rangle$ represents the one-phonon state with the frequency of the phonon ω_j and the rotational momentum $m = \pm 1$, and

$$\begin{aligned} S^{(v,v')}_{J,J\pm1} = \sum_n \Big[& C^{(v',J\pm1}_{2n} (C^{(v,J}_{2n} \sqrt{n + J \pm 1/2} + C^{(v,J}_{2n\pm2} \sqrt{n + 1/2 \pm 1/2}) \\ & + C^{(v',J\pm1}_{2n+1} (C^{(v,J}_{2n+1} \sqrt{n + J + 1 \pm 1/2} + C^{(v,J}_{2n+1\pm2} \sqrt{n + 1/2 \pm 1/2}) \Big]. \end{aligned} \tag{60}$$

Applying Fermi Golden Rule, we obtain the following equation for transition rates:

$$\Gamma_{v,J\rightarrow v',J\pm1} = \frac{2\pi}{\hbar} \left| S^{(v,v')}_{J,J\pm1} \right|^2 \int_0^{\omega_M} d\omega \vartheta^2(\omega) \delta(E_{v,J} - E_{v',J\pm1} - \hbar\omega), \tag{61}$$

where $\vartheta^2(\omega) = \sum_j \vartheta_j^2 \delta(\omega - \omega_j)$, and ω_M is the top phonon frequency.[Pub VI]

Knowing the rates of vibronic transitions enables the description of the time dependence of the relaxation of the vibronic system by solving the rate (kinetic) equations:

$$\dot{\rho}_{v,J} \approx -\Gamma_{v,J} \rho_{v,J} + \sum_{v'} \left(\Gamma_{v',J+1\rightarrow v,J} \, \rho_{v',J+1} + \Gamma_{v',J-1\rightarrow v,J} \, \rho_{v',J-1} \right), \tag{62}$$

where $\rho_{v,J}$ represents the population density of the vibronic level v, J and

$$\Gamma_{v,J} = \sum_{v'} \left(\Gamma_{v,J\rightarrow v',J+1} + \Gamma_{v,J\rightarrow v',J-1} \right) \tag{63}$$

is the total decay rate of the vibronic level v, J.[Pub VI] Eq. (62) was solved numerically for various initial conditions of the population factors.

7.3 Results

Applying the presented theory, it is possible to calculate relaxation from any energy level with $|v \geq 0, J \geq 1/2\rangle$. Considering all possible transitions where $\Delta_m = \pm 1$ and $\Delta E \leq \omega_M$ are taken into account allows for the consideration of all energy levels participating in the relaxation process. Here are presented three exemplary cases for relaxation with different initial states.

7.3.1 Relaxation of a purely rotating state $v = 0, J > 1/2$

At first, we consider the relaxation of a purely rotating state ($v = 0$) and $J > 1/2$, where the initial wave packet gradually loses its rotational momentum and ends up at a vibronic state $|v = 0, J = 1/2\rangle$. Fig. 21 depicts the energy levels of the linear vibronic system found by solving the eigenvalue problem Eq. (7) for different $J = \pm 1/2, \pm 3/2, \pm 5/2, \ldots$.

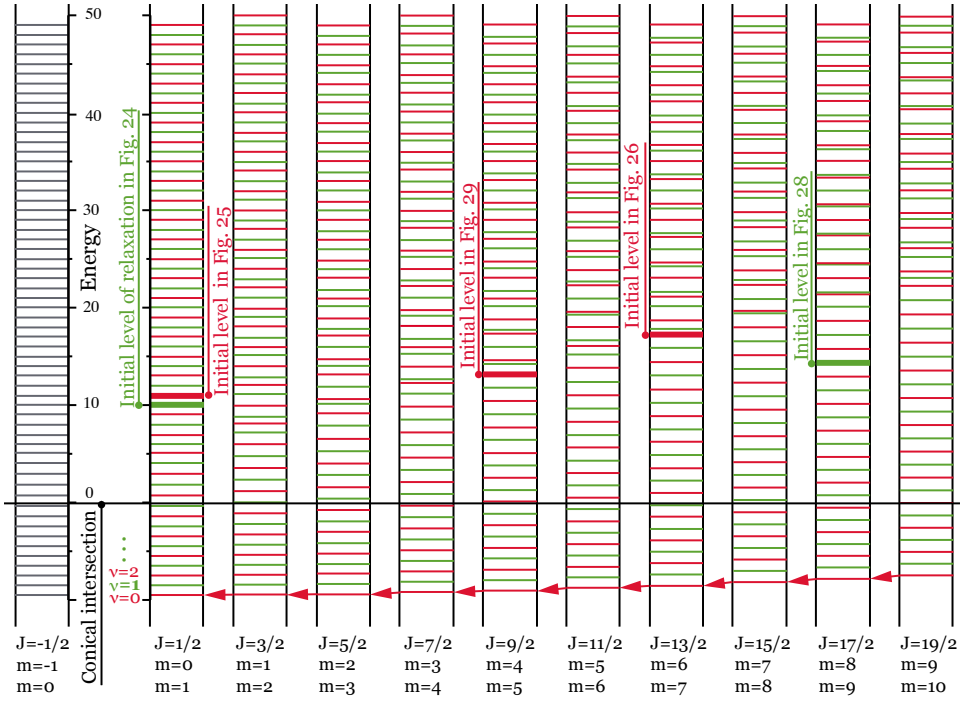

Fig. 21. Energy level diagram with different J values, $D = 10$. "Left side" of the diagram with negative J values is omitted, as energy levels for $\pm J$ are mutually equal. Red arrows mark the relaxation path of purely rotating state ($v = 0$) and $J > 1/2$.[Pub. VI]

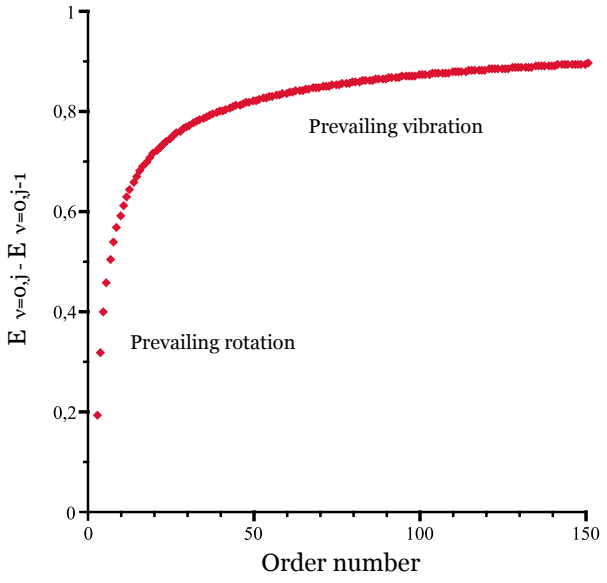

Fig. 22. Difference between adjacent energy levels in case of $D = 10$, $v = 0$, $J = 1/2\ldots 199/2$. [Pub. VI]

Fig. 22 illustrates the differences between adjacent energy levels of purely rotational states ($v=0$) and $J \geq 1/2$. For small values of J, these differences are in good agreement with the energy of the pseudorotation $\hbar\omega_0 \frac{J^2}{4D}\left(1+\frac{J^2}{16D^2}\right)$ as defined in Eq. (58). The linear dependence of energy differences on J indicates that the system exhibits rotational behaviour in these states.[Pub VI] However, when J becomes very large, the vibronic interaction becomes negligible, and the system behaves akin to a circular oscillator. This is the reason, why differences between adjacent levels are close to the vibrational quantum in case of large J.[Pub VI]

In Fig. 23, the relaxation from vibronic level $|v = 0, J = 79/2\rangle$ is depicted. The figure highlights the difference in relaxation rates between high-energy vibrational-like states (upper states) and rotational-like states near the bottom of the potential surface, with vibrational-like states exhibiting a higher relaxation rate. The deceleration of the relaxation near the bottom of the APES stems from the decreasing energy differences between vibronic levels and the corresponding smaller density of states of the phonons, which can lead to decay transitions.

It's noteworthy that the deceleration of relaxation in its final stages is attributed to two factors: a) moving away from the conical intersection, and b) reducing energy differences between adjacent levels: a decrease in energy difference results in smaller phonon quanta at corresponding energies, leading to fewer contributing phonons (smaller density of states). Additionally, the relaxation rate decreases for large J due to the diminishing vibronic contribution to these states as J increases. As mentioned in the previous chapter, the time unit in the graph is

of order of 0,1 ps. For the systems and initial states studied in the current chapter, the characteristic time of total relaxation is around 300–500 ω_0^{-1} (30–50 ps), and the characteristic time of passing through the conical intersection is ~2,5 ps.

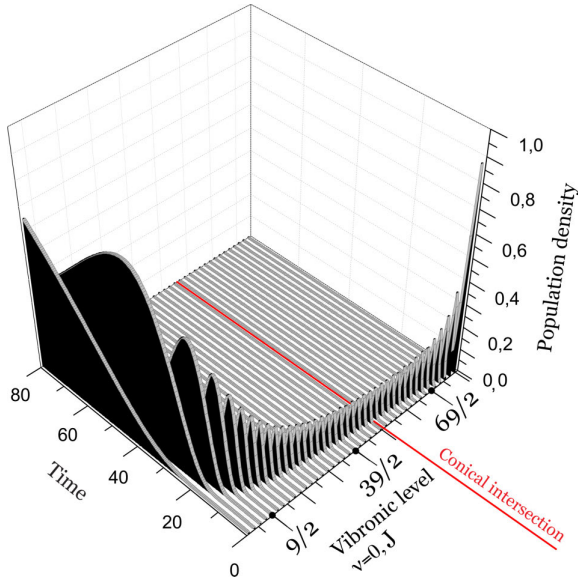

Fig. 23. Temporal dependence of the population densities of the vibronic levels with different J for relaxation from vibronic level $|v = 0,\ J = 79/2\rangle$, D = 0, $\omega_M = 1{,}3$, $\lambda^2 = 0{,}01$. In crystals, the used time unit is typically of the order 0,1 ps.[Pub. VI]

7.3.2 Relaxation of combined vibrational-rotational states

a) Relaxation from vibronic level $|v > 0,\ J = 1/2\rangle$.

Next, relaxation from the states $|v > 0,\ J = +1/2\rangle$ to the states $|v = 0,\ J = +1/2\rangle$ and $|v = 0,\ J = -1/2\rangle$ was studied. All possible transitions, where $\Delta m = \pm 1$ and $\Delta E \leq \hbar\omega_M$ are taken into account. An intriguing result emerges: in this type of excitation the vibronic levels with $J > 1/2$ also participate in the relaxation process. Transition probabilities to states with higher $|J|$ (higher rotational momenta $|m|$ of vibrations), are in some cases found to be comparable to transition probabilities to states with lower $|J|$ (lower $|m|$).[Pub VI]

Fig. 24 shows the relaxation from vibronic level $|v = 19,\ J = 1/2\rangle$, while Fig. 25 illustrates the relaxation from vibronic level $|v = 20,\ J = 1/2\rangle$. With a vibronic interaction strength of $D = 10$, the conical intersection is between levels $v = 9$ and $v = 10$. The graphs group vibronic levels with equal v and varying $J = -19/2,\ -17/2,\ \ldots\ 19/2$. So each group comprises twenty levels with fixed v, level $J = -1/2$ is highlighted with a red line. See also Fig. 27, which explains the principle how the levels are depicted in the figures. Since in both cases is excited level $J = 1/2$, the graph vividly illustrates how the population spreads to levels

with $J > 1/2$. Transitions tend to conserve the sign of rotational momentum (direction of rotation), meaning transitions between states $|J = 1/2\rangle \rightarrow |J = 3/2\rangle$ are generally more probable than transitions $|J = 1/2\rangle \rightarrow |J = -1/2\rangle$.[Pub VI] This tendency is evident in the graphs, where the population density tends to maintain either left or right side from the red line (level $J = -1/2$). However, Slonczewski resonances can alter the course of relaxation. This effect is apparent in Fig. 25, where the starting point for relaxation is level $|v = 20, J = 1/2\rangle$, but $|v = 19, J = -1/2\rangle$ serves as a resonance level, leading to relaxation mainly through vibronic levels with negative J. Additionally, there is faster relaxation observed above the conical intersection.

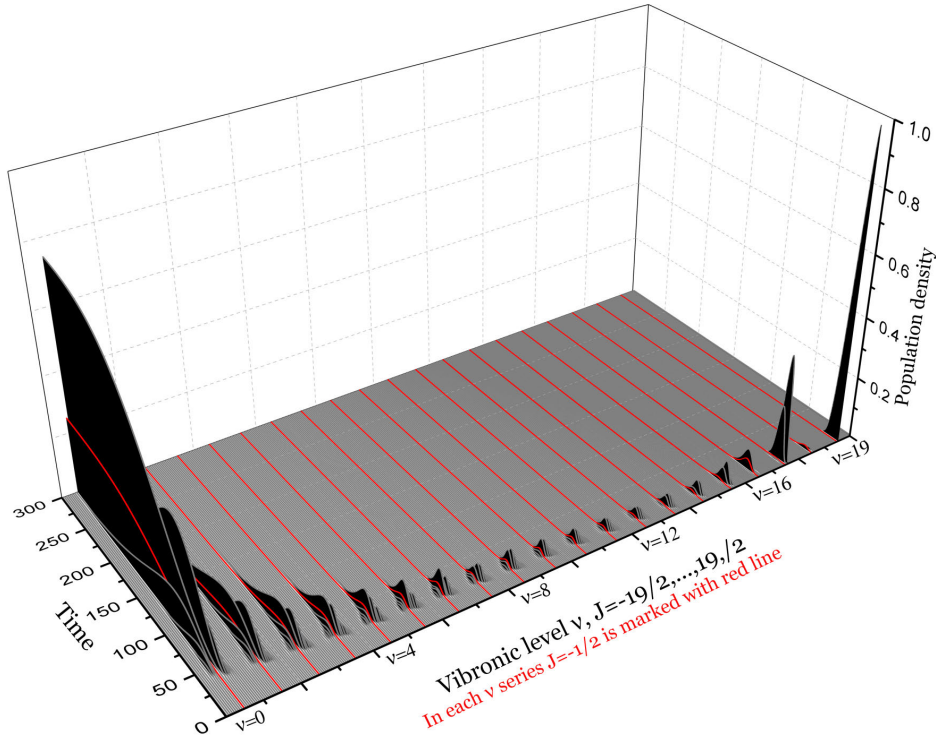

Fig. 24. Temporal dependence of the population densities of the vibronic levels with different v and J. Initial state for relaxation is chosen vibronic state $|v = 19, J = 1/2\rangle$ with local vibronic interaction strength $D = 10$ and parameters for relaxation $\omega_M = 1{,}3$, $\lambda^2 = 0{,}01$. The unit of the measurement of time in the order of magnitude is 0,1 ps. Red lines correspond to population densities of levels with $J = -1/2$ and varying v. Other lines, deviating from these, correspond to the same v but with other J (line position in one group with fixed v corresponds to varying value of $J = -19/2, \ldots, 19/2$). See also Fig. 27, to comprehend in detail vibronic levels representation in the graphs. For particular case (starting position $J = 1/2$) dominant values of J are typically positive, indicating general maintenance of dominant rotation direction during relaxation.[Pub. VI]

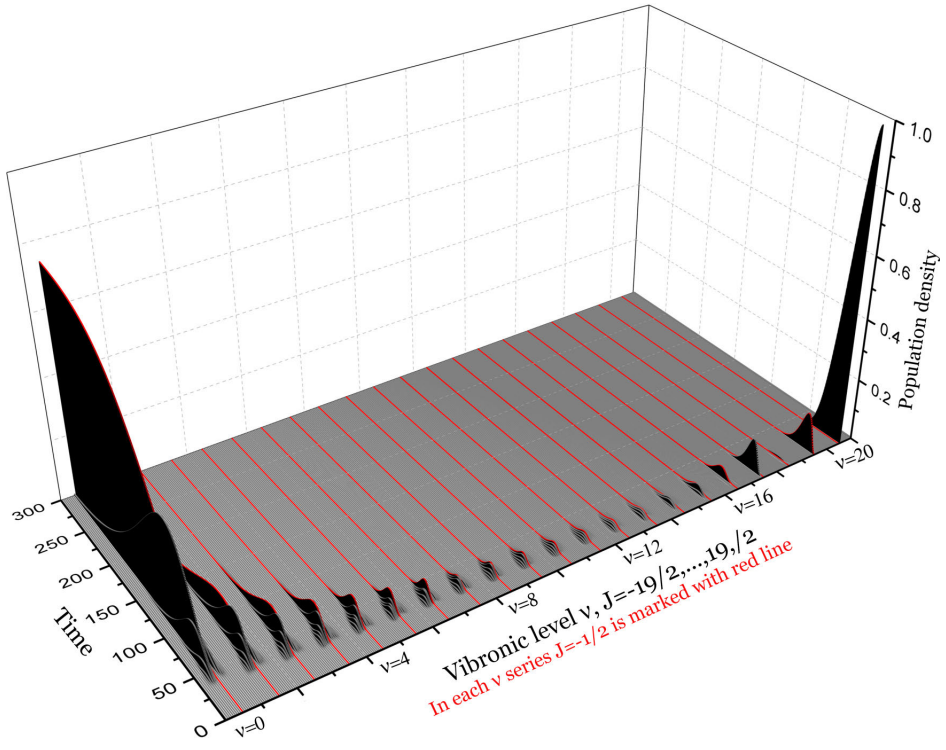

Fig. 25. Similar to Fig. 24 but for initial vibronic state $|v = 20, J = 1/2\rangle$. The unit of the measurement of time in the order of magnitude is 0,1 ps. Note that after reaching level $v = 20, J = 1/2$, dominant rotation direction changes. [Pub. VI]

b) Relaxation from vibronic level $|v > 0, J > 1/2\rangle$.

As for cases above, the calculations are performed for a vibronic interaction strength $D = 10$. Fig. 26 showcases relaxation from the vibronic level $|v = 20, J = 13/2\rangle$. For $J = 13/2$ the conical intersection area is between levels $v = 7$–8 (for $J = 1/2$ it was $v = 9$–10). It's observed that relaxation occurs more rapidly directly above and in the conical intersection area. Generally, transitions to states with smaller $|J|$ are more probable, except the transitions from $|J| = 1/2$, as discussed earlier.[Pub VI]

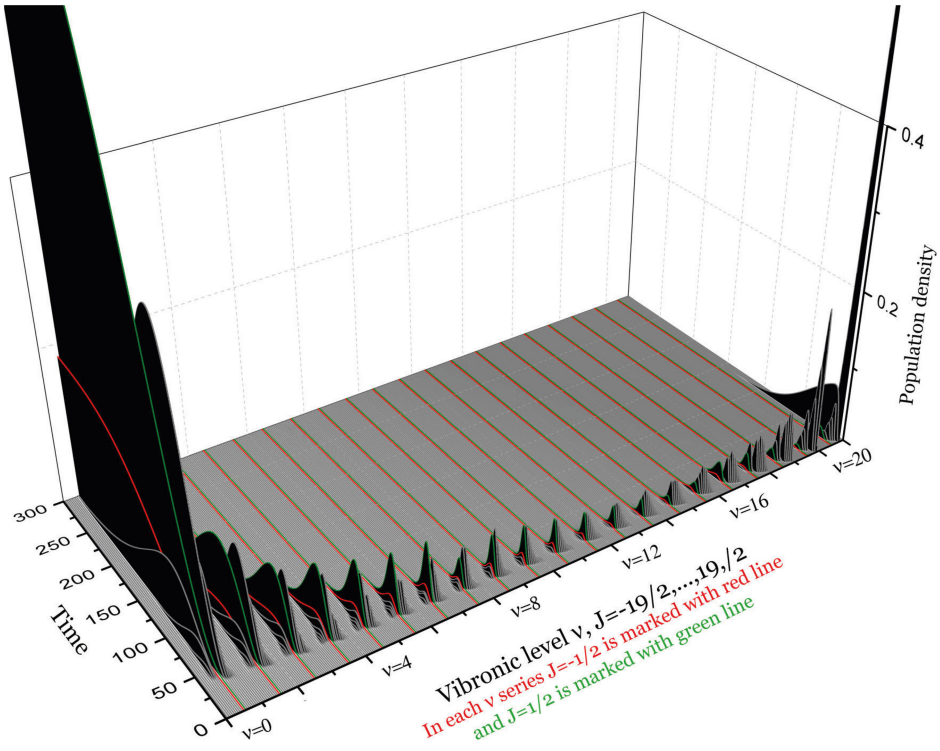

Fig. 26. Relaxation of the $E \otimes e$-system with vibronic interaction strength $D = 10$ from vibronic state $|v = 20, J = 13/2\rangle$ for relaxation parameters $\omega_M = 1{,}3$, $\lambda^2 = 0{,}01$. The unit of the measurement of time in the order of magnitude is 0,1 ps.[Pub. VI]

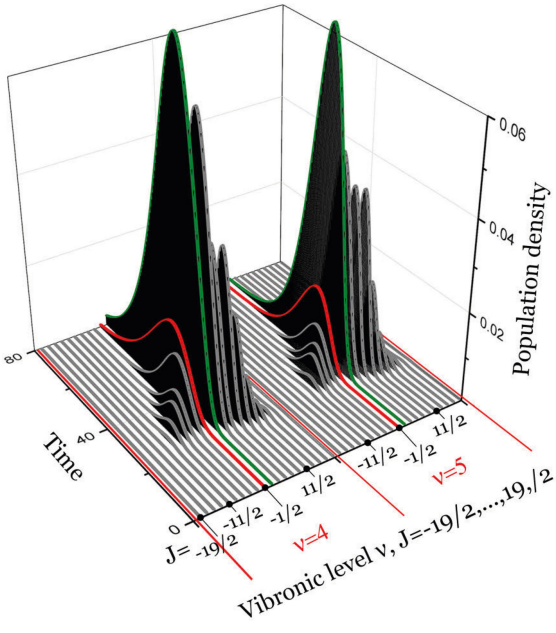

Fig. 27. Enlarged fragment of Fig. 26. For fixed v vibronic levels with varying $J = -19/2, -17/2, \ldots, 19/2$ are shown. Same principle of vibronic levels representation is applied in Fig. 24–Fig. 29.[Pub. VI]

Fig. 28 displays results for relaxation calculations with a vibronic interaction strength of $D = 3$, with the initial state being $|v = 18, J = 17/2\rangle$. The conical intersection area lies between $v = 3\ldots1$ for $D = 3$, and $J = 1/2\ldots13/2$.[Pub VI]

Slonczewski resonances alter the energy gap between adjacent levels, affecting relaxation time and whether J increases or decreases during the relaxation process. For certain adjacent levels, the gap may exceed the maximum phonon frequency, resulting in slower relaxation, as depicted in Fig. 29 for level $|v = 10, J = 15/2\rangle$. Relaxation to the level with $J = 13/2$ in the one-phonon approximation is impossible, and relaxation to the level with $J = 17/2$ is very slow due to the small vibronic factor S for transition $|v = 10, J = 15/2\rangle \rightarrow |v = 9, J = 17/2\rangle$.

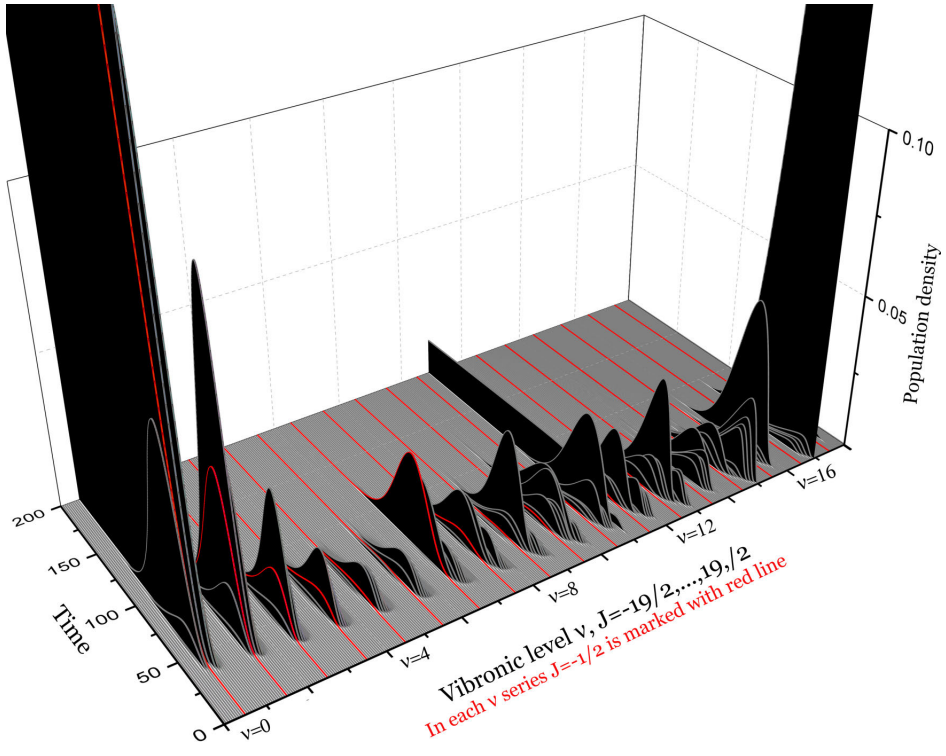

Fig. 28. Relaxation of the $E \otimes e$-system with vibronic interaction strength $D = 3$ from vibronic level $|v = 17, J = 17/2\rangle$ for relaxation parameters $\omega_M = 1{,}3$, $\lambda^2 = 0{,}01$.[Pub. VI]

The transition probabilities to levels with higher rotational momenta $|m|$ may become comparable to those of levels with smaller rotational momenta due to the Slonczewski resonances. Fig. 29 depicts such a scenario when the excited level is $|v = 18, J = 9/2\rangle$.[Pub VI] Calculations reveal that even states with $J = 17/2$ become populated during relaxation. This increase in rotational momenta is solely a quantum effect. As mentioned earlier, the phenomenon lies in the quantum origin of these resonances, making the quantum effects of rotational friction crucial in this context.

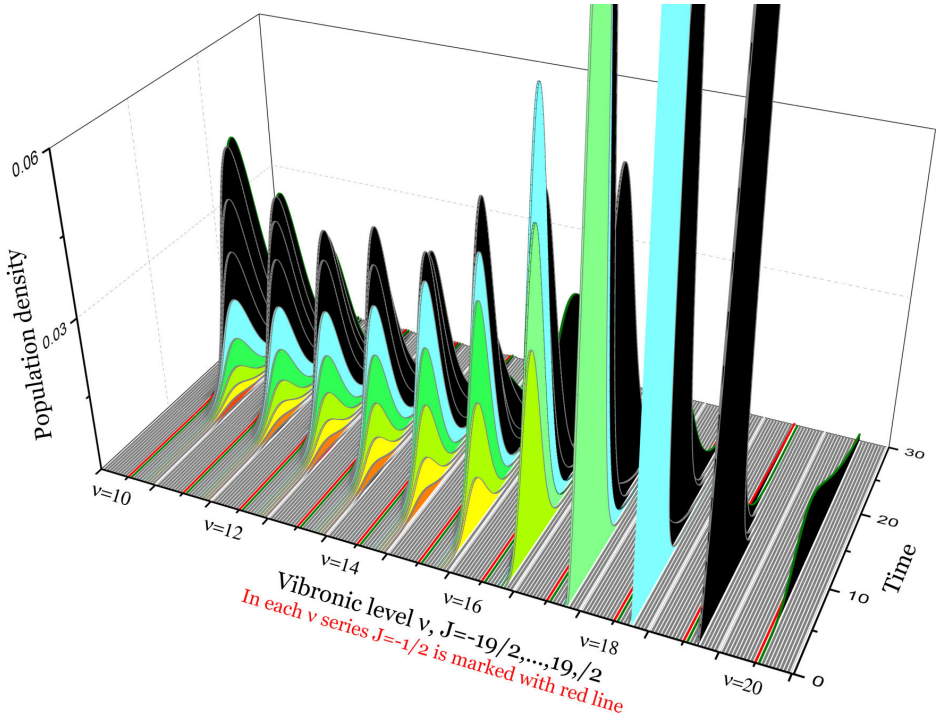

Fig. 29. Relaxation of the $E \otimes e$-system from the vibronic level $|v = 18, J = 9/2\rangle$, $D = 10$, $\omega_M = 1{,}3$, $\lambda^2 = 0{,}01$ (fragment of the graph). The unit of the measurement of time in the order of magnitude is 0,1 ps. White stripes separate the areas with fixed v but different J. Black curves correspond to $J < 9/2$, blue curves correspond to levels with $J = 9/2$, green curves to $J = 11/2$, green-yellow curves to $J = 13/2$, yellow curves to $J = 15/2$, and orange curves to $J = 17/2$. Reaching states with $J > 9/2$ (from initial blue to orange and even red) implies acceleration of pseudorotation during relaxation.[Pub. VI]

8 FURTHER DEVELOPMENTS

In addition to the problems addressed and discussed in this dissertation, there are several other aspects regarding vibronic interaction that warrant further consideration in the near future. Vibronic interactions are responsible for numerous fundamental processes across a wide range of systems. In order to comprehend and describe these processes, a thorough understanding of the ground electronic states of vibronic system, as well as all excited states with energies of several electronvolts, is necessary. Applying Density Functional Theory (DFT) is today a main way for the theoretical investigation of atomic and molecular systems. However, a significant limitation of this method is its strictly justified applicability only for describing the ground electronic state of solids, as well as for atomic and molecular systems. There have been numerous efforts to adapt the DFT with certain modifications to calculate excited states, but these modifications allow us to calculate only the first few excited states, and the justification for the applicability of these methods still leaves much to be desired. A solution to this problem for localized systems with a finite number of valence electrons has recently been proposed in papers published by researchers from the University of Tartu.[81–83]

The proposed method[81–83] is applicable to vibronic systems where the primary contribution to the considered properties arise from a finite (and not excessively large) number of valence electrons and nuclear degrees of freedom. Constraining the number of the electronic and vibrational degrees of freedom allows formulating a theoretical model of the system, which enables to study the vibronic effects that are caused by all the considered degrees of freedom. The underlying principle behind the solution is as follows: utilizing the theoretical model of valence electrons allows by diagonalization of the vibronic energy matrix to observe changes in all electronic states, including the ground state, due to alterations in the system's configuration. By comparing the theoretically derived characteristics of the ground state for different (distorted) configurations with the DFT calculations of this state for the same configurations it is possible to determine all vibronic interaction parameters. Subsequently, this allows us to identify potential energies, their conical intersections and other cross-sections for all significant excited states. This knowledge forms the foundation for describing vibronic processes triggered by various perturbations of the system. This method was applied in Refs[81–83] on several systems, such as bi-benzene, benzene stacks, and chemically bound benzene-graphene structures, revealing the pivotal role played by Jahn-Teller and pseudo-Jahn Teller effects in the formation of fundamental structures. We intend to conduct similar studies on other molecular systems, including DNA and graphene.

As mentioned in Section 4.4, vibronic interaction in Jahn-Teller systems may lead to interaction between centres situated apart. This interaction may prove crucial for systems which are close to structural phase transitions with non-totally

symmetric vibrations contributing significantly to the interaction, responsible for the transitions. We aim to revisit this problem in future by employing the methodology outlined in this thesis to describe the interaction of JTE systems with the phonon continuum. Additionally, the method allows for the investigation of the interaction between Jahn-Teller systems and low-energy acoustic phonons, including sound.

SUMMARY

Herein lie the principal findings of the thesis concerning the theory of electron-phonon interaction in molecular systems and impurity centres in crystals with degenerate electronic states.

The doctoral thesis deals with the interaction between local nuclear vibrations and the motion of electrons in solid and molecular systems, which is called the vibronic interaction. Often this interaction is small and is neglected to simplify calculations. However, there are systems where the consideration of this interaction is necessary for an adequate description of the characteristic properties of the system, and it is responsible for important quantum effects. The main focus of the doctoral thesis is to study the impurity centre of the crystal in the excited state, in which there is a vibronic interaction and which in turn interacts with the vibrations of the crystal lattice, the numerical magnitude of which is $\sim 10^{23}$. A purely quantum mechanical theory and corresponding calculations are presented to describe the interaction between the crystal impurity centre and the crystal lattice vibrations.

The interaction of degenerate electronic and vibrational states causes spontaneous symmetry breaking and mixing of electronic and vibrational states in the system. A remarkable manifestation of the vibronic interaction in systems with electronic degeneracy (or quasi-degeneracy) is the existence of conical intersections within the adiabatic potentials of these systems. Extensive literature examines the role of conical intersections in chemical transformations, as it largely determines the photochemical properties of the systems. The $E \otimes e$ Jahn-Teller system serves as an archetype of such systems with a conical intersection. As shown by Slonczewski, a distinctive quantum phenomenon emerges from a conical intersection – high-energy quantum states in the upper (conical) part of the potential with a mixed electron-vibrational (vibronic) origin. These states are called Slonczewski resonances. A clear manifestation of these states was independently discovered in 1972 by V. Loorits (University of Tartu) and M. C. M. O'Brien and S. N. Evangelou (University of Oxford) in a numerical study of the optical spectra of $E \otimes e$-systems. A complementary numerical study of these resonances in optical spectra was pursued in my bachelor thesis,[53] with particular focus on states demonstrating high pseudorotational momentum. In **Publication VI** was proposed an analytical theory of these resonant states, employing Airy functions with appropriately formulated boundary conditions as the basic states. The obtained analytical theory is consistent with the numerical results.

1. Ground state symmetry of Jahn-Teller $E \otimes e$-system

A longstanding query regarding the Jahn-Teller effect concerns the symmetry of the ground state of the vibronic $E \otimes e$-system. Initially, I. Bersuker posited arguments supporting the hypothesis that this state is non-degenerate and possesses

A_1-symmetry. Subsequent studies by M. C. M. O'Brien, F. S.Ham, and others demonstrated that in case of the dominant linear vibronic interaction in the $E \otimes e$-system, the degenerate E-state exhibits the lowest energy, attributed to the existence of Berry phase in a vibronic system with electronic degeneracy. However, the consideration of the Berry phase is based on the adiabatic approximation. But in the $E \otimes e$-problem, this approximation is not always applicable, which affects the determination of the ground state.

In **Publication VII**, a series of numerical calculations were conducted on numerous vibronic $E \otimes e$-states for various strengths of linear and quadratic vibronic coupling, with rigorous consideration for non-adiabaticity. The calculations revealed that, indeed, in case of a strong quadratic vibronic coupling, the ground state became non-degenerate, underscoring the decisive role of non-adiabaticity in determining the ground state within the $E \otimes e$-system. Furthermore, it turned out that the change in the nature of the ground state in case of a strong quadratic interaction is associated with change in the origin of the pseudorotations: for linear vibronic coupling, the pseudorotations are characterized by half-integer rotational quanta, while in the case of a quadratic vibronic coupling, the rotational quanta are characterized by integer.

In performing calculations, a novel approach to addressing $E \otimes e$-problem in case of quadratic vibronic interaction was employed. It based on the use of vibronic states in the RWA as the ground states. This significantly reduced the calculation time required for determining vibronic states in case of a strong quadratic vibronic coupling.

2. Interaction of electron-vibrational impurity centre with phonon continuum of crystal

As stated above, the doctoral thesis focuses on the impurity centres of crystals, where the doubly degenerated excited electronic state interacts with the doubly degenerated local mode of nuclear vibrations (Jahn-Teller system) and in turn with all the vibrations of the crystal lattice. An inherent characteristic of the Jahn-Teller effect in impurity centres and molecular systems within crystals is the cooperative nature of atomic (or ionic) motion within the crystal, resulting in interaction between valence electrons and the phonon continuum. The interaction of optical electronics with the phonon quasi-continuum is fully responsible for the irreversible evolution in time and the loss of energy of excited Jahn-Teller systems. Despite of the importance of this interaction, a rigorous quantum mechanical method for its consideration has been lacking. Recent advances in this field include calculations of the time evolution of vibronic systems with electronic degeneracy, including up to 10 vibrational degrees of freedom. In such systems, energy is redistributed in time between these vibrational degrees of freedom, yet remains localized within the same system. The emission of phonons into the crystal, which is necessary for energy dissipation and relaxation, does not occur.

Developing a method, which makes possible to consider emission of phonons by excited vibronic system is a primary objective of this research.

2.1 Method to calculate the phonon emission of excited vibronic system

This problem was solved in **Publications I–III.** Initially, it was demonstrated that the vibronic interaction with non-totally symmetric phonons of the phonon continuum can be effectively substituted by a purely vibrational interaction of the local (or pseudolocal) Jahn-Teller modes with phonons, and based on that the corresponding vibrational Hamiltonian was derived. This advancement facilitated the computation of phonon relaxation of vibronic states. In this case, the resultant quadratic interaction Hamiltonian was treated as a perturbation that leads to the transitions between the numerically pre-calculated localized vibronic states of the Jahn-Teller system leading to the generation (destruction) of phonons. It gave for the first time opportunity to perform calculations of the relaxation of the vibronic system through the conical intersection. The computational framework incorporated the master equation for the density matrix, which was solved numerically taking into account single-phonon transitions. Consequently, it became for the first time possible to prove, within the framework of a rigorous quantum mechanical theory, the paramount importance of conic intersections in the temporal evolution and relaxation of vibronic systems. Additionally, these findings substantially refined the prevailing notion that conical intersections, due to strong non-adiabatic effects proximate to them, significantly accelerate vibronic transformations, allowing them to occur on a femtosecond time scale. Notably, calculations unveiled that despite the strongly non-adiabatic dynamics adjacent the conical intersection, relaxation through the section typically unfolds over a picosecond or slightly longer temporal domain.

2.2 Energy dissipation of excited impurity centre due to phonon emission

Furthermore, leveraging the resulting vibrational Hamiltonian, **Publication V** pioneered the calculation of the irreversible temporal evolution of configurational coordinates of strongly excited Jahn-Teller systems caused by phonon-assisted relaxation. Employing a cumulant expansion of the time evolution operator the density function of the configuration coordinates was delineated. Two first cumulants were taken into account. In calculations it was possible to trace the evolution of the density function over time, step by step (with a sub-picosecond time step), starting from its initial value in the highly excited state to its final, equilibrium value obtained after the complete loss of the excitation energy. At the same time, it was possible to show by strict quantum calculation the noticeable effect of Slonczewski resonances on relaxation.

2.3 Excitation spectra of resonant Raman scattering and absorption spectra

The developed method of accounting for the contribution of the phonon continuum to the vibrations active in the Jan-Teller effect was used to calculate the absorption and excitation spectra of resonant Raman scattering (termed Raman Excitation Profiles or REPs) for different strengths of vibronic interaction with nontotally symmetric local (pseudo-local) modes and phonons in **Publication IV**. Analysis unveiled that the phonon continuum causes specific Fano dips in the spectra. It was also found that the effects of non-adiabaticity are manifesting more prominently in REPs than absorption spectra. The same applies to Fano effects – they are more clearly manifested in REPs than in absorption spectra. Additionally, REPs demonstrated much stronger quantum effects of stimulated transitions, particularly evident in the pronounced Slonchewski resonances. The interference of the second order resonant Raman scattering with different total rotational momenta of the two created vibrational quanta is also detected for the first time in the form of new minima in the REPs.

2.4 Quantum friction of pseudorotation

A very interesting property of the Jahn-Teller problem with linear vibronic coupling is the presence of an axis of symmetry in the adiabatic potential (which in this case has the shape of a Mexican hat). The existence of this axis of symmetry leads to the existence of a pseudo-rotation – the rotation of the distorted state. This rotation is characterised by the half-integer rotational quanta. The volume phonons of the E-symmetry of crystal with an impurity in $E \otimes e$-state are also characterized by a rotational quantum. Therefore, in addition to energy relaxation, the developed theory of the interaction of the Jahn-Teller system with phonons allows for the first time to study the rotational relaxation associated with the emission of phonons with rotational momentum. In **Publication VI** were done detailed calculations of these emission processes for many different vibronic states of $E \otimes e$-system. It was found that there is a finite probability of quantum transitions, which lead not only to a decrease, but also to an increase in the rotational quantum of the Jahn-Teller system. In classical systems, the interaction with the environment causes the rotation to slow down due to friction. It is interesting that such anomalous quantum processes have increased probability near the Slonczewski resonances. Thus, the quantum friction of the rotation in the Jahn Teller system may differ from the classical one – at the intermediate stages of rotation, the rotational moment may even exceed its initial value. This is an unexpected phenomenon, which is possible in quantum systems.

SUMMARY IN ESTONIAN

Elektron-foonon interaktsioonid tahkiste lokaalsetes kõdunud elektronolekutes

Doktoritöö käsitleb tahkistes ja molekulaarsüsteemides esinevat interaktsiooni lokaalsete tuumade võnkumiste ja elektronide liikumise vahel, mida nimetatakse vibrooninteraktsiooniks. Sageli on see interaktsioon väike ja jäetakse arvutuste lihtsustamiseks arvesse võtmata. Siiski esineb süsteeme, kus antud interaktsiooni arvestamine on vajalik süsteemi iseloomulike omaduste piisavaks kirjeldamiseks ning sellega kaasnevad omapärased ja olulised kvantefektid. Doktoritöö pearõhk on uurida ergastatud olekus kristalli lisanditsentrit, milles esineb vibrooninteraktsioon ja mis on omakorda interaktsioonis kristallvõre võnkumistega, mille arvuline suurusjärk on $\sim 10^{23}$. Niisugune elektron-foononinteraktsioon määrab oluliselt aine (foto)füüsikalised omadused. Esmakordselt on esitatud rangelt kvantmehaaniline teooria ja vastavad arvutused kristalli lisanditsentri ja kristallvõre võnkumiste vastasmõju kirjeldamiseks. See tegi esmakordselt võimalikuks kirjeldada arvutuslikult ergastatud vibrooninteraktsiooniga lisanditsentri energia üleminekut kristallvõre võnkumistesse (relaksatsiooni).

Kõdunud elektron- ja võnkeolekute interaktsioonil tekib süsteemis spontaanne sümmeetria rikkumine ning elektron- ja võnkeolekute segunemine. Selliste süsteemide potentsiaalset energiat saab kirjeldada koonilise lõikumisega potentsiaalipinnaga. Koonusekujulised potentsiaalipindade lõikumised on tavapärased näiteks ergastatud biomolekulides. Viimaste vastupidavust UV-kiirgusele selgitatakse kiire, femtosekund-skaalas toimuva relaksatsioonimehhanismiga. Kuna koonilised potentsiaalipindade lõikumised määravad suuresti molekulaarsüsteemide ja tahkiste fotofüüsikalised ja -keemilised omadused, on nende süsteemide uurimine viimastel aastakümnetel, eriti pärast femtosekundlahutusega ekperimendimeetodite arenemist tublisti hoogu kogunud. Töös uuritud Jahn-Telleri $E \otimes e$ süsteem on kõige tüüpilisem koonilise potentsiaalilõikega vibroonsüsteesteem. Slonczewski on näidanud, et koonilise potentsiaalilõikega vibroonsüsteemides on segunenud elektron- ja võnkeolekud potensiaali ülaosas asuvad kõrge energiaga kvantolekud. Niisugusi olekuid nimetatakse Slonczewski resonantsideks ja need kujundavad vibroonsüsteemi omadusi ning kvantefekte. Slonczewski resonantside olemasolu on arvutuslikult $E \otimes e$ süsteemi optilises spektris näidanud V. Loorits (1972, Tartu Ülikool) ning M. C. M. O'Brien ja S. N. Evangelou (1972, Oxfordi ülikool). Oma bakalaureusetöös[53] arvutasin erineva vibrooninteraktsiooni tugevusega $E \otimes e$ süsteemi optilised spektrid, käsitledes lisaks ka suurema kui põhiarvulise pseudopöördmomendiga süsteeme. **Artiklis VI** on esitatud analüütiline teooria Slonczewski resonantside arvutamiseks Airy funktsioonide abil, mis on kooskõlas numbriliste tulemustega.

1. $E \otimes e$ põhioleku sümmeetria

Pikki aastaid on olnud vaidluse all $E \otimes e$ vibroonsüsteemi ja Renner-Telleri süsteemi põhioleku sümmeetria. I. Bersuker on esitanud põhjendusi kõdumata A_1 sümmeetria kasuks. M. C. M. O'Brien, F. S. Ham ja teised näitasid, et kui süsteemis domineerib lineaarne vibrooninteraktsioon on madalaima energiaga kahekordselt kõdunud E olek. Nad lähtusid eeldusest, et kõdunud olekuga vibrooninteraktsioniga süsteemis eksisteerib Berry faas. Kuid Berry faasi olemasolu põhineb adiabaatilisel lähendusel, mida ei saa $E \otimes e$ probleemi puhul alati kasutada.

Doktoritöös on uuritud vibroonsüsteemi põhioleku ja madalaima ergastatud oleku sümmeetria sõltuvust lineaarse ja ruutvibrooninteraktsiooni tugevusest. **Artiklis VII** on arvutatud rida vibroonseid olekuid erinevate lineaarsete ja teist järku vibrooninteraktsioonitugevuste puhul võttes arvesse mitteadiabaatilisust. Näidatud on, et sõltuvalt esimest ja teist järku vibrooninteraktsiooni tugevusest, võib põhiolek olla kõdumata A_1 olek või kõdunud E olek. Arvutustest lähtub, et tugeva ruutvibrooninteraktsiooni puhul ja nõrga (või puuduva) lineaarse vibrooninteraktsiooni puhul on põhiolek kõdumata A_1 olek, millest võib omakorda järeldada, et sellisel juhul määrab põhioleku mitteadiabaatilisus. Nõrga (või puuduva) ruutvibrooninteraktsiooni puhul ja iga lineaarse vibrooninteraktsiooni puhul on põhiolek kõdunud E olek. Lisaks selgus, et põhioleku sümmeetria tugeva ruutvibrooninteraktsiooni korral on määratud pseudopöördmomendi päritolu muutusega: lineaarse vibrooninteraktsiooni puhul on pseudopöördmoment kirjeldatud poolarvuliste suurustega ja ruutvibrooninteraktsiooni puhul täisarvuliste suurustega.

2. Elektoron-võnke süsteemi interaktsioon kristallvõre foononitega

Nagu eelpool öeldud, keskendub doktoritöö kristallide lisanditsenritele, kus kahekordselt kõdunud ergastatud elektronolek on interaktsioonis kahekordselt kõdunud lokaalse tuumade võnkemoodiga (Jahn-Telleri $E \otimes e$ süsteem) ja omakorda kõigi kristallvõre võnkumistega. Kristallide lisanditsentrites ja molekulaarsüsteemidele on iseloomulik valentselektronide interaktsioon kõigi kristallvõre võnkumistega (foononkontiinumiga). Optiliste elektronide interaktsioon kristallvõre foonkontiinumiga põhjustab energiarelaksatsiooni (energia hajumise) ergastatud Jahn-Telleri süsteemis. Ehkki see interaktsioon on oluline, on seni puudunud rangelt kvantmehhaaniline meetod selle kirjeldamiseks. Varasemad arvutusmeetodid suudavad arvesse võtta kuni paarkümmend võnkemoodi ning suudavad seetõttu kirjeldada energia ümberjaotamist lokaliseeritud süsteemis kuid mitte foononite emiteerimist kristalli, mis on tarvilik ergastatud lisanditsentri relaksatsiooni (energia hajumine kiirguseta) kirjeldamiseks. Loodud on meetod, mis võimaldab arvutada lisanditsentri interaktsiooni kristallvõre võnkumistega ja kirjeldada olulisi kvantmehhaanilisi efekte.

2.1 Meetod ergastatud vibroonsüsteemi foononite emissiooni arvutuseks

Meetodi loomine, mis suudaks kirjeldada ergastatud vibroonsüsteemi foononite emissiooni, on doktoritöö üks keskseid teemasid. Selle ülesande lahendamist on käsitletud **Artiklites I–III**. Esmalt on näidatud, et vibrooninteraktsiooni foononkontiinumi mittetäielikult sümmeetriliste foononitega võib asendada võnkeinteraktsiooniga lokaalse (või pseudolokaalse) Jahn-Telleri moodi ja foononite vahel. Leitud on vastav võnkehamiltoniaan, mille abil on võimalik arvutada vibroonolekute energia ülekandumine kristallvõre võnkumistesse. Saadud ruutinteraktsiooni Hamiltoniaani käsitletakse häiritusena, mis põhjustab üleminekuid eelnevalt numbriliselt arvutatud lokaliseeritud Jahn-Telleri süsteemi vibroonolekute vahel ja viib foononite tekkimiseni (või kadumiseni). See võimaldas esmakordselt arvutada vibroonsüsteemi relaksatsiooni potentsiaalipindade koonilise lõikepunkti kaudu. Alusvõrrandi (master equation) abil leiti tihedusmaatriks, mis lahendati numbriliselt, võttes arvesse ühefoononilisi üleminekuid.

2.2 Ergastatud lisanditsentri energia hajumine foononite emissiooni kaudu

Tänu sellele oli esmakordselt võimalik näidata range kvantmehhaanilise teooria raames kooniliste lõikepunktide suurt tähtsust aja evolutsioonis ja vibroonsüsteemide relaksatsioonis. Saadud tulemused võimaldasid ka oluliselt parandada üldtunnustatud arvamust, et koonilised lõikepunktid kiirendavad märkimisväärselt vibroonüleminekuid (tugevate mitteadiabaatiliste efektide tõttu nende lähedal), võimaldades üleminekutel toimuda femtosekundi ajaskaalal. Arvutused näitasid, et hoolimata tugevast mitteadiabaatilisest dünaamikast koonilise lõikepunktiga lähedal, toimub relaksatsioon selle kaudu tavaliselt pikosekundi või veidi pikemal ajaskaalal.

Tänu maintud võnkehamiltoniaanile oli **Artiklis V** võimalik esmakordselt arvutada tugevalt ergastatud Jahn-Telleri süsteemi konfiguratsioonikoordinaatide pöördumatut muutumist foononrelaksatsiooni käigus. Selleks kasutati aja evolutsiooni operaatori kumulantarendust, mille abil saab leida konfiguratsioonikoordinaatide tihedusfunktsiooni. Arvesse on võetud kahte esimest kumulanti. Arvutustes oli võimalik jälgida tihedusfunktsiooni evolutsiooni ajas sammsammult (väiksema kui pikosekundi sammuga), alates tihedusfunktsiooni algväärtusest kõrgelt ergastatud olekus kuni selle lõpliku, tasakaalulise väärtuseni pärast ergastuse energia täielikku hajumist. Samuti tuli välja Slonczewski resonantside märgatav mõju relaksatsiooniprotsessile.

2.3 Ramanhajumise ja neeldusmisspekid

Loodud meetodit foononkontiinumi mõju arvestamiseks aktiivsetele Jahn-Telleri võnkemoodidele kasutati **Artiklis IV** neeldumisspektrite ja resonantse Raman hajumise ergastusspektrite (Raman excitation profiles – REPs) arvutamiseks erineva tugevusega vibrooninteraktsiooni puhul mittetäielikult sümmeetriliste

lokaalsete (pseudo-lokaalsete) võnkemoodide ja foononite vahel. Ilmnes, et foononkontiinum põhjustab spektrites spetsiifilisi Fano miinimume. Lisaks tuli välja, et mitteadiabaatilisuse efektid on REP-des märgatavamad kui neeldumisspektrites. Sama kehtib ka Fano efektide kohta – need avalduvad REP-des selgemalt kui neeldumisspektrites. Lisaks ilmnevad REP-des oluliselt tugevamini stimuleeritud üleminekute kvantefektid – kõrge energiaga Slonchewski resonantsid on REP-des selgemalt välja joonistunud kui neeldumisspektrites. Arvutatud spektrites on esmakordselt jälgitav teist järku resonantse Raman hajumise interferents, mida põhjustab kahe erineva summaarse pöörlemismomentidega võnkekvandi tekkimine.

2.4 Kvanthõõrdumine pöörlemisel

Jahn-Telleri süsteemi oluline omadus on lineaarse vibrooninteraktsiooni puhul sümmeetriatelje olemasolu adiabaatilises potentsiaalis (potentsiaal on sel juhul mehhiko kübara kujuline). Selle sümmeetriatelje tõttu esineb süsteemis pseudopöörlemine ehk moonutatud oleku pöörlemine, mida iseloomustavad pooltäisarvulised pöörlemiskvandid. Kristalli foononeid iseloomustab samuti pöörlemiskvant. Seetõttu võimaldab Jahn-Telleri süsteemi interaktsiooni foononitega kirjeldav teooria lisaks energia relaksatsioonile esmakordselt uurida ka pöörlemisrelaksatsiooni, mis on seotud pöörlemismomenti omavate foononite emiteerimisega. **Artiklis VI** on tehtud arvutused nende emissiooniprotsesside kohta paljude erinevate $E \otimes e$ vibroonolekute puhul. Ilmnes, et on olemas lõplik tõenäosus kvantüleminekutele, mis viivad mitte ainult Jahn-Telleri süsteemi pöörlemiskvandi vähenemiseni, vaid ka suurenemiseni. Klassikalistes süsteemides põhjustab keskkonnaga interaktsioon hõõrdumise tõttu pöörlemise aeglustumist. Kuid nagu arvutused näitavad, võib pöörlemise kvanthõõrdumine Jahn-Telleri süsteemis erineda klassikalisest – pöörlemismoment võib pöörlemise vahefaasides kasvada ja ületada isegi esialgset väärtust. Slonczewski resonantside lähedal toimuvad sellised anomaalsed kvantprotsessid suurema tõenäosusega. Tegu on ootamatu nähtusega, mis on võimalik kvantsüsteemides.

REFERENCES

[1] R. Englman, *The Jahn-Teller Effect in Molecules and Crystals* (Wiley-Interscience, London, 1972).
[2] H.A. Jahn and E. Teller, Proc. R. Soc. London. Ser. A – Math. Phys. Sci. **161**, 220 (1937).
[3] I.B. Bersuker, *The Jahn–Teller Effect* (Cambridge University Press, Cambridge, 2006).
[4] K. Dressler, D.A. Ramsay, and G. Herzberg, Philos. Trans. R. Soc. London. Ser. A, Math. Phys. Sci. **251**, 553 (1959).
[5] R.J. Buenker, M. Peric, S.D. Peyerimhoff, and R. Marian, Mol. Phys. **43**, 987 (1981).
[6] I.B. Bersuker, Chem. Rev. **101**, 1067 (2001).
[7] I.B. Bersuker, in *Adv. Quantum Chem.* (Academic Press, 2003), pp. 1–12.
[8] R. Oerter, *The Theory of Almost Everything: The Standard Model, the Unsung Triumph of Modern Physics* (Penguin Group, 2006).
[9] G.A. Gehring and K.A. Gehring, Rep. Prog. Phys **1**, 1 (1975).
[10] B.G. Kaplan, Michael D.; Vekhter, *Coopewrative Phenomena in Jahn-Teller Effect* (Springer US, 1995).
[11] R.H. Zadik, Y. Takabayashi, G. Klupp, R.H. Colman, A.Y. Ganin, A. Potočnik, P. Jeglič, D. Arčon, P. Matus, K. Kamarás, Y. Kasahara, Y. Iwasa, A.N. Fitch, Y. Ohishi, G. Garbarino, K. Kato, M.J. Rosseinsky, and K. Prassides, Sci. Adv. **1**, e1500059 (2015).
[12] A.L. Sobolewski and W. Domcke, Eur. Phys. J. D **20**, 369 (2002).
[13] A.L. Sobolewski and W. Domcke, Phys. Chem. Chem. Phys. **6**, 2763 (2004).
[14] Sobolewski, Andrzej L. and Domcke, Wolfgang, Europhys. News **37**, 20 (2006).
[15] R. Stones and A. Olaya-Castro, Chem **1**, 822 (2016).
[16] D.L. Miller and M.A. Weinstock, J. Am. Acad. Dermatol. **30**, 774 (1994).
[17] A.N. Houghton and D. Polsky, Cancer Cell **2**, 275 (2002).
[18] Y.E. Perlin and B.S. Tsukerblat, *Electron-Vibrational Interaction in Optical Spectra of Impurity Paramagnetic Ions* (Shtintsa, Kishinev, 1974).
[19] I.B. Bersuker and V.Z. Polinger, *Vibronic Interactions in Molecules and Crystals* (Springer, Berlin, 1989).
[20] Y. Toyozawa, *Optical Processes in Solids* (Cambridge University Press, Cambridge, 2003).
[21] V.Z. Polinger and I.B. Bersuker, Phys. Stat. Sol. B **96**, 153 (1979).
[22] Y.B. Rosenfeld and A.V. Vaisleib, Sov. Phys. JETP **86**, 1059 (1984).
[23] Y.E. Perlin and B.S. Tsukerblat, *Optical Bands and Polarization Dichroism of Jahn–Teller Centers, in: Dynamical Jahn–Teller Effect in Localized Systems* (Elsevier, Amsterdam, 1984).
[24] H.-D. Meyer, U. Manthe, and L.S. Cederbaum, Chem. Phys. Lett. **165**, 73 (1990).
[25] U. Manthe, H.-D. Meyer, and L.S. Cederbaum, J. Chem. Phys. **97**, 3199 (1992).
[26] M. Beck, A. Jäckle, G.A. Worth, and H.-D. Meyer, Phys. Rep. **324**, 1 (2000).
[27] H.-D. Meyer and G.A. Worth, Theor. Chem. Acc. **109**, 251 (2003).
[28] S. Faraji, H.-D. Meyer, and H. Köppel, J. Chem. Phys. **129**, 074311 (2008).
[29] M. Nooijen and J.G. Snijders, Int. J. Quantum Chem. **44**, 55 (1992).
[30] J.F. Stanton and J. Gauss, J. Chem. Phys. **101**, 8938 (1994).
[31] M.C.M. O'Brien, J. Phys. C Solid State Phys. **5**, 2045 (1972).
[32] H. Köppel, E. Haller, L.S. Cederbaum, and W. Domcke, Mol. Phys **41**, 669 (1980).
[33] I.B. Bersuker, Opt. Spectrosc. **11**, 319 (1961).
[34] I.B. Bersuker, Zh. Eksp. Teor. Fiz. **43**, 1315 (1962).

[35] M.C.M. O'Brien, Proc. R. Soc. A Math. Phys. Eng. Sci. **281**, 323 (1964).
[36] F.S. Ham, Phys. Rev. **166**, 307 (1968).
[37] M.V. Berry, Proc. R. Soc. London, Ser A **392**, 45 (1984).
[38] C.P. Moate, M.C.M. O'Brien, J.L. Dunn, C.A. Bates, Y.M. Liu, and V.Z. Polinger, Phys. Rev. Lett. **77**, 4362 (1996).
[39] P. De Los Rios, N. Manini, and E. Tosatti, Phys. Rev. B **54**, 7157 (1996).
[40] H. Koizumi and I.B. Bersuker, Phys. Rev. Lett. **83**, 3009 (1999).
[41] J.W. Zwanziger and E.R. Grant, J. Chem. Phys. **87**, 2954 (1987).
[42] S. Sookhun, J.L. Dunn, and C.A. Bates, Phys. Rev. B **68**, 235403 (2003).
[43] H. Koizumi, I.B. Bersuker, J.E. Boggs, and V.Z. Polinger, J. Chem. Phys. **112**, 8470 (2000).
[44] V.Z. Polinger, R. Huang, J.L. Dunn, and C.A. Bates, J. Chem. Phys. **117**, 4340 (2002).
[45] H. Li, V.Z. Polinger, J.L. Dunn, and C.A. Bates, in *Adv. Quantum Chem.* (Academic Press, 2003), pp. 89–102.
[46] G. Bevilacqua, I.B. Bersuker, and L. Martinelli, in *Vibronic Interact. Jahn-Teller Eff. Cryst. Mol.*, edited by M.D. Kaplan and G.O. Zimmerman, 1st ed. (Springer Netherlands, 2001), pp. 229–233.
[47] B. Beagley, A. Eriksson, J. Lindgren, I. Persson, L.G.M. Pettersson, M. Sandstrom, U. Wahlgren, and E.W. White, J. Phys. Condens. Matter **1**, 2395 (1989).
[48] K.A. Müller, in *Magn. Reson. Relax.*, edited by R. Blinc (Nort Holland, Amsterdam, 1967).
[49] H.C. Longuet-Higgins, U. Öpik, M.H.L. Pryce, and R.A. Sack, Proc. R. Soc. London A Math. Phys. Eng. Sci. **244**, 1 (1958).
[50] V. Loorits, Izv. Akad. Nauk. ESSR, Fiz-Mat. **29**, 208 (1980).
[51] M.C.M. O'Brien and S.N. Evangelou, Solid State Commun. **36**, 29 (1980).
[52] K. Pae and V. Hizhnyakov, J. Chem. Phys. **138**, 104103 (2013).
[53] K. Pae, Elektronsiirded Tugeva Vibrooninteraktsiooniga Sümmeetrilistes Süsteemides [Unpublished Bachelor Thesis], University of Tartu, 2009.
[54] K. Ghiassi and R.J. Lancashire, Libr. Chem. (2017).
[55] T.A. Barckholtz, M.-C. Yang, and T.A. Miller, (1999).
[56] I. Sioutis, V. Stakhursky, G. Tarczay, and T. Miller, J. Chem. Phys. **128**, 84311 (2008).
[57] V. Gudkov and I. Bersuker, in *Vibronic Interact. Jahn-Teller Eff.* (2011), pp. 143–161.
[58] M.N. Sarychev, W.A.L. Hosseny, A.S. Bondarevskaya, I. V Zhevstovskikh, A. V Egranov, O.S. Grunskiy, V.T. Surikov, N.S. Averkiev, and V. V Gudkov, J. Alloys Compd. **848**, 156167 (2020).
[59] S. Matsika and P. Krause, Annu. Rev. Phys. Chem. **62**, 621 (2011).
[60] M.C.E. Galbraith, S. Scheit, N. V Golubev, G. Reitsma, N. Zhavoronkov, V. Despré, F. Lépine, A.I. Kuleff, M.J.J. Vrakking, O. Kornilov, H. Köppel, and J. Mikosch, Nat. Commun. **8**, 1018 (2017).
[61] *Vibronic Coupling and Electron-Phonon Interactions in Molecules and Crystals: XXIII International Symposium on the Jahn-Teller Effect* (IOP Publishing, 2017).
[62] *XXIV International Symposium on the Jahn-Teller Effect* (IOP Publishing, 2018).
[63] J. Slonczewski, Phys. Rev. **131**, 1596 (1963).
[64] L.D. Landau and E.M. Lifshitz, *Quantum Mechanics*, Third Edit (Butterworth Heinemann, Amsterdam, 2003).
[65] E.R. Bernstein and J.D. Webb, Mol. Phys. **36**, 1113 (1978).
[66] N. Sakamoto, J. Phys. C Solid State Phys. **15**, 6379 (1982).
[67] V. Hizhnyakov, K. Pae, and T. Vaikjärv, Chem. Phys. Lett. **525**–**526**, (2012).

[68] I. Tehver, G. Benedek, V. Boltrushko, V. Hizhnyakov, and T. Vaikjärv, in *Vibronic Interact. Jahn-Teller Eff. Theory Appl.*, edited by M. Atanasov (Springer, 2012), p. 163–177.
[69] T. Vaikjärv and V. Hizhnyakov, J. Chem. Phys. **140**, 064105 (2014).
[70] A.A. Maradudin, E.W. Montroll, G.H. Weiss, and I.P. Ipatova, in *Solid State Physics, Suppl. 3*, edited by D.T. H. Ehrenreich, F. Seitz, 2nd ed. (Academic Press, New York, 1971).
[71] P.M. Champion and A.C. Albrecht, Annu. Rev. Phys. Chem. **33**, 353 (1982).
[72] V. Loorits and V. Hizhnyakov, in *Phys. Impurity Centers Cryst.*, edited by G.S. Zavt (Academy of Sciences Of Estonia, Tallinn, 1972).
[73] V. Hizhyakov and I. Tehver, in *Proc. Second Int. Conf. Light Scatt. Solids* (Flammarion Science, Paris, 1972), pp. 57–61.
[74] Y. Toyozawa and M. Inoue, J. Phys. Soc. Japan **21**, 1663 (1966).
[75] S. Muramatsu and K. Nasu, J. Phys. Soc. Japan **46**, 189 (1979).
[76] V. Hizhyakov and I. Tehver, Phys. Status Solidi **21**, 755 (1967).
[77] V. Hizhnyakov and I. Tehver, J. Raman Spectrosc. **24**, 653 (1993).
[78] W. Domcke and D.R. Yarkony, Annu. Rev. Phys. Chem. **63**, 325 (2012).
[79] N. Manini and P.D.L. Rios, J. Phys. Condens. Matter **10**, 8485 (1998).
[80] G. Lindblad, Commun. Math. Phys. **48**, 119 (1976).
[81] V. Boltrushko, V. Krasnenko, and V. Hizhnyakov, Chem. Phys. **460**, 90 (2015).
[82] V. Krasnenko, V. Boltrushko, and V. Hizhnyakov, J. Chem. Phys. **144**, 134708 (2016).
[83] V. Krasnenko, V. Boltrushko, and V. Hizhnyakov, J. Phys. Conf. Ser. **833**, 12009 (2017).
[84] A. Bill, V. Hizhnyakov, D. Nevedrov, G. Seibold, and Z. Sigmund, Zeitschrift Für Phys. B Condens. Matter **104**, 753 (1997).
[85] A. Bill, V. Hizhnyakov, G. Seibold, and E. Sigmund, in *Spec. Contrib. Honour K. Alex Müller Occas. His 80th Birthd.* (Springer, 2007), p. 143–156.
[86] A. Bill, V. Hizhnyakov, and G. Seibold, in *High-Tc Copp. Oxide Supercond. Relat. Nov. Mater. to Prof. K. A. Müller Occas. His 90th Birthd.*, edited by A. Bussmann-Holder, H. Keller, and A. Bianconi, Springer S (Springer, 2017), pp. 1–14.
[87] K. Pae and V. Hizhnyakov, J. Chem. Phys. **145**, 64108 (2016).

ACKNOWLEDGEMENT

I extend heartfelt gratitude to my supervisor professor Vladmir Hižnjakov for guiding me on this journey to the enjoyably fundamental nature of matter, offering glimpses into the inherent structures of the universe. The imagination together with mathematics has led to exploration of the most peculiar properties within the quantum realm. I am indebted to the Jahn-Teller community for their generous support, as well as to my dear current and former colleagues at the Institute of Physics in Tartu. My co-PhD student, Taavi Vaikjärv, has been a constant source of discussion and interpretation. My coursemates from physics studies were a happy bunch of people, who taught that great things get done with joy. My dear friends Maria and Liina elaborated this joy and we have spent many indispensable moments in the lap of invigorating Estonian woods and lakes. I am grateful to Toomas and Silver for being there and supporting my journey. My parents have been also incredible supportive, and they have shown that will and imagination are powerful tools. Being part of "Rocket 69" community has filled my heart with joy – it has been pure privilege to encourage young people on their path of exploration and if they would only know how much they have inspired me; same and much more holds for the whole team of "Rocket 69". I am also deeply grateful to Tartu's humanitarian and artistic community for being there and opportunity to share the path with you. Discussions with you reinforced my belief that the true aim of science and the human mind is to create new worlds, not merely to predict or describe.

PUBLICATIONS

CURRICULUM VITAE

Name Kaja Pae
Date of Birth November 13, 1979
Nationality Estonian
Email kaja.pae@gmail.com
Phone +372 569 5767

Education

2010–2024 University of Tartu, doctoral studies (Physics)
1999–2006, 2009–2010 Estonian Academy of Arts, Bachelor's and Master's studies (Architecture and Urban Planning, 5-year integrated program)
2007–2009 University of Tartu, Bachelor's studies (major in Theoretical Physics, *cum laude*)

Career

2022–... Ministry of Climate (formerly Ministry of Economic Affairs and Communications until 2023), Head of Construction and Living Environment Department
2017–2022 Editor-in-Chief of the Estonian architecture magazine "Maja"
2017–2023 Member of the Board of Arhitektuurikirjastus NGO
2016–2019 Junior Researcher at the Institute of Physics, University of Tartu
2012–2015 Engineer at the Institute of Physics, University of Tartu, Center of Excellence in Research "Theory of Mesoscopic Systems and Applications"
2013–... Contract Lecturer at the Faculty of Architecture, Estonian Academy of Arts
2012–... Freelance Architect
2009–2011 Head of Urban Forums at the Estonian Centre of Architecture
2009 Research Assistant at the Institute of Physics, University of Tartu
2003–2007 Urban Mark Architecture Office, Architect
2002–2003 Vahur Sova Architecture Office, Architect

Public Activities

2016–... Judge of the science popularization TV-program "Rakett 69"
2023–... Member of the Heritage Conservation Council

Awards

2021 Estonian Association of Architects' Medal of Merit "Mõtestaja"
2017 Estonian Landscape Architects Union's Annual Achievement Award for the exhibition "Who Makes the City?"
2017 Estonian Academy of Arts' Annual Creative Award for the exhibition "Who Makes the City?"

2014 Nominee for Tartu's Cultural Carrier of the Year (Annelinn Portal and Vision Competition)
2014 Best Poster at the International Jahn-Teller Symposium in Graz, Austria
2012 Best Poster at the International Jahn-Teller Symposium in Tsukuba, Japan
2011 Estonian Cultural Endowment's Architecture Foundation Activity Award for organizing Urban Forums
2009 Second Prize in the Estonian Academy of Sciences Student Research Competition (for the work "Electron Transitions in Symmetrical Systems with Strong Vibronic Interaction")
2007 Nominee for the Estonian Cultural Endowment's Annual Architecture Award
2007 1st–2nd Place in the Built Architectural Small Form Competition "Small 2002–2006" for the Estonian Bank Gallery; with Ülar Mark
2006 Award for Steel Construction of the Year
2006 Selected to represent Estonia at the Venice X Architecture Biennale; with Ülar Mark and Rein Ahas
2003 1st Place in the Tartu University Social Sciences Faculty New Building Project Competition; with Ülar Mark

Scholarships

2002 Estonian National Culture Fund Scholarship
2002 Construction World Scholarship
2012 World Scientists Organization Scholarship
2014 Kristjan Jaagu Travel Scholarship
2015 Kristjan Jaagu Travel Scholarship

Publications

Physics

Hizhnyakov, V.; Pae, K.; Boltrushko, V.; Köppel, H. (2018). Vibronic states in conical intersections: manifestations of centrifugal energy and non-adiabaticity in optical spectra of Jahn-Teller systems. Journal of Physics: Conference Series, 1148.

Pae, K.; Hizhnyakov, V. (2017). Ground state in $E \otimes e$ Jahn-Teller and Renner-Teller systems: Account of nonadiabaticity. Journal of Chemical Physics, 147 (8).

Pae, K.; Hizhnyakov, V. (2016). Quantum friction of pseudorotation in Jahn-Teller system: Passage through conical intersection. Journal of Chemical Physics, 145, 064108.

Pae, K.; Hizhnyakov, V. (2014). Time-dependent Jahn-Teller Problem: Phonon Induced Relaxation through Conical Intersection. Journal of Chemical Physics, 141(23), 234113.

Pae, K.; Hizhnyakov, V. (2013). Nonadiabaticity in a Jahn-Teller system probed by absorption and resonance Raman scattering. Journal of Chemical Physics, 138(10), 104103.

Pae, K.; Hizhnyakov, V. (2013). Optical Jahn-Teller effect: contribution of phonons. Journal of Physics: Conference Series, 428,

Hizhnyakov, V.; Pae, K.; Vaikjärv, T. (2012). Optical Jahn-Teller effect in the case of local modes and phonons. Chemical Physics Letters, 525–526, 64–68.

Hizhnyakov, V.; Boltrushko, V.; Pae, K.; Vaikjarv, T. (2011). Zero-phonon lines: Novel manifestations of vibronic interactions in impurity centres of solids. Optika i Spektroskopiya, 111(3), 398–406.

Hizhnyakov, V.; Pae, K.; Vaikjärv, T. (2011). Vibronic Transitions to a State with Jahn-Teller Effect: Contribution of Phonons. M.Atanasov et al. (Toim.). Vibronic Interactions and the Jahn–Teller Effect: Theory and Applications (179–191).Springer.

Architecture and Urban Planning

Books:

Urban Forums / Linnafoorumid. 2011, compiled and edited by. 356 pages. Tallinn: Estonian Architecture Centre. In Estonian and English.

Jointspace – Open Source on Mobile Positioning and Urban Studies. 2006, compiled and edited by. 174 pages. Tallinn: Positium. In English.

Compiled Publications and Edited Works:

Estonian Architecturl Review "Maja" 2017–3, 2017–4, 2018–1, 2018–2/3, 2018–4, 2019–1, 2019–2, 2019–3, 2019–4, 2020–1, 2020–2/3, 2020–4, 2021–1, 2021–2, 2021–3, 2021–4, 2022–1, 2022–2, 2022–3-4, 2023–1.

Tartu Spatial Gluttony Map, 2016.

Guest Editor of Maja Journal, Issues 1–2, 2016.

Compilation of the Homely Annelinn Information Brochure, 2015.

Articles

Suburbanization: spatial chances of euphoria of freedom and pragmatic power lines. History of Estonian urban planning. Volume II, 2024.

Spatial Agency – the key to a good living environment. Maja Winter 2023.

Vision Creation. Maja Winter 2022.

How Should We Live? Maja Winter 2022.

Culture of Abundance: End of Typologies or New Typologies? Maja Autumn 2021.

Encounter of Non-Aesthetics and High Aesthetics. Maja Spring 2021.

What's in the Air? Maja Spring 2021.

Vision + Education. Maja Summer–Autumn 2020.

Public Space. Temporality as a Means. Vikerkaar, October 2020.

The Graceful Power Lines of the World. Postimees, May 20, 2020.

Beauty Makes Believing in People Important. Maja Winter 2020.

Collection of Thoughts on New Beauty Forms. Postimees, Oct 21, 2019.

Public Space in Declining Estonian Small Towns. Müürileht, September 2019.
Confrontations and Measurements – between architecture and art. Maja, Summer, 2019.
Why Do We Need a Weak Monument? Maja, Summer–Autumn, 2018.
Catalog of Good Taste. Maja, Summer–Autumn, 2018.
The Shining Tip of the Iceberg. Sirp, Oct 6, 2017.
The Inertness of Free Plan Areas: Towards Step-By-Step Organizing Urbanism. The Baltic Atlas, Sternberg Press, 2016. Baltic Pavilion Book at the 2016 Venice Architecture Biennale.
You Would Prefer Not To. On Public Space, Control, and Responsibility. Ehituskunst, 2016.
Annelinn Community? Müürileht, October 2015.
Sublime and Everyday. Maja, No. 1, 2015.
Towards Annelinn. Sirp, Nov 28, 2014.
Aesthetics of Inevitability. Vihik, 2013 (Journal of the Estonian Literary Society)
Divergent Practices of Tartu. Positions. Reading of New Estonian Architecture, 2012.
10Pi. Not-Tartu, 2012.
Living in Dystopia. Ehituskunst. Estonian Architectural Review No. 53/54 2011.
Recognizing the Unrepeatable. Urban Forums / Linnafoorumid. 2011.
University to the Field? Eesti Päevaleht Nov 18, 2010.
Cities in Our Heads. Vihik No. 15, 2010 (Journal of the Estonian Literary Society)
Tissue of Uncertainty. Maja No. 3, 2008.
Divergent Practices of Tartu. Maja No. 2, 2007.
People in the City. Estonian Exhibition Joint Space at the Venice X Architecture Biennale. Maja No. 4, 2006.
Turning Inside Out – Identity Shifts in Space – Open Source on Mobile Positioning and Urban Studies. 2006.

Interviews

Art and Science: Equally Incomprehensible? Sirp, April 30, 2021. Interviewed by Arko Olesk.
About the Stairs of Tallinn. Interview in the cultural show OP, April 22, 2021. Interviewed by Margit Kilumets.
A Hundred Critical Architectural Discussions. Maja Spring 2020. Interviewed by Andres Kurg.
Takeoff – Kaja Pae, Chief Editor of the Estonian Architecture Journal Maja. Sirp, Sept 22, 2017. Interviewed by Merle Karro-Kalberg.
Architect: Annelinn has great potential. Linnaleht, Sept 18, 2014.
Urban Forum Arrives in Tartu. Sirp, Apr 23, 2010. Interviewed by Reet Varblane.

Translations

Pliny the Younger's letter 2.17. Maja, No. 1–2, 2016. (Translated from Latin Epistulae 2.17).

Other Significant Creative Activities

2022 Estonian-Irish Architects Joint Exhibition "My House Isn't Made of Trees Growing Behind My House in the Woods" in Navan, Ireland; with Paco Ulman.

2020–2021 Participation in the Estonian-Irish Architects' Wood Architecture-focused Creative Research "Wood Works" organized by the Estonian Architecture Centre; with Paco Ulman.

2016 "Five Pleasures." Work at the XV Venice Architecture Biennale; with Paco Ulman.

2015 "Tartu Parenthesis (( )". Participation in the UIT City Festival's site-specific literature project.

2014 Artistic Work for the Conference on Happiness; with Paco Ulman.

2013 Installation Series "Study of lines in nature"; with Paco Ulman.

2012 Photo Series on the Boundaries of Tartu in the short story collection "Not-Tartu."

2009 Prose Flyer Project as part of the Tartu Art Month; with Sven Vabar.

2006 Preparation of the Estonian Exhibition for the X Venice Architecture Biennale; with Ülar Mark, Rein Ahas, Yoko Alender, Raul Kalvo, Anto Aasa, Margus Tiru, and Erki Saluveer.

2005 Participation in the architecture exhibition in Berlin, "Emerging Identities – EAST" (Selected overview exhibition of modern architecture from the Eastern European region).

2002 Participation in the photography exhibition "Free Will" (Selected overview exhibition of works by young photographers).

Public Speeches and Panel Discussions

2024 Panel Discussion "Wood as a Sustainable Building Material and Carbon Sink", Postimees Rural Live Studio debate, April 18, Tartu Rural Fair.

2024 Presentation "Inspiring or Predicting: Examples of Artificial Intelligence Use in Spatial Design and What Could be the Role of the State?" March 15, Planning Conference, Tartu.

2023 Panel Discussion "Challenges of Nationwide Planning on the Threshold of the Great Transition", March 30, Planning Conference, Tartu.

2023 Presentation at the Äripäev Architecture and Development Conference, Sept 28, Radisson Blue Hotel, Tallinn.

2023 How Does Spatial Heritage Help Cope with Contemporary Challenges? Heritage Protection Conference, Haapsalu.

2023 Discussion on Building Renovation at "sLenderhood". June 5, EKA.

2022 Presentation at the Construction Conference, Nov 9, Hotel Euroopa, Tallinn.

2021 Participation in the Panel Discussion “Art and Science: Equally Incomprehensible?” February 11, Kumu.
2019 Moderator of the Tallinn Architecture Biennale Symposium “Beauty Matters”.
2019 Presentation “How does Tallinn Move”, May 30, conference “Human-Centered Greater Tallinn”, Tallinn Harbor A-Terminal (public presentation of the Tallinn mobility study).
2019 Panel Discussion “What to Do with Obsolete Architecture?” Moderator and Organizer, May 11, Kumu.
2019 Presentation at the EAL General Meeting, March 28, Kumu.
2019 Participation in the EAL Curated Exhibition “Almost Zero” Panel Discussion, March 6, Aparaaditehas.
2018 Presentation at HTG’s 105th Anniversary Conference as a Prominent Alumni.
2018 Moderator of the Narva UrbanLab Narva-Detroit Panel Discussion “Shrinking Urban Space: Changes and Adaptation”, Aug 24, Narva Art Residency.
2018 Initiator and Moderator of the Opinion Festival Discussion “There’s Space, but No Public”, Aug 10, Paide.
2018 Presentation at the Architecture Flash Lecture, Feb 7, Von Krahl Theatre.
2017 Lasnaidee Inspiration Seminar “What’s the Potential of Stone City?” Dec 10.
2017 Planning Conference Presentation on November 2, Tartu.
2017 Presentation at the Raikküla Manor Conference “Space in Time, Man in Space.” May 19, Raikküla Manor.
2017 Discussion on Tallinn’s Waterfront Vision, April 1, Estonian Museum of Architecture.
2016 Appearance at the Tartu Art Museum Museum Academy.
2016 Participation in a panel discussion at the Narva Prejudice Festival.
2016 “Quantum Friction of Pseudorotation: Relaxation through Conical Intersection in Long Time-scale” at the XXII International Symposium on the Jahn-Teller Effect, Tartu.
2015 “Step-by-step Organizing Urbanism” at the Tartu Planning Conference 2015.
2015 “Time Evolution of Optical Centres with Jahn-Teller Effect in Excited State – Contribution of Phonons”, St. Petersburg, Russia.
2015 “Theory of Optical Centres with Jahn-Teller Effect in Excited States – Contribution of Phonons”, Budva, Montenegro.
2015 Presentation “Experience with Annelinn” at the E-Click Landscapes Conference “Landscapes as Possibilities”, Estonian University of Life Sciences, Tartu.
2015 Presentation at the Architecture and Urbanism Conference The Good, the Bad and the Ugly, Vene Draamateater, Tallinn.
2015 From the Edges of Panel Districts. Kondase keskus Peripheral Series, Kondase keskus, Viljandi.

2015 Moderation of the Architecture Flash Lecture "What Does It Mean to Be Contemporary?", TÜ Church, Tartu.
2014 "About Free Planning and Annelinn" (Annelinn branch library).
2014 "You Would Prefer Not To" in the Architecture Flash Lectures series (Telliskivi Creative City).
2014 "Relaxation through Conical Intersection Caused by Emission of Phonons", Graz, Austria.
2014 Introduction to Architectural Films and Discussion. Elektriteater, Tartu.
2014 "About Annelinn Space" at the Annelinn Festival, Tartu.
2014 "About Naming" at the Affect><Effect Conference, Tartu.
2013 Architecture Flash Lecture "On the Border of Language" (Tartu Health Care College).
2012 "Experience of Locality", Estonian Photographic Art Fair (Telliskivi Creative City).
2012 "Human City or Not" TÜ and TTÜ Autumn School See This City and the Other. From Emajõe Athens to Supilinn (Kesklinna kool, Tartu).
2012 "Vibronic Transitions to a State with Jahn–Teller Effect: Contribution of Phonons in Case of $E \otimes e$ – Problem" at the XXIst International Symposium on the Jahn–Teller Effect (Tsukuba, Japan).
2012 "Aesthetics of Inevitability" at the Aesthetics and Politics of Indecision Conference (Estonian Literary Society House, Tartu).
2011 Presentation on "Non-adiabaticity in Vibronic Transitions of Centers with Jahn–Teller Effect" (Cottbus, Germany).
2011 Conference Presentation "Recognition" at the Happiness Conference (as part of Prima Vista) (May 3, Nooruse Gallery, Tartu).
2010 Public Conversation at the Artishok Art Biennial (artist talk) with Toomas Thetloff and Taavi Piibemann (Sept 3, Tartu Art House).
2010 Presentation at the Biosemiotics Summer School "Living in Dystopia" (July 10, Nüpli)..
2010 Utopia Seminar Presentation (June 11, Estonian Literary Society House).
2008 Seminar Presentation "How the City Captivates" "Situationists and Pessoa" (Estonian Literary Society House).
2006 Presentation at the Plektrum Festival "Possibilities for Microurbanism". (Culture Factory Polymer, Tallinn).
2004 Alvar Aalto Conference "Mobile Positioning in Urbanism" (Villa Tammekann, Tartu).

Exhibitions and Events Organized

2023 Member of Estonian Annual Wood Building Jury.
2019–2022 Publication of the Maja and Sirp Space Publication Award.
2019 Establishment of the Maja and Sirp Space Publication Award (with Merle Karro-Kalberg).
2019 Creation of the Architecture Awards website (with Kaire Pärnpuu).

2018, 2019 Member of the Estonian Landscape Architects Union Annual Awards Jury.
2018 Creation of the new website for the architecture magazine Maja (with Kaire Pärnpuu).
2018 Organization and moderation of the Opinion Festival discussion "There's Space, but No Public".
2017 Exhibition "Who Makes the City?" with Pille Epner at the Estonian Museum of Architecture.
2016 Curation of the exhibition "Who Makes the City?" with Pille Epner at the Tartu Art Museum. An overview exhibition of initiatives and institutions shaping the urban space of Tartu.
2013–2016 Annelinn Vision Competition, workshops, and discussions.
2015 Moderation of the Architecture Flash Lecture "What Does It Mean to Be Modern?".
2014 Curator of the Exhibition "A(nne)linnad"; with Tanel Rander.
2014 Guest Judge on the Science Popularization TV-show "Rocket 69".
2014–2020 Initiator and leader of the Annelinn website project; with Ave Kongo.
2009–2010 Chief Organizer of the Urban Forums series.
2007–2008 Co-organizer of the seminar series "How the City Captivates"; with Sven Vabar and Jaak Tomberg.

Teaching and Other Academic Activities
Supervised eight master's theses, taught various courses, served on the defense committees of the Estonian Aviation Academy's Aircraft Construction and Maintenance program and the Estonian Academy of Arts' Interior Architecture master's theses.

ELULOOKIRJELDUS

Nimi Kaja Pae
Sünniaeg 13. november 1979
Kodakondsus eestlane
E-mail kaja.pae@gmail.com
Telefon +372 5695767

Haridus

2010–2024 Tartu Ülikool, doktoriõpingud (füüsika)
1999–2006, 2009–2010 Eesti Kunstiakadeemia, bakalaureuse ja magistriõpingud (arhitektuur- ja linnaplaneerimine, 5-aastane integreeritud õpe)
2007–2009 Tartu Ülikool, bakalaureuseõpingud (teoreetilise füüsika suund, *cum laude*)

Töökäik

2022–... Kliimaministeerium (kuni 2023 Majandus- ja Kommunikatsiooniministeerium), Ehituse ja elukeskkonna osakonna juhataja
2017–2022 Eesti arhitektuuriajakirja Maja peatoimetaja
2017–2023 Arhitektuurikirjastus MTÜ juhatuse liige
2016–2019 Tartu Ülikooli Füüsika Instituut, teoreetilise füüsika osakonna nooremteadur
2012–2015 Tartu Ülikooli Füüsika Instituut, teoreetilise füüsika osakond, teaduse tippkeskus „Mesosüsteemide teooria ja rakendused“, insener
2013–… Eesti Kunstiakadeemia arhitektuuriteaduskond, lepinguline õppejõud
2012–… vabakutseline arhitekt.
2009–2011 Eesti Arhitektuurikeskus, linnafoorumite eestvedaja
2009 Tartu Ülikooli Füüsika Instituut, teoreetilise füüsika osakond
2003–2007 Urban Mark arhitektuuribüroo, arhitekt
2002–2003 Vahur Sova arhitektuuribüroo, arhitekt

Ühiskondlik tegevus

2016–… Teaduse populariseerimise saate „Rakett 69“ põhikohtunik
2023–… Muinsuskaitsenõukogu liige

Tunnustused

2021 Eesti Arhitektide Liidu Mõtestaja teenetemedal
2017 Eesti Maastikuarhitektide Liidu aasta teo preemia näituse „Kes loob linna?“ eest
2017 Eesti Kunstiakadeemia aasta loomepreemia näituse „Kes loob linna?“ eest

2014	Tartu aasta kultuurikandaja nominent (Annelinnaportaal ja visioonikonkurss)
2014	Parim poster rahvusvahelisel Jahn-Telleri sümpoosiumil Grazis, Austrias
2012	Parim poster rahvusvahelisel Jahn-Telleri sümpoosiumil Tsukubas, Jaapanis
2011	Eesti Kultuurkapitali arhitektuuri sihtkapitali tegevuspreemia Linnafoorumite korraldamise eest
2009	II auhind Eesti Teaduste Akadeemia üliõpilastööde konkursil (Töö „Elektronsiirded tugeva vibrooninteraktsiooniga sümmeetrilistes süsteemides“ eest)
2007	Eesti Kultuurkapitali arhitektuuri aastapreemia nominent
2007	1–2. koht ehitatud arhitektuursete väikevormide võistlusel „Väike 2002–2006“ Eesti Panga galerii eest; koos Ülar Margiga
2006	aasta teraskonstruktsiooni auhind
2006	Valitud esindama Eestit väljapanekuga Veneetsia X arhtektuuribiennaalil; koos Ülar Margi ja Rein Ahasega
2003	1. koht Tartu Ülikooli Sotsiaalteaduskonna uue õppehoone projekti konkursil; koos Ülar Margiga

Stipendiumid

2002	Eesti Rahvuskultuuri Fondi stipendium
2002	Ehitusmaailma stipendium
2012	Maailma Teadlaste Organisatsiooni stipendium
2014	Kristjan Jaagu välissõidu stipendium
2015	Kristjan Jaagu välissõidu stipendium

Olulisemad publikatsioonid

Füüsikas:

Hizhnyakov, V.; Pae, K.; Boltrushko, V.; Köppel, H. (2018). Vibronic states in conical intersections: manifestations of centrifugal energy and non-adiabaticity in optical spectra of Jahn-Teller systems. Journal of Physics: Conference Series , 1148.

Pae, K.; Hizhnyakov, V. (2017). Ground state in $E \otimes e$ Jahn-Teller and Renner-Teller systems: Account of nonadiabaticity. Journal of Chemical Physics, 147 (8).

Pae, K.; Hizhnyakov, V. (2016). Quantum friction of pseudorotation in Jahn-Teller system: Passage through conical intersection. Journal of Chemical Physics, 145, 064108.

Pae, K.; Hizhnyakov, V. (2014). Time-dependent Jahn-Teller Problem: Phonon Induced Relaxation through Conical Intersection. Journal of Chemical Physics, 141(23), 234113.

Pae, K.; Hizhnyakov, V. (2013). Nonadiabaticity in a Jahn-Teller system probed by absorption and resonance Raman scattering. Journal of Chemical Physics, 138(10), 104103.
Pae, K.; Hizhnyakov, V. (2013). Optical Jahn-Teller effect: contribution of phonons. Journal of Physics: Conference Series , 428,
Hizhnyakov, V.; Pae, K.; Vaikjärv, T. (2012). Optical Jahn-Teller effect in the case of local modes and phonons. Chemical Physics Letters, 525–526, 64–68.
Hizhnyakov, V.; Boltrushko, V.; Pae, K.; Vaikjarv, T. (2011). Zero-phonon lines: Novel manifestations of vibronic interactions in impurity centres of solids. Optika i Spektroskopiya, 111(3), 398–406.
Hizhnyakov, V.; Pae, K.; Vaikjärv, T. (2011). Vibronic Transitions to a State with Jahn-Teller Effect: Contribution of Phonons. M.Atanasov et al. (Toim.). Vibronic Interactions and the Jahn–Teller Effect: Theory and Applications (179–191). Springer.

Arhitekuuris ja linnaplaneerimises

Raamatud:

Linnafoorumid / Urban Forums. 2011, koostaja ja toimetaja. 356lk. Tallinn: Eesti Arhitektuurikeskus. Eesti ja inglise keeles.
Jointspace – Open Source on Mobile Positioning and Urban Studies. 2006, koostaja ja toimetaja. 174lk. Tallinn: Positium. Inglise keeles.

Koostatud trükised ja toimetised:

Ajakiri Maja 2017–3, 2017–4, 2018–1, 2018–2/3, 2018–4, 2019–1, 2019–2, 2019–3, 2019–4, 2020–1, 2020–2/3, 2020–4, 2021–1, 2021–2, 2021–3, 2021–4, 2022–1, 2022–2, 2022–3-4, 2023–1.
Tartu ruumigurmaani kaart, 2016.
Ajakirja Maja külalistoimetaja nr 1–2, 2016.
Teavitusvoldiku *Kodune Annelinn* koostamine, 2015.

Artiklid:

Eeslinnastumine: vabaduse eufooria ruumilised juhused ja pragmaatilised jõujooned. Eesti linnaehituse ajalugu II köide, 2024.
Ruumiamet – hea elukeskkonna võti. Maja talv 2023.
Visiooniloome. Maja talv 2022.
Kuidas ikkagi elada? Maja talv 2022.
Ülekülluse kultuur: tüpoloogiate lõpp või uued tüpoloogiad? Maja sügis 2021.
Mitte-esteetika ja kõrg-esteetika kohtumine. Maja kevad 2021.
Mis on õhus? Maja kevad 2021.
Nägemus + haridus. Maja suvi–sügis 2020.
Avalik ruum. Ajutisus kui vahend. Vikerkaar, oktoober 2020
Maailma graatsilised jõujooned. Postimees, 20. mai 2020.
Ilu muudab oluliseks usk inimesse. Maja talv 2020.
Mõtete kogum uutest iluvormidest. Postimees, 21. okt. 2019.

Avalik ruum hääbuvates Eesti väikelinnades. Müürileht, september 2019.
Vastasseisud ja mõõduvõtud – arhitektuuri ja kunsti vahel. Maja, suvi, 2019.
Milleks meile nõrk monument? Maja, suvi–sügis, 2018.
Hea maitse kataloog. Maja, suvi–sügis, 2018.
Jäämäe küütlev tipp. Sirp, 6.okt 2017.
The Inertness of Free Plan Areas: Towards Step-By-Step Organizing Urbanism. The Baltic Atlas, Sternberg Press, 2016. Balti paviljoni raamat 2016. aasta Veneetsia arhitektuuribiennaalil.
Sa eelistaksid mitte. Avalikust ruumist, kontrollist ja vastutusest. Ehituskunst 2016.
Annelinna kogukond? Müürileht, oktoober 2015.
Ülev ja igapäevane. Maja, nr1, 2015.
Annelinna poole. Sirp, 28.nov 2014.
Paratamatuse esteetika. Vihik, 2013 (Eesti Kirjanduse Seltsi ajakiri)
Tartu hargnevad praktikad. Positsioonid. Lugemik uuest Eesti arhitektuurist, 2012.
10Pi. Mitte-Tartu, 2012.
Elades düstoopias. Ehituskunst. Estonian Architectural Review nr53/54 2011.
Tunda ära korratamatut. Linnafoorumid / Urban Forums. 2011.
Ülikool põllule? Eesti Päevaleht 18.nov. 2010.
Linnad meie peas. Vihik nr15, 2010 (Eesti Kirjanduse Seltsi ajakiri)
Määramatus koes. Maja nr 3, 2008.
Tartu hargnevad praktikad. Maja nr 2, 2007.
Inimesed linnas. Eesti näitus Joint Space Veneetsia X arhitektuuribiennaalil. Maja nr 4, 2006.
Turning Inside Out – Identy Shifts in Space – Open Source on Mobile Positioning and Urban Studies. 2006.

Intervjuud:
Kunst ja teadus: ühtviisi arusaamatud mõlemad? Sirp 30.04.2021. Küsis Arko Olesk.
Tallinna treppidest. Intervjuu kultuurisaates OP 22.04.2021. Küsis Margit Kilumets.
Sada numbrit kriitilist arhitektuuridiskussiooni. Maja kevad 2020. Küsis Andres Kurg.
Pealelend – Kaja Pae, Eesti arhitektuuriajakirja Maja peatoimetaja. Sirp 22.09.2017. Küsis Merle Karro-Kalberg.
Arhitekt: Annelinnal on suur potentsiaal. Linnaleht 18.sept 2014.
Linnafoorum jõuab Tartusse. 23.04.2010 Sirp. Küsis Reet Varblane.

Tõlked
Plinius Noorema kiri 2.17. Maja, nr 1–2, 2016. (Ladina keelest Epistulae 2.17).

Muu olulisem loominguline tegevus
2022 Eesti-Iiri arhitektide ühisnäitus „Mu maja pole tehtud puudest, mis kasvavad mu maja taga metsas“ Navanis Iirimaal; koos Paco Ulmaniga.

2020–2021 Osalemine Eesti Arhitektuurikeskuse korraldatud Eesti-Iiri arhitektide puitarhitektuurile keskenduvas loomeuurimuses „Wood Works“; koos Paco Ulmaniga.
2016 „Five Pleasures“. Töö XV Veneetsia Arhitektuuribiennaalil; koos Paco Ulmaniga.
2015 „Tartu sulg (( )“. Osalemine Linnafestivali UIT kohaspetsiifilise kirjanduse projektis.
2014 Õnnekonverentsi kunstnikutöö; koos Paco Ulmaniga.
2013 Installatsioonisari „Study of lines in a nature“; koos Paco Ulmaniga.
2012 Fotoseeria Tartu piiridest novellikogus „Mitte-Tartu“.
2009 Proosaflaierite projekt Tartu Kunstikuu raames; koos Sven Vabariga.
2006 Eesti ekspositsiooni koostamine X Veneetsia Arhitektuuribiennaalile; koos Ülar Margi, Rein Ahase, Yoko Alendri, Raul Kalvo, Anto Aasa, Margus Tiru ja Erki Saluveeriga.
2005 Osalemine töödega arhitektuurinäitusel Berliinis näitusel „Emerging Identities – EAST“ (Valitud ülevaatenäitus Ida–Euroopa regiooni moodsast arhitektuurist).
2002 Osalemine töödega fotonäitusel „Vaba voli“ (Valitud ülevaatenäitus noorte fotograafide töödest).

Avalikud ettekanded ja vestlusringid

2024 Euroopa Komisjoni arutelu „Puit kui kestlik ehitusmaterjal ja süsiniku siduja“. Postimehe Maa Elu TV Maamessil, 18. aprill, Tartu.
2024 Ettekanne „Innustav või ennustav: näiteid tehisaru kasutamisest ruumiloomes ja mis võiks olla riigi roll?“ 15. märts Planeerimiskonverents, Tartu.
2023 Paneelarutelu „Üle riigi planeerimise väljakutsed Suure Siirde lävel“, 30. märts Planeerimiskonverents, Tartu.
2023 Ettekanne Äripäeva Arhitektuuri ja arenduse konverentsil, 28 sept hotell Radisson Blue, Tallinn
2023 Kuidas aitab ruumiline pärand toime tulla nüüdisaegsete väljakutsetega?
2023 Hoonete renoveerimisteemaline vestlusring sLenderhood. 5 juuni EKA.
2022 Ettekanne Ehituskonverentsil, 9 nov, hotell Euroopa, Tallinn.
2021 Osalemine vestlusringis „Kunst ja teadus: ühtviisi arusaamatud mõlemad?“, 11. veebruar Kumu.
2019 Tallinna Arhitektuuribiennaali sümpoosioni „Beauty Matters“ moderaator. 2019 Ettekanne „Kuidas liigub Tallinn“, 30.mai konverentsil „Inimkeskne Suur-Tallinn“ Tallinna sadama A-terminalis (Tallinna liikuvusuuringu avalik esitlus).
2019 Vestlusringi „Mida peale hakata kasutuks muutunud arhitektuuriga?“ moderaator ja korraldaja, 11. mai Kumu.
2019 Ettekanne EALi üldkogule, 28. märts Kumu.
2019 Osalemine EALi kuraatornäituse „Liginull“ vestlusringis, 6. märts Aparaaditehas.
2018 Tuntud vilistlase ettekanne HTG 105. juubelikonverentsil.

2018 Narva UrbanLab Narva-Detroit vestlusringi „Shrinking Urban Space: Changes and Adaptation“ moderaator, 24. aug Narva kunstiresidents.
2018 Arvamusfestivali arutelu „Ruumi on, aga avalikkust pole“ algataja ja moderaator, 10. aug Paide.
2018 Ettekanne „Ground state of E x e Jahn-Teller system. Account of non-adiabaticity“. Santander, Hispaania.
2018 Tartu 2024 – Euroopa kultuuripealinnaks, vestlusringi moderaator 9.mai ERM.
2018 Ettekanne arhitektuuri välkloengul 7. veeb Von Krahli teatris.
2017 Lasnaidee inspiratsiooniseminar „Milles peitub kivilinna potentsiaal?“ 10. dets.
2017 Planeerimiskonverentsi ettekanne 2. novembril.
2017 Raikküla mõisakonverentsil „Ruum ajas, inimene ruumis“. 19. mai Raikküla mõis.
2017 Arutelu Tallinna mereääre visiooni teemal, 1. aprill Eesti Arhitektuurimuuseum.
2016 Esinemine Tartu Kunstimuuseumi muuseumiakadeemias.
2016 Osalemine vestlusringis Narva eelarvamusfestivalil.
2016 „Quantum friction of pseudorotation: relaxation through conical intersection in long time-scale“ konverentsil XXII Internationa Symposium on the Jahn-Teller Effect, Tartu.
2015 „Samm-sammult organiseeruv urbanism“ Tartu planeerimiskonverents 2015.
2015 „Time evolution of optical centres with Jahn-Teller effect in excited state – contribution of phonons“. (Peterburi, Venemaa)
2015 Theory of optical centres with Jahn-Teller effect in excited states – contribution of phonons. (Budva, Montenegro)
2015 Annelinnaga töötamise kogemusest. E-Click’i maastike konverentsil „Landscapes as Possibilities“, Eesti Maaülikool, Tartu.
2015 Ettekanne arhitektuuri- ja urbanismi konverentsil The Good, the Bad and the Ugly, Vene Draamateater, Tallinn.
2015 Paneelpiirkondade äärtest. Kondase keskuse äärealade sarjas, Kondase keskus, Viljandi.
2015 Arhitektuuri välkloengu „Mida tähendab olla kaasaegne ?“ modereerimine, TÜ kirikus, Tartu.
2014 „Vabaplaneeringust ja Annelinnast“ (Annelinna haruraamatukogu).
2014 „Sa eelistaksid mitte“ Arhitektuuri välkloengute sarjas (Telliskivi loomelinnak).
2014 „Relaxation through Conical Intersection Caused by Emission of Phonons“, Graz, Austria.
2014 Arhitektuurifilimide sissejuhatus ja vestlus. Elektriteater, Tartu.
2014 „Annelinna ruumist“ Annelinna festivalil, Tartu.
2014 „Nimetusest“ konverentsil Afekt><Efekt, Tartu.
2013 Arhitektuuri välkloeng „Keele piiril“ (Tartu Tervishoiu kõrgkool).
2012 „Kohalikkuse kogemus“, Eesti Fotokunstimess (Telliskivi loomelinnak).

2012 „Inimese linn või mitte“ TÜ ja TTÜ sügiskool See linn ja teine. Emajõe Ateenast Supilinna (Kesklinna kool, Tartu).
2012 „Vibronic transitions to a state with Jahn–Teller effect: contribution of phonons in case of $E \otimes e$-problem“ XXIst International Symposium on the Jahn–Teller Effect (Tsukuba, Jaapan)
2012 „Paratamatuse esteetika“ konverentsil Esteetika ja otsustamatuse poliitika (Eesti Kirjanduse Seltsi maja, Tartu)
2011 Ettekanne „Non-adiabaticity in vibronic transitions of centres with Jahn-Teller effect“ (Cottbus, Saksamaa)
2011 Õnnekonverentsi ettekanne „Äratundmine“ (Prima Vista raames) (3.mai, Nooruse galerii, Tartu)
2010 Artishoki kunstibiennaali avalik jutuajamine (artist talk) Toomas Thetloffi ja Taavi Piibemanniga (3.september, Tartu Kunstimaja)
2010 Biosemiootika suvekooli ettekanne „Elades düstoopias“ (10.juuli, Nüpli)
2010 Utoopia seminari ettekanne (11.juuni, Eesti Kirjanduse Seltsi maja)
2008 Seminari „Kuidas linn köidab“ ettekanne „Situatsionistid ja Pessoa“ (Eesti Kirjanduse Seltsi maja)
2006 Ettekanne Plektrummi festivalil „Possibilities for Microurbanism“. (Kultuuritehas Polymer, Tallinn)
2004 Alvar Aalto konverents „Mobile Positioning in Urbanism“ (Villa Tammekann, Tartu)

Korraldatud näitused ja üritused

2019–2022 Maja ja Sirbi ruumipublikatsioonipreemia väljaandmine.
2019 Maja ja Sirbi ruumipublikatsioonipreemia loomine (koos Merle Karro-Kalbergiga).
2019 Arhitektuuripreemiate kodulehe loomine (koos Kaire Pärnpuuga).
2018, 2019 Eesti Maastikuarhitektide Liidu aastapreemiate žürii liige.
2018 Arhitektuuriajakirja Maja uue kodulehele loomine (koos Kaire Pärnpuuga).
2018 Arvamusfestivali arutelu „Ruumi on, aga avalikkust pole“ korraldamine ja modereerimine.
2017 Näitus „Kes loob linna?“ koos Pille Epneriga Eesti Arhitektuurimuuseumis.
2016 Näituse „Kes loob linna?“ kureerimine koos Pille Epneriga Tartu Kunstimuuseumis. Ülevaatenäituse Tartu linnaruumi kujundavatest initsiatiividest ja institutsioonidest.
2013–2016 Annelinna visioonikonkurss, töötoad ja arutelud.
2015 Arhitektuuri välkloengu „Mida tähendab olla kaasaegne?“ moderaator.
2014 Näituse „A(nne)linnad“ kuraator; koos Tanel Randeriga.
2014 Teaduse populariseerimissaate „Rakett 69“ külaliskohtunik.
2014–2020 Annelinna veebilehe eestvedaja; koos Ave Kongoga.
2009–2010 Linnafoorumite sarja peakorraldaja.

2007–2008 Kaaskorraldaja seminarisarjal „Kuidas linn köidab“; koos Sven Vabari ja Jaak Tombergiga.

Õpetamine ja muu akadeemiline tegevus

Juhendanud kaheksa magistritööd, õpetanud erinevaid kursusi, kuulunud Eesti Lennuakadeemia Õhusõiduki ehitamise ja hoolduse eriala lõputööde kaitsmiskomisjoni ja Eesti Kunstiakadeemia sisearhitektuuri eriala magistritööde kaitsmiskomisjoni.

DISSERTATIONES PHYSICAE UNIVERSITATIS TARTUENSIS

1. **Andrus Ausmees.** XUV-induced electron emission and electron-phonon interaction in alkali halides. Tartu, 1991.
2. **Heiki Sõnajalg.** Shaping and recalling of light pulses by optical elements based on spectral hole burning. Tartu, 1991.
3. **Sergei Savihhin.** Ultrafast dynamics of F-centers and bound excitons from picosecond spectroscopy data. Tartu, 1991.
4. **Ergo Nõmmiste.** Leelishalogeniidide röntgenelektronemissioon kiiritamisel footonitega energiaga 70–140 eV. Tartu, 1991.
5. **Margus Rätsep.** Spectral gratings and their relaxation in some low-temperature impurity-doped glasses and crystals. Tartu, 1991.
6. **Tõnu Pullerits.** Primary energy transfer in photosynthesis. Model calculations. Tartu, 1991.
7. **Olev Saks.** Attoampri diapasoonis voolude mõõtmise füüsikalised alused. Tartu, 1991.
8. **Andres Virro.** AlGaAsSb/GaSb heterostructure injection lasers. Tartu, 1991.
9. **Hans Korge.** Investigation of negative point discharge in pure nitrogen at atmospheric pressure. Tartu, 1992.
10. **Jüri Maksimov.** Nonlinear generation of laser VUV radiation for high-resolution spectroscopy. Tartu, 1992.
11. **Mark Aizengendler.** Photostimulated transformation of aggregate defects and spectral hole burning in a neutron-irradiated sapphire. Tartu, 1992.
12. **Hele Siimon.** Atomic layer molecular beam epitaxy of A^2B^6 compounds described on the basis of kinetic equations model. Tartu, 1992.
13. **Tõnu Reinot.** The kinetics of polariton luminescence, energy transfer and relaxation in anthracene. Tartu, 1992.
14. **Toomas Rõõm.** Paramagnetic H^{2-} and F^{+} centers in CaO crystals: spectra, relaxation and recombination luminescence. Tallinn, 1993.
15. **Erko Jalviste.** Laser spectroscopy of some jet-cooled organic molecules. Tartu, 1993.
16. **Alvo Aabloo.** Studies of crystalline celluloses using potential energy calculations. Tartu, 1994.
17. **Peeter Paris.** Initiation of corona pulses. Tartu, 1994.
18. **Павел Рубин.** Локальные дефектные состояния в CuO_2 плоскостях высокотемпературных сверхпроводников. Тарту, 1994.
19. **Olavi Ollikainen.** Applications of persistent spectral hole burning in ultrafast optical neural networks, time-resolved spectroscopy and holographic interferometry. Tartu, 1996.
20. **Ülo Mets.** Methodological aspects of fluorescence correlation spectroscopy. Tartu, 1996.
21. **Mikhail Danilkin.** Interaction of intrinsic and impurity defects in CaS:Eu luminophors. Tartu, 1997.

22. **Ирина Кудрявцева.** Создание и стабилизация дефектов в кристаллах KBr, KCl, RbCl при облучении ВУФ-радиацией. Тарту, 1997.
23. **Andres Osvet.** Photochromic properties of radiation-induced defects in diamond. Tartu, 1998.
24. **Jüri Örd.** Classical and quantum aspects of geodesic multiplication. Tartu, 1998.
25. **Priit Sarv.** High resolution solid-state NMR studies of zeolites. Tartu, 1998.
26. **Сергей Долгов.** Электронные возбуждения и дефектообразование в некоторых оксидах металлов. Тарту, 1998.
27. **Kaupo Kukli.** Atomic layer deposition of artificially structured dielectric materials. Tartu, 1999.
28. **Ivo Heinmaa.** Nuclear resonance studies of local structure in $RBa_2Cu_3O_{6+x}$ compounds. Tartu, 1999.
29. **Aleksander Shelkan.** Hole states in CuO_2 planes of high temperature superconducting materials. Tartu, 1999.
30. **Dmitri Nevedrov.** Nonlinear effects in quantum lattices. Tartu, 1999.
31. **Rein Ruus.** Collapse of 3d (4f) orbitals in 2p (3d) excited configurations and its effect on the x-ray and electron spectra. Tartu, 1999.
32. **Valter Zazubovich.** Local relaxation in incommensurate and glassy solids studied by Spectral Hole Burning. Tartu, 1999.
33. **Indrek Reimand.** Picosecond dynamics of optical excitations in GaAs and other excitonic systems. Tartu, 2000.
34. **Vladimir Babin.** Spectroscopy of exciton states in some halide macro- and nanocrystals. Tartu, 2001.
35. **Toomas Plank.** Positive corona at combined DC and AC voltage. Tartu, 2001.
36. **Kristjan Leiger.** Pressure-induced effects in inhomogeneous spectra of doped solids. Tartu, 2002.
37. **Helle Kaasik.** Nonperturbative theory of multiphonon vibrational relaxation and nonradiative transitions. Tartu, 2002.
38. **Tõnu Laas.** Propagation of waves in curved spacetimes. Tartu, 2002.
39. **Rünno Lõhmus.** Application of novel hybrid methods in SPM studies of nanostructural materials. Tartu, 2002.
40. **Kaido Reivelt.** Optical implementation of propagation-invariant pulsed free-space wave fields. Tartu, 2003.
41. **Heiki Kasemägi.** The effect of nanoparticle additives on lithium-ion mobility in a polymer electrolyte. Tartu, 2003.
42. **Villu Repän.** Low current mode of negative corona. Tartu, 2004.
43. **Алексей Котлов.** Оксианионные диэлектрические кристаллы: зонная структура и электронные возбуждения. Tartu, 2004.
44. **Jaak Talts.** Continuous non-invasive blood pressure measurement: comparative and methodological studies of the differential servo-oscillometric method. Tartu, 2004.
45. **Margus Saal.** Studies of pre-big bang and braneworld cosmology. Tartu, 2004.

46. **Eduard Gerškevitš.** Dose to bone marrow and leukaemia risk in external beam radiotherapy of prostate cancer. Tartu, 2005.
47. **Sergey Shchemelyov.** Sum-frequency generation and multiphoton ionization in xenon under excitation by conical laser beams. Tartu, 2006.
48. **Valter Kiisk.** Optical investigation of metal-oxide thin films. Tartu, 2006.
49. **Jaan Aarik.** Atomic layer deposition of titanium, zirconium and hafnium dioxides: growth mechanisms and properties of thin films. Tartu, 2007.
50. **Astrid Rekker.** Colored-noise-controlled anomalous transport and phase transitions in complex systems. Tartu, 2007.
51. **Andres Punning.** Electromechanical characterization of ionic polymer-metal composite sensing actuators. Tartu, 2007.
52. **Indrek Jõgi.** Conduction mechanisms in thin atomic layer deposited films containing TiO_2. Tartu, 2007.
53. **Aleksei Krasnikov.** Luminescence and defects creation processes in lead tungstate crystals. Tartu, 2007.
54. **Küllike Rägo.** Superconducting properties of MgB_2 in a scenario with intra- and interband pairing channels. Tartu, 2008.
55. **Els Heinsalu.** Normal and anomalously slow diffusion under external fields. Tartu, 2008.
56. **Kuno Kooser.** Soft x-ray induced radiative and nonradiative core-hole decay processes in thin films and solids. Tartu, 2008.
57. **Vadim Boltrushko.** Theory of vibronic transitions with strong nonlinear vibronic interaction in solids. Tartu, 2008.
58. **Andi Hektor.** Neutrino Physics beyond the Standard Model. Tartu, 2008.
59. **Raavo Josepson.** Photoinduced field-assisted electron emission into gases. Tartu, 2008.
60. **Martti Pärs.** Study of spontaneous and photoinduced processes in molecular solids using high-resolution optical spectroscopy. Tartu, 2008.
61. **Kristjan Kannike.** Implications of neutrino masses. Tartu, 2008.
62. **Vigen Issahhanjan.** Hole and interstitial centres in radiation-resistant MgO single crystals. Tartu, 2008.
63. **Veera Krasnenko.** Computational modeling of fluorescent proteins. Tartu, 2008.
64. **Mait Müntel.** Detection of doubly charged higgs boson in the CMS detector. Tartu, 2008.
65. **Kalle Kepler.** Optimisation of patient doses and image quality in diagnostic radiology. Tartu, 2009.
66. **Jüri Raud.** Study of negative glow and positive column regions of capillary HF discharge. Tartu, 2009.
67. **Sven Lange.** Spectroscopic and phase-stabilisation properties of pure and rare-earth ions activated ZrO_2 and HfO_2. Tartu, 2010.
68. **Aarne Kasikov.** Optical characterization of inhomogeneous thin films. Tartu, 2010.
69. **Heli Valtna-Lukner.** Superluminally propagating localized optical pulses. Tartu, 2010.

70. **Artjom Vargunin.** Stochastic and deterministic features of ordering in the systems with a phase transition. Tartu, 2010.
71. **Hannes Liivat.** Probing new physics in e+e− annihilations into heavy particles via spin orientation effects. Tartu, 2010.
72. **Tanel Mullari.** On the second order relativistic deviation equation and its applications. Tartu, 2010.
73. **Aleksandr Lissovski.** Pulsed high-pressure discharge in argon: spectroscopic diagnostics, modeling and development. Tartu, 2010.
74. **Aile Tamm.** Atomic layer deposition of high-permittivity insulators from cyclopentadienyl-based precursors. Tartu, 2010.
75. **Janek Uin.** Electrical separation for generating standard aerosols in a wide particle size range. Tartu, 2011.
76. **Svetlana Ganina.** Hajusandmetega ülesanded kui üks võimalus füüsikaõppe efektiivsuse tõstmiseks. Tartu, 2011
77. **Joel Kuusk.** Measurement of top-of-canopy spectral reflectance of forests for developing vegetation radiative transfer models. Tartu, 2011.
78. **Raul Rammula**. Atomic layer deposition of HfO_2 – nucleation, growth and structure development of thin films. Tartu, 2011.
79. **Сергей Наконечный.** Исследование электронно-дырочных и интерстициал-вакансионных процессов в монокристаллах MgO и LiF методами термоактивационной спектроскопии. Тарту, 2011.
80. **Niina Voropajeva.** Elementary excitations near the boundary of a strongly correlated crystal. Tartu, 2011.
81. **Martin Timusk.** Development and characterization of hybrid electro-optical materials. Tartu, 2012, 106 p.
82. **Merle Lust.** Assessment of dose components to Estonian population. Tartu, 2012, 84 p.
83. **Karl Kruusamäe.** Deformation-dependent electrode impedance of ionic electromechanically active polymers. Tartu, 2012, 128 p.
84. **Liis Rebane.** Measurement of the $W \to \tau\nu$ cross section and a search for a doubly charged Higgs boson decaying to τ-leptons with the CMS detector. Tartu, 2012, 156 p.
85. **Jevgeni Šablonin.** Processes of structural defect creation in pure and doped MgO and NaCl single crystals under condition of low or super high density of electronic excitations. Tartu, 2013, 145 p.
86. **Riho Vendt**. Combined method for establishment and dissemination of the international temperature scale. Tartu, 2013, 108 p.
87. **Peeter Piksarv.** Spatiotemporal characterization of diffractive and non-diffractive light pulses. Tartu, 2013, 156 p.
88. **Anna Šugai.** Creation of structural defects under superhigh-dense irradiation of wide-gap metal oxides. Tartu, 2013, 108 p.
89. **Ivar Kuusik.** Soft X-ray spectroscopy of insulators. Tartu, 2013, 113 p.
90. **Viktor Vabson**. Measurement uncertainty in Estonian Standard Laboratory for Mass. Tartu, 2013, 134 p.

91. **Kaupo Voormansik.** X-band synthetic aperture radar applications for environmental monitoring. Tartu, 2014, 117 p.
92. **Deivid Pugal.** hp-FEM model of IPMC deformation. Tartu, 2014, 143 p.
93. **Siim Pikker.** Modification in the emission and spectral shape of photostable fluorophores by nanometallic structures. Tartu, 2014, 98 p.
94. **Mihkel Pajusalu**. Localized Photosynthetic Excitons. Tartu, 2014, 183 p.
95. **Taavi Vaikjärv.** Consideration of non-adiabaticity of the Pseudo-Jahn-Teller effect: contribution of phonons. Tartu, 2014, 129 p.
96. **Martin Vilbaste.** Uncertainty sources and analysis methods in realizing SI units of air humidity in Estonia. Tartu, 2014, 111 p.
97. **Mihkel Rähn.** Experimental nanophotonics: single-photon sources- and nanofiber-related studies. Tartu, 2015, 107 p.
98. **Raul Laasner.** Excited state dynamics under high excitation densities in tungstates. Tartu, 2015, 125 p.
99. **Andris Slavinskis.** EST Cube-1 attitude determination. Tartu, 2015, 104 p.
100. **Karlis Zalite**. Radar Remote Sensing for Monitoring Forest Floods and Agricultural Grasslands. Tartu, 2016, 124 p.
101. **Kaarel Piip.** Development of LIBS for *in-situ* study of ITER relevant materials. Tartu, 2016, 93 p.
102. **Kadri Isakar.** ^{210}Pb in Estonian air: long term study of activity concentrations and origin of radioactive lead. Tartu, 2016, 107 p.
103. **Artur Tamm.** High entropy alloys: study of structural properties and irradiation response. Tartu, 2016, 115 p.
104. **Rasmus Talviste.** Atmospheric-pressure He plasma jet: effect of dielectric tube diameter. Tartu, 2016, 107 p.
105. **Andres Tiko.** Measurement of single top quark properties with the CMS detector. Tartu, 2016, 161 p.
106. **Aire Olesk.** Hemiboreal Forest Mapping with Interferometric Synthetic Aperture Radar. Tartu, 2016, 121 p.
107. **Fred Valk.** Nitrogen emission spectrum as a measure of electric field strength in low-temperature gas discharges. Tartu, 2016, 149 p.
108. **Manoop Chenchiliyan.** Nano-structural Constraints for the Picosecond Excitation Energy Migration and Trapping in Photosynthetic Membranes of Bacteria. Tartu, 2016, 115p.
109. **Lauri Kaldamäe.** Fermion mass and spin polarisation effects in top quark pair production and the decay of the higgs boson. Tartu, 2017, 104 p.
110. **Marek Oja.** Investigation of nano-size α- and transition alumina by means of VUV and cathodoluminescence spectroscopy. Tartu, 2017, 89 p.
111. **Viktoriia Levushkina.** Energy transfer processes in the solid solutions of complex oxides. Tartu, 2017, 101 p.
112. **Mikk Antsov.** Tribomechanical properties of individual 1D nanostructures: experimental measurements supported by finite element method simulations. Tartu, 2017, 101 p.
113. **Hardi Veermäe.** Dark matter with long range vector-mediated interactions. Tartu, 2017, 137 p.

114. **Aris Auzans.** Development of computational model for nuclear energy systems analysis: natural resources optimisation and radiological impact minimization. Tartu, 2018, 138 p.
115. **Aleksandr Gurev**. Coherent fluctuating nephelometry application in laboratory practice. Tartu, 2018, 150 p.
116. **Ardi Loot**. Enhanced spontaneous parametric downconversion in plasmonic and dielectric structures. Tartu, 2018, 164 p.
117. **Andreas Valdmann.** Generation and characterization of accelerating light pulses. Tartu, 2019, 85 p.
118. **Mikk Vahtrus.** Structure-dependent mechanical properties of individual one-dimensional metal-oxide nanostructures. Tartu, 2019, 110 p.
119. **Ott Vilson.** Transformation properties and invariants in scalar-tensor theories of gravity. Tartu, 2019, 183 p.
120. **Indrek Sünter.** Design and characterisation of subsystems and software for ESTCube-1 nanosatellite. Tartu, 2019, 195 p.
121. **Marko Eltermann**. Analysis of samarium doped TiO_2 optical and multi-response oxygen sensing capabilities. Tartu, 2019, 113 p.
122. **Kalev Erme**. The effect of catalysts in plasma oxidation of nitrogen oxides. Tartu, 2019, 114 p.
123. **Sergey Koshkarev.** A phenomenological feasibility study of the possible impact of the intrinsic heavy quark (charm) mechanism on the production of doubly heavy mesons and baryons. Tartu, 2020, 134 p.
124. **Kristi Uudeberg.** Optical Water Type Guided Approach to Estimate Water Quality in Inland and Coastal Waters. Tartu, 2020, 222 p.
125. **Daniel Blixt.** Hamiltonian analysis of covariant teleparallel theories of gravity. Tartu, 2021, 142 p.
126. **Ulbossyn Ualikhanova.** Gravity theories based on torsion: theoretical and observational constraints. Tartu, 2021, 154 p.
127. **Iaroslav Iakubivskyi**. Nanospacecraft for Technology Demonstration and Science Missions. Tartu, 2021, 177 p.
128. **Heido Trofimov.** Polluted clouds at air pollution hot spots help to better understand anthropogenic impacts on Earth's climate. Tartu, 2022, 96 p.
129. **Ott Rebane.** *In situ* non-contact sensing of microbiological contamination by fluorescence spectroscopy. Tartu, 2022, 157 p.
130. **Juhan Saaring.** Ultrafast Relaxation Processes in Ternary Hexafluorides Studied under Synchrotron Radiation Excitation. Tartu, 2022, 106 p.
131. **Ahmet Ilker Topuz.** Quantitative and qualitative investigations for muon scattering tomography via GEANT4 simulations: A computational study. Tartu, 2023, 163 p.
132. **Nico Benincasa.** Phase transitions and gravitational waves in models of dark matter. Tartu, 2023, 206 p.